Optimisation of a Propagation Model for Last Mile Connectivity with Low Altitude Platforms using Machine Learning

A thesis submitted for the degree of Doctor of Philosophy

By

Faris Abdullah Almalki

BSc, MSc

College of Engineering Design and Physical Sciences

Brunel University

London

December 2017

Abstract

Our related research review on propagation models reveals six factors that are significant in last mile connectivity via LAP: path loss, elevation angle, LAP altitude, coverage area, power consumption, operation frequency, interference, and antenna type. These factors can help with monitoring system performance, network planning, coverage footprint, receivers' line-of-sight, quality of service requirements, and data rates which may all vary in response to geomorphology characteristics. Several competing propagation models have been proposed over the years but whilst they collectively raise many shortcomings such as limited altitude up to few tens of meters, lack of cover across different environments, low perdition accuracy they also exhibit several advantages. Four propagation models, which are representatives of their types, have been selected since they exhibit advantages in relation to high altitude, wide coverage range, adaption across different terrains. In addition, all four have been extensively deployed in the past and as a result their correction factors have evolved over the years to yield extremely accurate results which makes the development and evaluation aspects of this research very precise. The four models are: ITU-R P.529-3, Okumura, Hata-Davidson, and ATG. The aim of this doctoral research is to design a new propagation model for last-mile connectivity using LAPs technology as an alternative to aerial base station that includes all six factors but does not exhibit any of the shortcomings of existing models. The new propagation model evolves from existing models using machine learning. The four models are first adapted to include the elevation angle alongside the multiple-input multiple-output diversity gain, our first novelty in propagation modelling. The four adapted models are then used as input in a Neural Network framework and their parameters are clustered in a Self-Organizing-Map using a minimax technique. The framework evolves an optimal propagation model that represents the main research contribution of this research. The optimal propagation model is deployed in two proof-of-concept applications, a wireless sensor network, and a cellular structure. The performance of the optimal model is evaluated and then validated against that of the four adapted models first in relation to predictions reported in the literature and then in the context of the two proof-of-concept applications. The predictions of the optimised model are significantly improved in comparison to those of the four adapted propagation models. Each of the two proof-of-concept applications also represent a research novelty.

Acknowledgements

First and foremost, I would like to thank God Almighty for giving me the ability and strength to complete this thesis.

It is my pleasure to thank great people who made this thesis possible. Predominantly, I would like to express my sincere gratitude to my principal supervisor Professor Marios Angelides for giving me this great opportunity to pursue my PhD; during which he provided an excellent research atmosphere and immense knowledge. I also would like to thank him for his patience, motivation, guidance, and experience that significantly added to my research skills. In addition to his continuous encouragement to engage with wider research community by attending international conferences, participating in scientific workshops, and submitting research work to respected journals. My thanks extended to my researcher development advisor, and annual panel review members: for their great mentor and valuable comments during the course of my PhD program. I would also like to thank the anonymous reviewers that spent considerable time reading and commenting on my published works.

I acknowledge the contribution of full financial support given by the Royal Saudi Embassy and the Saudi Cultural Bureau in London, as well as Taif University back in the Kingdom of Saudi Arabia whom gave me a scholarship to pursue my PhD study, and funding me to present my work in three international conferences. I am in debt to my beloved wife the entrepreneur Bushra for her encouragement, and for being tremendously supportive during my PhD. My endless gratitude to my father Professor Abdullah for opening my eyes to the charm of science and for inculcating the love of research, and to my mother Ms Amani for her immeasurable care, love and prayers she gave me. Extended thanks to my brother Dr Fahad and sisters Aljoharah, Alanoud, Dr Alhanouf, and Almaha for their great support, constant encouragement and love that I have relied on during my studies. Last but certainly not least, thanks to my 4-year old daughter Judy who motivate me to be an awesome dad, and I always want to be successful and a great role model for her. During this work, many ideas, and laughs have been shared with my friend Abdullah Alotaibi, which will be memorable times. I wish the research work in the College of Engineering, Design and Physical Sciences at Brunel university London to continue and flourish many years to come.

Author's Declaration

I hereby declare that this thesis is my own work and effort and that it has not been submitted anywhere for any award. Where other sources of information have been used, they have been acknowledged.

Faris Abdullah Almalki

December 2017

List of Publications and Participations in Students Conferences

Journal

- **F. A. Almalki**, M. C. Angelides, “Optimization of a Propagation Model for Last-Mile Connectivity using a Low Altitude Platform”, under consideration
- S. Alsamhi, **F. A. Almalki**, M. C. Angelides, S. Gapta, O. Ma, "Tethered Balloon Technology for Emergency Communication and Disaster Relief Deployment", *Springer Telecommunication Systems*, forthcoming.

Conferences Proceedings

- J. Cole, **F. A. Almalki,** and P. R. Young, "Chipless RF Liquid Sensor," 2015 IEEE International Microwave and RF Conference (IMaRC), Hyderabad, India, December 2015
- **F. A. Almalki**, M. C. Angelides, “Considering Near Space Platforms to Close the Coverage Gap in Wireless Communications; the Case of the Kingdom of Saudi Arabia”, IEEE 2016 - Future Technologies Conference (FTC), San Francisco, US, December 2016
- **F. A. Almalki**, M. C. Angelides, “Empirical Evolution of a Propagation Model for Low Altitude Platforms”, IEEE Computing Conference 2017, London, UK, July 2017
- **F. A. Almalki**, M. C. Angelides, “Propagation Modelling and Performance Assessment of Aerial Platforms Deployed During Emergencies”, *12th IEEE International Conference for Internet Technology and Secured Transactions (ICITST-2017)*, Cambridge, UK, December 2017

Participation in conferences

- "Chipless RF Sensors for wireless Gas and Liquids Monitoring", 8th Saudi Students Conference in the UK, Imperial College London, February 2015.
- “Three Minute Thesis Competition” organized by the Saudi Cultural Bureau in London and the Saudi Scientific Society in the UK, Imperial College London, June 2015, **Second prize**.
- "Provision of Wireless Services in KSA using High Altitude Platforms", 9th Saudi Students Conference in the UK, Birmingham University, February 2016.
- “Three Minute Thesis Competition Finals” organized by the Brunel Graduate School, March 2017, **People’s choice third prize**.

Table of Contents

Table of Figures

Table of Tables

List of Acronyms

AP	Access Point
ATA	Air-To-Air
AWGN	Additive White Gaussian Noise
ABSOLUTE	Aerial Base Stations with Opportunistic Links for Unexpected & Temporary Events
AR	Action Research
ATG	Air-To-Ground
AoDs	Angles of Departure
BS	Base Station
BER	Bit Error Rate
CB	Collaborative Beamforming
COST-231	Cooperative for Scientific and Technical Research-231
dB	Decibel
dBm	Decibel-milliwatt
dBi	Decibels relative to an isotropic radiator
DL	Down Link
ESA	European Space Agency
ETRI	Electronics and Telecommunications Research Institute
ECC-33	Electronic Communication Committee-33
EPM-73	Empirical Propagation Model-73
EIRP	Effective Isotropic Radiated Power
FSPL	Free Space Path Loss
FSOs	Free Space Optics
FDD	Frequency-Division Duplex
GPRS	General Packet Radio Service
GEO	Geostationary Earth Orbit
GoS	Grade of Service
HS	Handset
HAP	High Altitude Platform
HALE-D	High-Altitude Long Endurance Defence
IoT	Internet of Things
ITU	International Telecommunication Union
IMT-Advanced	International Mobile Telecommunications-Advanced
JAXA	Japan Aerospace Exploration Agency
KARI	Korean Aerospace Research Institute
KSA	Kingdom of Saudi Arabia
LAP	Low Altitude Platform
LTE	Long Term Evolution
LTE-A	Long Term Evolution-Advanced
LoS	Line-of-Sight
LEO	Low Earth Orbit
MAPL	Maximum Allowable Path Loss
MIMO	Multiple Input Multiple Output
ML	Machine Learning
MEO	Medium Earth Orbit
NLoS	No Line-of-Sight
NASA	National Aeronautics and Space Administration
NICT	National Institute of Information and Communications Technology
Neural Networks	NNs

OFDMA	Orthogonal Frequency-Division Multiple Access
OPNET	Optimised Network Engineering Tool
PL	Path loss
PSO	Particle Swarm Optimisation
PTS	Portable Terrestrial Stations
PSATRI	Prince Sultan Advanced Technology Research Institute
P_B	Probability of Blocking
QoS	Quality of Service
QPSK	Quadrature Phase Shift Keying
QAM	Quadrature Amplitude Modulation
RF	Radio Frequency
RSS	Received Signal Strength
RMSE	Root Mean Square Error
RSL	Received Signal Level
RTT	Round-trip time
SISO	Single Input Single Output
SSI	Sky Stations International Inc
SUI	Stanford University Interim
SINR	Signal-to-Interference-Noise Ratio
SNR	Signal-to-Noise Ratio
Self-Organizing Map	SOM
TCP	Transmission Control Protocol
TETRA	Terrestrial Trunked Radio
TDD	Time-Division Duplex
UL	Up Link
UMTS	Universal Mobile Telecommunications Service
WiMAX	Worldwide Interoperability for Microwave Access
WiGiG	Gigabit WiFi
WiFi	Wireless Fidelity
WiMAX	Worldwide Interoperability for Microwave Access
WSN	Wireless Sensor Network
W-I	Walfisch–Ikegami
3D	Three-Dimensional
3GPP	Third Generation Partnership Project
4G	Fourth Generation
5G	Fifth Generation

Chapter 1 : Last Mile Connectivity

Wireless communication systems are enabled either by terrestrial base stations (BSs) or space-based systems such as satellites, High Altitude Platforms (HAPs), and Low Altitude Platforms (LAPs). Aerial platforms are stationed, but are not stationary, between terrestrial and space-based systems and benefit from their strengths, whilst avoiding some of their weaknesses. Traditional wireless communication systems provide services with a good level of data rates, re-configurable provision with various dynamic coverage demands. However, the deployment of these enabling technologies has led to a huge rise in the demand for mobile communications, partly due to the exponential growth in multimedia traffic, and partly due to the emergence of new type of technology such as Internet of Things (IoT), or Big Data. Researchers have begun considering aerial platforms as a wireless communication system as it can add value to the wireless communication technology. This chapter presents a review of related research on last mile connectivity with deploying LAPs as an alternative to BSs. There are several factors that play an important role in quantifying the link budget performance of the last mile wireless communication link using LAPs across various environments, urban, suburban, and rural. These factors include: propagation path loss model, elevation angle, LAP altitude and coverage area, power consumption, operation frequency, interference, and antenna specification include gain, height, transmission power, and loss. The chapter then draws the own research rationale that motivates the research aim and objectives, and the research methodologies that have been used in pursuing each objective.

1.1 Channel Modelling for Last Mile Connectivity using LAP

Although, HAPs have number of merits, including a capability of providing regional footprint and a long endurance deploying them, they remain an expensive option when considering the delivery of wireless communications in remote areas. Therefore, in the case of short-term large-scale events or during and immediately after natural disasters, LAPs are preferred for providing dynamic and scalable networks as they can cover fairly quickly a wide area with a radius running into tens of kilometres, depending on configuration and communication payloads [1-3]. LAPs can be stationed up to a maximum altitude of 5km above ground, whether they are unmanned solar-powered

airships [4] or tethered platforms that use ultra-strong but light-weight tethers for power and communications. The following subsections aim to highlight the key six parameters that reportedly affect the last mile connectivity using LAPs, as shown on Figure 1.1.

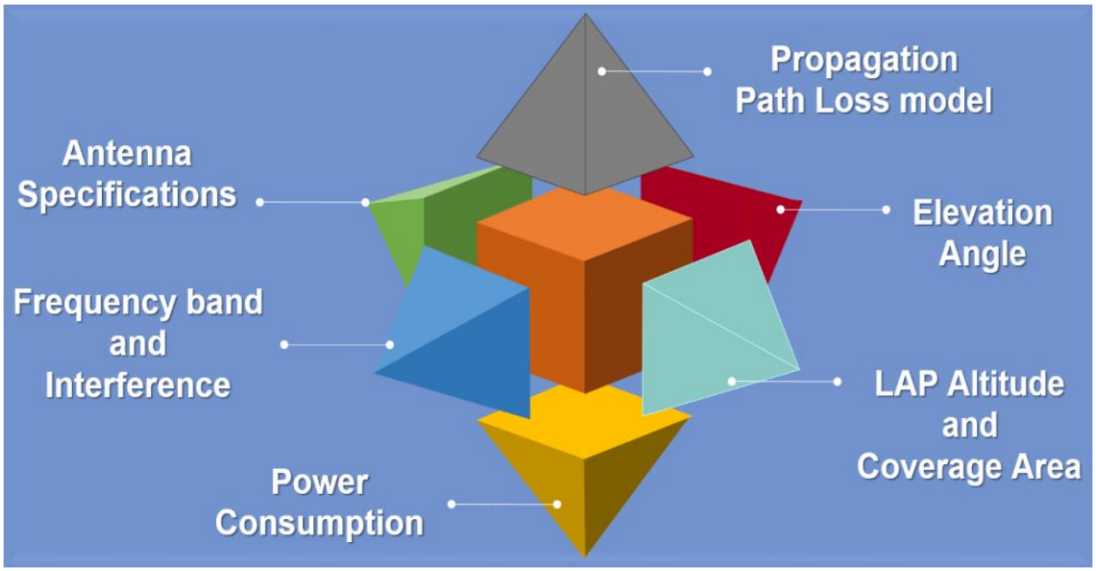

Figure 1.1: Last mile connectivity issues with using LAP

1.1.1 Propagation Path Loss Models

Propagation models predict signal attenuation or path loss as a measure of the power density of an electromagnetic wave as it propagates through space from a transmitter. Calculating path loss is useful for monitoring system performance, network planning and coverage to achieve perfect reception. Many factors may affect a signal when propagating to a maximum distance such as terrain, frequency, transmitter and receiver antenna heights [5]. Propagation models are classified into three types: Stochastic, Physical (deterministic), and Empirical (statistical). *Stochastic* models are the least accurate path loss prediction models, as they use the least information about the environment and much less processing power to generate predications. *Deterministic* models use Maxwell's equation along with reflection and diffraction laws. These models use basic physical methods. Air-To-Ground (ATG) with ray tracing exemplify deterministic models. *Empirical* models use existing equations derived from several measured experiments. Empirical and deterministic path loss models give the most accurate results. The empirical propagation models that are considered use a pre-defined set of constants and constraints for different topographies, and different geographical factors such as hills, terrain, streets, and building heights [6-8].

Researching prorogation path loss models would be helpful for Radio Frequency (RF) engineers in choosing the propagation model that is suitable for a given environment. With aerial platforms propagation path loss models, radio signals propagate through free space until reaching the complex ground ubiquitous environment, where shadowing, scattering and other effects occur by nature and/or man-made structures. Therefore, it is essential to identify the different type of environments that have been categorized by International Telecommunication Union (ITU) namely: Urban, Suburban, and Rural [2, 9]. Table 1.1 lists three environments alongside their characteristics. Besides terrain types, there are several common parameters across propagation models that effect the overall performance, such as frequency of operation, distance between transmitter and receiver (coverage radius), transmitter antenna height, receiver antenna height, as well as antenna gain, and transmission power [9, 10].

Table 1.1: ITU categorization of environments influenced by radio wave propagation

Environment	Description and propagation impairments of concern
Urban	• Typified by wide streets • Characterized by streets lined with tall buildings with several floors • Building height renders contribution to roof-top propagation unlikely • Reflections and shadowing from moving vehicles occur • Primary effects are long delays
Suburban	• Single and double storey dwellings • Roads are generally two lanes wide with cars parked along sides • Heavy to light foliage possible • Motor traffic usually light
Rural	• Small houses surrounded by large gardens • Influence of topography height • Heavy to light foliage possible • Motor traffic sometimes high

Figure 1.2 below shows the conceptual propagation model from a LAP perspective in different environments. In each environment, factors such as path loss, Received Signal Strength (RSS), coverage, and other link budget parameters may vary in response to geometrical and topography characteristics as well as user profiles.

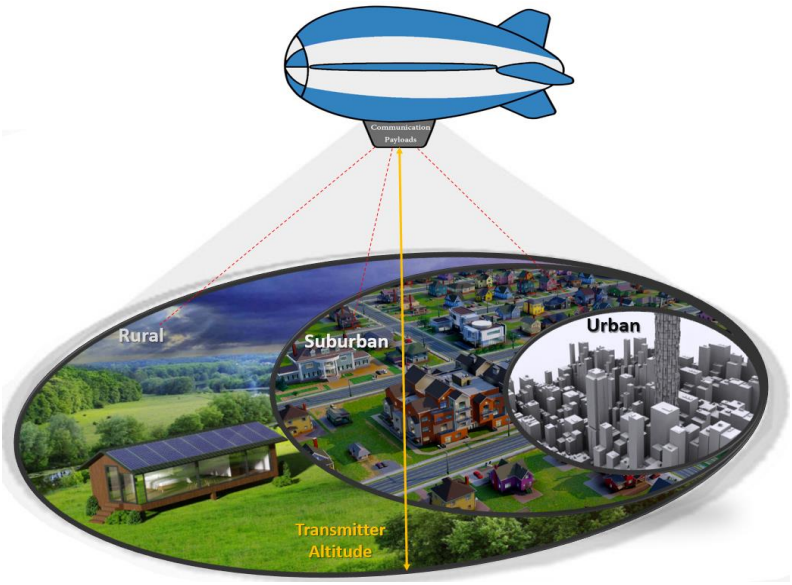

Figure 1.2: Conceptual bird's-eye-view of a LAP propagation model in different environments

The propagation models for LAPs technology reported in literature are broadly based either on empirical propagation [11-16], or ATG-based models [2, 9, 17-19, 20-26]. Researchers in [11] deploy tethered balloon technology for mobile communication purposes at altitudes of 0.1km, 0.15km and 0.2km above ground and make calculations on path loss, coverage area, and balloon height using the Hata empirical propagation model. The results show an increase in the coverage area as well as improved RSS when altitude and or transmission power increase. Path losses decrease as the altitude of the tethered balloon varies at a fixed transmission power. In [12], the Hata propagation model considers extending LAP's coverage using mutli-tethered platforms that consist of Worldwide Interoperability for Microwave Access (WiMAX) payload. The architecture is simulated at different LAP altitude using Optimised Network Engineering Tool (OPNET) modeller to monitor Quality of Service (QoS) parameters. The performance of the network implementation shows high efficiency in providing wireless communication services for large coverage areas based on the QoS parameters (delay, traffic and throughput).

In [13], a set of empirical propagation models (SUI, Hata, COST-231, free space, log-distance model, and ITU indoor and outdoor) have been chosen for evaluation based on a mixed outdoor-indoor scenario using flying LAP at less than a 0.1km altitude in an urban area. The motivation is to determine whether these models are suitable for the real-world experiment, besides developing their own propagation model for outdoor-indoor scenario. The evaluation measurements of RSS show that their

adapted log-distance model is suited for an outdoor-indoor scenario based on the root mean square error (RMSE) value of 6.05, while the selected ITU indoor model represents the second best of their measured data with an RMSE value of 6.3. The researchers also highlight some of the selected models' limitations, where the Log-distance model is too general, whilst the empirical models suffer from limited antenna heights and short transmission distance, while ITU indoor-outdoor models require advance knowledge of environment characteristics. Further investigation is set to be carried out as future work in terms of increasing the number of walls that separates an indoor receiver and a LAP.

Authors in [14] investigate the performance of Long-Term Evolution (LTE) and Wireless Fidelity (Wi-Fi) technologies in an urban Australian environment using a tethered LAP. A ray tracing ATG path loss model is simulated at many LAP altitudes, and considers four network performance indicators (path loss, outage probability, delay, and throughput). Then a comparison is made between the ray-tracing model and three empirical propagation models, namely WINNER II, Okumura-Hata and COST231-Hata at a 25m aerial platform altitude. Results show that LTE outperforms WiFi in all environments, while it is inferred that cost, coverage, and deployment time should also be considered in the selection of suitable technology for LAPs. One of the great enhancements presented by LAPs is the ability to increase the footprint area compared to terrestrial networks due to increased Line-of-Sight (LoS) probability, yet this enhancement depends on the LAP's altitude, frequency band, and antenna type.

Authors in [15] consider Friis, and WINNER D1 empirical propagation path loss models in a field experiment to increase network connectivity using aerial platform. The WiFi network measures RSS, coverage, throughput and energy efficiency in rural environment for two modes: access point (AP), and ad-hoc at very low altitudes, 10 and 25m. A comparison of the two experimental WiFi scenarios show that the overall performance of the AP mode is better than the ad-hoc mode in terms of RSS and throughput. However, the ad-hoc mode is more responsive and shows better energy efficiency, while the WINNER D1 model is more restrictive in terms of altitude, frequency band, and footprint. The authors emphasise the importance of investigating more models and approaches to extend telecommunications beyond their current conservative limits to increase wireless network connectivity, and meet the exponential growth in multimedia traffic.

An experimental channel measurement is conducted in [16] to evaluate path loss, RSS, and coverage parameters in various propagation models, namely, ATG, Okumura-Hata, COST-Hata and COST Walfish-Ikegami (COST-WI) using a tethered balloon at different altitudes of upto 0.5km. Results show that exceeding transmitter altitude which represents the balloon in this case beyond its maximum limit leads to intolerable errors especially in urban areas, whereas the Okumura-Hata model is in part accurate in rural terrains. The RSS results are in line with expectations, and decline linearly with the altitude. More LoS is connectivity achieved with higher altitudes where the impact of high rise buildings is decreased. The antenna directivity effect decreases RSS as altitude increases, due to the power density of it focused on the ground plane. For future work, the authors aim to consider a fuller range of link budget parameters to include throughputs, packet error rates and delays for higher LAP altitudes.

However, the ATG propagation model is reportedly preferred in the literature for LAP deployments. In [2, 9, 21] path loss is calculated by using a closed-form method between a LAP and terrestrial receivers based on two key ATG propagation types. The first type is a LoS condition or near-Line-of-Sight condition, the second type is No Line-of-Sight (NLoS) condition, but still receiving coverage via strong reflections and diffractions. Recommendations have been raised in [2, 9] about the significance of investigating various LAP propagation models that can identify the optimum altitude and achieve maximum coverage area in different rural or urban environments.

In [17] the ATG path loss is modelled at altitudes ranging between 0.2km to 3km in urban sites to estimate Signal-to-Interference-Noise Ratio (SINR), and expected throughput. Two aspects are considered in modelling urban environments: the geometry of buildings and the surface materials of all structures that interact with electromagnetic waves caused by the LAP transmitter and result in reflection. The Doppler effect is not considered since an assumption is made on quasi-stationary LAP. Diffraction and scattering of other potential urban geometry effects, e.g. trees, streetlights and mobile objects are not considered either. However, an assumption is made that the large-scale building geometry and its electromagnetic features dominate average path loss. The results show clear tendency towards two different propagation groups for outdoor receivers: LoS and NLoS.

In [18] authors discuss the performance of LTE aerial stations at altitudes of 1km above ground in terms of coverage and capacity for public safety networks in different channel propagation properties. The ATG path loss models two components: Free Space Path-Loss (FSPL) and excessive path-loss, which is additional loss caused by the urban environment. The results demonstrate an improvement in cell capacity and coverage in downlink with little effect caused by temperature. However, environment properties, and bandwidth affect considerably the LAP capacity, thus need more investigation.

In [20] researchers propose a unified propagation model, which is a combination of large-scale fading model, and small-scale fading model. The former model is appropriate for a flat environment, which concerns mainly free space attenuation. The latter model is appropriate for urbans or hilly environments, which mainly concerns multipath fading factors. Since ATG is a general free space model, authors in [21] indicate that when increasing a LAP altitude in order to increase coverage an opposing effect occurs, where users experience more LoS connectivity, but at a higher path loss. Urban statistics, if known in advance, may help achieve the goals of maximizing footprint and throughput whilst maintaining LoS.

Authors in [22] consider the ATG propagation path loss model in a simulation work to increase network connectivity using LAPs. The WiFi network simulation calculates RSS, coverage, in two modes: access point, and ad-hoc in dense urban and rural environments at altitudes up to 0.5km. The results show that more LAPs are required for dense urban with at a higher LAP altitude in comparison to rural areas. They argue the benefits of using directive antennas. However, the work does not include a comparative analysis of the two modes of performance. In [23] the ATG model is used to locate the Three-Dimensional (3D) LAP position in an area with different user and traffic profiles using a Particle Swarm Optimisation (PSO) algorithm. The work aims to solve the trade-off between increasing LAP's altitude and/or transmit power and path loss besides minimizing the number of LAP deployed. Results confirm that acceptable performance can be obtained when the LAP altitude floats between an upper and a lower bound in urban environments to guarantee large coverage and capacity, and minimize interference to the users that are not served by their LAP.

In [26] a two-ray air to air (ATA) and an ATG propagation model is considered to enable cost-effective and broadband connectivity to mariners in remote oceans using tethered LAPs. Standard access technologies such as General Packet Radio Service (GPRS), Universal Mobile Telecommunications Service (UMTS), LTE and Wi-Fi are used at altitudes of 0.12km and transmission power of 30dBm, whereas underwater communications are mainly achieved using acoustic links. Results show the ability of transmitting data from these mariners to shore via tethered LAPs to range of upto 100km, and at a throughput of over 2Mbit/s for ATA model, whilst the ATG model achieves ranges of upto 50km and a throughput of over 1Mbit/s using low frequency bands. Results confirm that higher transmission power and/or lower frequency lead to wider connectivity.

The propagation path loss that can be considered for LAPs is broader in comparison to either satellites or terrestrial systems, despite the advantages of satellites systems, e.g. global coverage, last-mile LoS connectivity for urban and rural environments, which offer flexible and cost-effective deployment of Ad Hoc networks for disaster relief and/or short term large scale events. Satellites use a limited range of propagation models, mainly based on free space ATG propagation models. In addition to this, path loss and signal delay are relatively high due to the large distance, especially for Geostationary Earth Orbit (GEO) satellites. When these are located at around 36,000km above ground, latency stands at 250ms. The number is quite small, but it causes an echo over telephone connections and low QoS for Transmission Control Protocol (TCP) connectivity. The signal delay and path loss of Medium Earth Orbit (MEO), Low Earth Orbit (LEO) satellites are much less than GEOs, which may serve the satellites characteristics. In contrast, the propagation path loss models considered and developed for terrestrial system are mainly stochastic or empirical propagation models. Despite, the wireless coverage ranges up to a certain limit and meets rapid demands for wireless service from subscribers in different geographical locations. Yet, multipath, limited LoS connectivity, and limited coverage area are unresolved issues [27, 28, 47, 74].

1.1.2 Elevation Angle

It is a necessary condition for ionospheric communication signals to propagate in a correct angle to enhance last mile connectivity. There are number of reasons for that:

The Earth curvature when calculating LoS path loss, the coverage distance, and terrain morphology. At lower elevation angles, path loss increases due to distance increases, whereas at high elevation angles more LoS connectivity is achieved but less footprint, thus it is a trade-off. Space-based wireless communication systems take into consideration the elevation angle in their channel FSPL calculation. Nevertheless, there is no consideration of the elevation angle in propagation models for terrestrial wireless communications, possibly due to a low transmitter altitude. In aerial platform technology, path loss in a propagation model depends on the elevation angle, aiming to achieve LoS most of the time [2, 9].

Authors of [29, 30] and ITU [31] argue that the elevation angle in urban environments can range between 30° and 90°, 15° and 30° in suburban, and 5° and 15°in rural. In [32] the authors are suggesting that the angle range of 30° to 90° is a realistic elevation range for near space platforms in dense urban areas. The proposed model in [17] sets 15° as the minimum elevation angle in urban, since NLoS occurs as a result of the shadowing effect and reflection of signals from interfering obstacles which in turn leads to an additional path loss especially with increasing distance [33]. The authors in [29] argue that a minimum elevation angle range of 20° to 30° is appropriate in urban areas.

In [34] a deployment plan of an aerial platform is considered to cover the entire country of Japan, where the lowest elevation angle is assumed to be 10° for all environments. Similarly, in [35] an elevation angle of 10° is assumed to provide smooth coverage for the whole of the United Kingdom with constellation of multiple interconnected aerial platforms. Authors in [36] assume an elevation angle range of 5° to 20° for an integrated wireless topology of aerial platforms and satellites for wireless sensor communications.

1.1.3 LAP Altitude and Coverage Area

Several wireless network topologies of aerial platforms that provide footprint coverage at different altitudes are reported in the literature: standalone, integrated terrestrial-aerial, and integrated terrestrial-aerial-satellite. Adopting any topology depends on the QoS requirements, type of application, payload weight, and power consumption, each with its own advantages and challenges [37-39]. The standalone topology resembles a star configuration and acts as the main hub to provide narrow/broadband wireless access within a coverage area for both stationary and mobile terminals on the ground.

Users within such a topology can communicate with each other, as well as with users in other networks using gateways on the ground. The capacity in each cell depends on the antenna spot beam design, bandwidth and transmission power [30, 31], [37-40]. This topology can serve the needs of different types of users ranging from long-term to short-term users. RSS is affected by distance and/or shadowing as signals experience reflection from interfering obstacles, as Figure 1.3 shows.

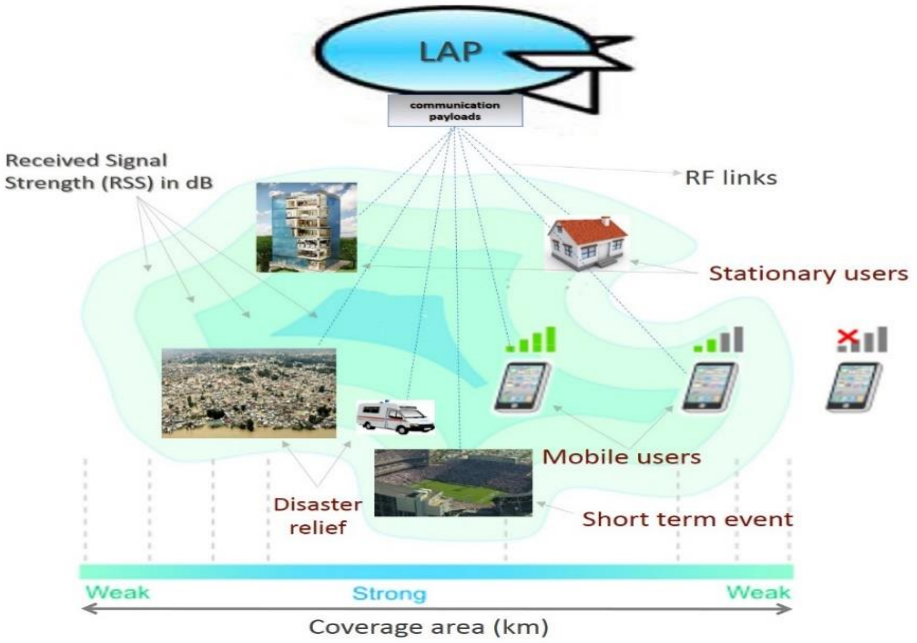

Figure 1.3: A standalone aerial platform topology

An integrated topology of aerial platforms and terrestrial systems offers many advantages, ranging from an increase in capacity demand, to more cellular coverage area for Fourth Generation (4G) and other networks, to endowing terrestrial networks with wireless communication services. Platforms can deliver an effective backhaul for remote areas with low population density, such as islands, mountains and deserts, at a competitive cost of deployment. Aerial platforms can include one or more macro cells to serve stationary/mobile users with high data rates as they use a higher frequency band. Aerial platforms may be linked to terrestrial networks via a gateway in those cases where the integration model uses similar cellular structure for both the aerial platforms and the terrestrial base stations. Designing this topology depends on the applications supported since some challenges that normally need to be considered include handover, interference, resource allocation, cell structures, and dynamic channel assignment [30, 31, 37-40].

The most complex configuration is the heterogeneous wireless topology, which can be achieved by deploying a multilayer approach that integrates a terrestrial system with a space system that includes both aerial platforms and satellites as depicted on Figure 1.4. This architecture consists of various layers whose aim is to support different applications and services. Each of the architecture's layers has different hardware and software capabilities to achieve the integration, for which it is necessary to take into consideration the available bandwidth, coverage, frequency ranges, uplink and downlink connectivity, and interface between terrestrial, aerial, and satellites systems. Communication between the integrated system can either be optical or Radio Frequency (RF) [30, 31, 37-40].

This heterogeneous topology includes an aerial platform network that is connected by inter-platform links. Some ground stations are linked by aerial platforms using both backhaul links, as well as hosting gateways to external networks, intermediate nodes are connected to the local wired or wireless and aerial platform systems, and satellite links use backhaul links towards aerial platforms and ground stations. This heterogeneous architecture may serve the needs of different types of usage that ranges from short-term to long-term, deliver seamless services over heterogeneous networks, and offer a high QoS for global connectivity in future communication systems and services [30, 37-40], [41-43].

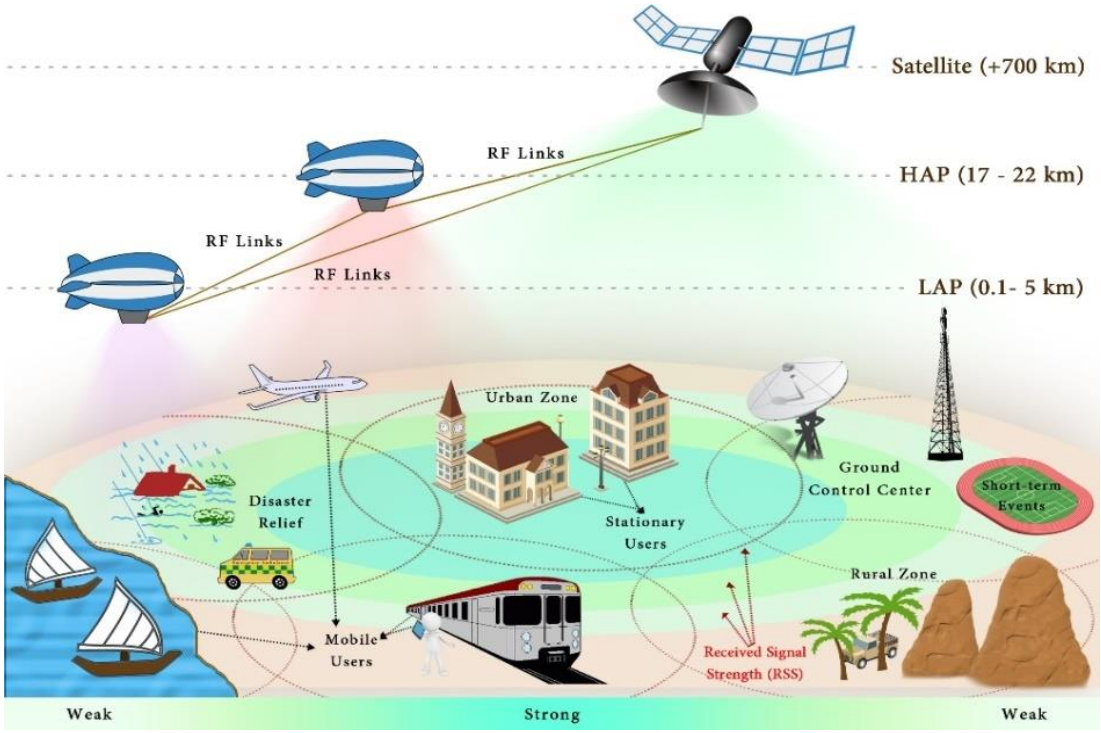

Figure 1.4: A heterogeneous topology of Terrestrial, LAP, HAP, and Satellite systems

As part of their continuous effort to bridge the coverage gap in wireless communication, researchers in [2, 9, 12, 24, 44] strive to maximise footprint coverage, by introducing an optimizing technique that identifies an optimum LAP altitude as a function of two parameters: the maximum allowable path loss (MAPL) and the statistical parameters of urban environments, which are standardised by the ITU. These ITU parameters are the percentage of a build-up area to the total land area, the number of buildings per unit area, and the statistical distribution of building heights according to Rayleigh's probability density function and LoS probability. The results illustrate that the service threshold is the total path loss between the LAP and a receiver and when this path loss exceeds the threshold the link is considered to have failed. This threshold defines MAPL, which in turn translates as the coverage zone for ground receivers.

A method in [9] introduces a way of selecting the optimum LAP's altitude in urban environments. Simulation results show that by checking the maximum service availability ratio amongst several simulations of different LAP altitudes, an optimum altitude is achieved at around 1.65km. This altitude is primarily based on the average building height, transmission power and on the target SINR. Furthermore, it has been observed that two factors that have an influence on getting better wireless service at the optimal altitude are coverage area and path loss. Both the coverage area and path loss increase as the LAP altitude rises from ground upto 1.65km above ground.

Researchers in [45-47] highlight the altitudes that suite aerial platforms as a result of the atmospheric effect. Troposphere and Stratosphere are two of the Earth's atmospheric distinct layers and are classified based on temperature, atmospheric pressure, air density, wind speed, and altitudes as Figure 1.5 shows. LAPs can work upto a 5km altitude whereas HAPs can reach upto 21km above ground. At these altitudes, several wireless communication services can be provided with lower transmission power compared to satellites. At 1km and 20km altitudes, the wind speed measures only a few m/s and the pressure decline to reach approximately 1hPa. At the stratosphere layer, HAP platforms are securely away from commercial air-traffic heights, and at an optimum height in relation to wind turbulence. Tethered LAPs can be deployed in the Troposphere layer using two tethers, one to tether the platform to the ground, the other to provide a communication link, e.g. optical, and/or power.

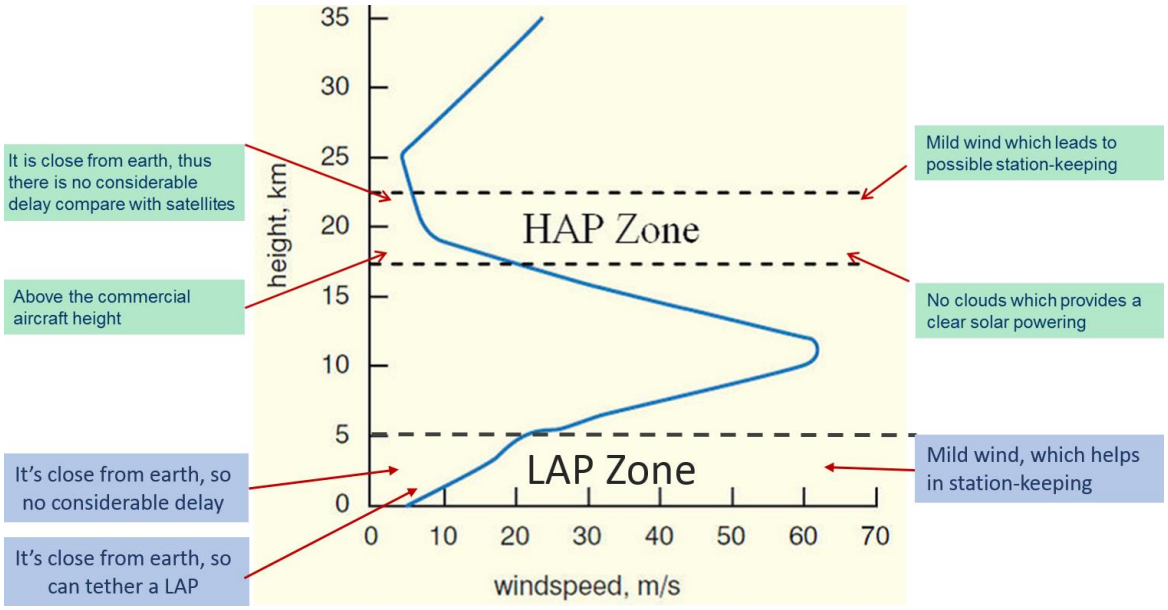

Figure 1.5: Wind velocity with respect to altitude [40]

Authors in [21] propose a closed-formula that aims to maximize the probability of LAP coverage, as well as identifying the optimum altitude and transmission power that could increase coverage footprint and throughput. Simulation results show high similarity in performance between the analytical and simulation results. However, knowing the ITU-R urban statistics is necessary. Future work suggests that experimental verification is considered for emergency services in Melbourne. In [12] an empirical propagation model is considered to extend LAP's coverage using mutli-tethered platforms that consist of a WiMAX payload. The performance of the network implementation shows efficiency in providing wireless communication services for large coverage areas upto 15km at 0.2km altitude using mutli-tethered LAPs.

In [22] an ATG propagation path loss model is considered in a simulation experiment to increase network connectivity using LAPs. The simulation of a WiFi network calculates RSS and coverage in both AP and ad-hoc modes in dense urban and rural environments. The results show that at a 0.5km LAP altitude, 2.4GHz frequency band, and a transmission power of 35dBm, it achieves a maximum urban radius of 6km, with a path loss of 120.5dB and an RSS of -80dBm. Additional LAPs may be necessary for dense urbans at a higher LAP altitude in comparison to rural areas, where a minimum LAP altitude is set at around 0.15km with directive antennas.

The evaluation in [4] is based on measured Received Signal Level (RSL) and Signal-to-Noise Ratio (SNR) using WiFi and WiMAX technologies onboard a LAP. At an altitude of 0.44km above ground, the balloon's coverage area is 47.39km^2 with a fixed 54Mb/s downlink throughput but as coverage increases to 72km^2 this results in fluctuating throughput. The WiFi gives a satisfactory performance for Internet access and achieves a LoS easily for rural users, but with challenging effects for urban users. The WiMAX provides more capacity, less interference, and has better coverage with NLoS, where objects block signals. The objective in [48] is to design an aerostat to provide wireless communications in remote areas. It is claimed that the rural residents in a large number of developing countries are still devoid of Internet connectivity, for reasons such as lack of infrastructure and high installation costs associated with terrestrial networks. The design has been set up to launch an aerostat with a wireless communication payload at an altitude of 0.2-0.25km above ground. Last-mile wireless connectivity is achieved using an omni-directional antenna and the WiFi 802.11b standard for a coverage radius of around 10km and data rates as high as 11Mbps.

Three experimental analyses of wireless temporary networks deployed by LAPs have been conducted in [49]. The experiments have been performed with hot-air balloons at altitudes ranging between 0.6km and 1.1km and equipped with low cost off-the-shelf communications equipment such as Terrestrial Trunked Radio (TETRA), WiFi and WiMAX, where RSS and throughput have been measured experimentally in a real environment. The coverage range in TETRA system is determined by the transmitted power, the receiver sensitivity and by the fade margin. The result show unstable coverage, and low throughput. The WiFi 2.4GHz band gives a longer range compared to the 5GHz band, but the interference possibility at 2.4 GHz remains high, as most users use this band. Transmission power and receiver sensitivity limit the range of WiFi. The unlicensed band WiFi suffers from the interference issue, whereas using WiMAX evades interference, as it uses a different licenced frequency band at 3.5GHz. The overall coverage is only few kilometres, however, the throughput achieved is high, and it could be improved by increasing the output power and/or controlling the beam direction of the balloon. Thus, directive smart antenna is suggested for future work.

In [42] an algorithm is proposed for dynamic utilization of a LAP in heterogeneous networks at an altitude of 1km. Results illustrate enhancement in QoS by balancing loads during high traffic. The coverage area changes rapidly based on traffic demands

and user density, which might serve short-term and disaster situations, but not long-term ones. Authors in [15] consider two propagation path loss models, free space ATG and empirical WINNER D1, in a field experiment to increase network connectivity using aerial platforms. The WiFi network measures RSS, coverage, throughput and energy efficiency in both AP and ad-hoc modes in a rural environment and at very low altitudes. A comparison between the two experimental WiFi scenarios shows that the overall coverage can be up to 7 km in diameter in open areas where there is clear trade-off between coverage and throughput.

Authors in [3] present an algorithm that calculates the optimal placement and the optimal coverage radius to cover an area using different station types: Portable Terrestrial Stations (PTS), and LAP systems equipped with LTE. The results confirm the advantage of LAPs in terms of higher bandwidth utilisation, wider coverage areas, and the total number of base stations required to cover a desired area which is generally lower than PTS. However, an increasing number of LAPs in a specific area can cause interference with terrestrial stations, therefore, it is recommended to locate LAPs on the boundaries over the disaster area, so that interference is reduced while coverage gaps are covered effectively.

Authors in [50] argue that the cost-effective way to provide Wi-Fi in rural areas is by using tethered aerostats at 0.1km above ground, which can be easily relocated at any time anywhere. Tethered aerostats can be lifted vertically upward and omni-directional antennas can be installed on a balloon to obtain an alignment requirement to cover the distance between user and access point up to 7.0km. The total cost of this re-locatable tethered balloon is found to be approximately 1/2 of that of a terrestrial based station.

Results in [3] endorse the effectiveness of LAPs in comparison to PTS for first responders in Hurricane Katrina in the USA. The efficiencies achieved include high bandwidth use, wide coverage area, LoS connectivity, as well as low cost and signal latency, portability and adaptability [4, 51, 52]. Flexibility is revealed in [9, 44] in terms of providing dynamic coverage especially for unexpected events, e.g. emergency, or short-term events, e.g. sport, by connecting with satellites via backhaul links in case of transmission failure in order to maintain global connectivity. Authors in [43, 50, 52-55] discuss rapid network connectivity communication via LAPs to provide Internet services in rural areas, or wireless sensor deployment for monitoring and surveillance, security applications, and high-resolution aerial imaging.

Providing wireless communications services in isolated areas with harsh terrains could be economically infeasible or physically impossible even with such a huge number of BSs. There could be several reasons for this, including LoS connectivity with other towers, supply of power to towers, operation and maintenance, cost and number of users even with a larger number of terrestrial BSs that have been deployed around the world, predicted to be 11.2 million by 2020 and almost 2.4 times in comparison to 2013. ITU in 2016, however, has indicated that still over 3 billion people, which is nearly half of the world's population, are not using the Internet for reasons of lack of infrastructure in rural and other difficult terrains [56, 57]. Another challenge that faces terrestrial networks is that they are extremely vulnerable to man-made and natural disasters [45, 58]. According to the ITU when a disaster occurs, the terrestrial telecommunications infrastructure usually fails due to the physical destruction of a network, disruption in the supporting network infrastructure and network congestion [59]. Whilst satellites can offer coverage of large area for long-term or short-term services, they require high gain antennas and coverage footprint has no regard for geographical or political boundaries, in addition to be an expensive system to manufacture and launch.

1.1.4 Power Consumption

Unmanned platforms are powered mostly by renewable energy from solar power, either directly using photovoltaic or indirectly using concentrated solar power. In [24, 60, 61] authors highlight powering communication equipment with energy to deliver Internet access and various wireless communication services during special events and in the aftermath of an emergency, as one of the LAP design and implementation challenges and open research issue. Thus, it is recommended to choose carefully the access technology to be installed on-board LAPs taking into account consumption by batteries or solar panels, in order to optimise the performance properly between LAP altitude and coverage area, and indeed path loss. The design in [62] places aerial platforms at a 0.3km altitude using LTE technology to support reliable communications for emergency or temporary events. At such an altitude, RF signals can overcome most ground-level obstacles (e.g. trees, buildings, streetlights), which enables most users to enjoy a LOS connectivity to the LAP, besides increasing an already large coverage area. One limitation observed is that increasing the LAP altitude increases the coverage range, which leads to an increase in power consumption.

In a comprehensive survey, [43] covers a significant open issue pertaining to the power consumption in aerial platforms, whereby it classifies power consumption as two main sources: power consumed by all on-board components and power consumed by the communication links to the terrestrial receivers and other aerial platforms using RF or optical inter-platform links. Thus, the authors indicate that minimizing power consumption can be achieved by high link quality and less network congestion and thus less energy is needed to reconnect to the network, as the transmitted power depends on the distance between the transmitter and the receiver.

Power consumption is also an open challenge for other wireless systems. Satellites in MEO and LEO orbits are moving around the world to provide a global coverage, thus de-orbiting within their positions, atmospheric drag, complex handover process, solar radiation pressure, and Earth's gravitational pull, often lead to a shorter satellite lifetime and consumption of high energy. Providing power supply to terrestrial BSs in isolated areas with harsh terrains could be economically infeasible or physically impossible, especially where researchers indicate that BSs consume approximately 80% of a cellular system's total energy [56]. Much effort has been strived by researchers on green innovation renewable energy not only for providing energy sources to BSs in isolated areas or difficult geographical terrains, but also for saving power consumption. Yet, this technology needs more time to be a cost-effective option for developing countries [27, 28, 47, 74].

Therefore, tackling the power consumption issue has received varied considerations, whereby some researchers are considering its hardware nature. For instance, authors in [9, 11] report that an increase in transmission power leads to an increase in the coverage area as well as improved RSS. However, that requires high power supply on board, which some LAPs cannot offer. Hence, others in [51, 63] propose providing a power supply over optical links to a tethered LAP via cables to minimize the weight on board and achieve the high capacity and wide coverage range. They claim that solar panels mounted on the top of the platform's envelope might not be sufficient for station-keeping processors, telecommunications, and fuel cell charges for flight at night and during eclipses [64]. Further hardware consideration involves using high-flexible sheets "Thin film PV panels" to cover the upper surfaces of the platform. Propellers are linked to small motors and can also be used to generate energy for the platform in flight. In [64] a commercially available, light-weight flexible amorphous silicon solar

panel with a peak power output of 64W is examined. In [65] lithium/polymer-based batteries are suggested.

In contrast, some researchers have looked at the issue from a software angle using some optimisation techniques and improving performance of many parameters that do not require an increase in transmission power. For instance, a directive lightweight antenna with a fixed beam is considered in [66] to improve system capacity on aerial platforms, and most importantly reduce energy consumption since the energy is focused only in a desired direction. However, it is inferred that complex smart antennas either steered or switched beam could provide better results, but it is difficult to mount on LAPs. At an altitude of 2km above ground, a LAP that is using an LTE system for emergency situations is proposed in [19]. A power-efficient radio resource allocation mechanism is proposed using game theory to test both Uplinks (ULs) and Downlinks (DLs). Simulation results reveal that the algorithm gives a trade-off between the feasible throughput and the power consumption to guarantee fairness amongst users.

Power consumption at the receiver ends have been considered widely from a wireless sensor network (WSN) performance prospective, and linked directly with transmission link characteristics. Thus, many approaches have been considered to improve QoS results, which in turn enhance power consumption. In [67] a Bit Error Rate (BER) power scheduling scheme in WSN is proposed to avoid retransmitting data. Simulation results show that the total energy consumption is reduced in the proposed model. In [68] authors introduce two ways to optimise power energy in WSN: modulation selection that depends on distance and link selection of the average BER at high SNR under Rayleigh's fading channel. Researchers in [69] consider packet retransmission to minimize energy consumption for WSN over an additive white Gaussian noise (AWGN) channel. Their optimisation aims to find an optimum target BER probability and packet length at different transmission distances. They give the results of two transmission distance scenarios: short and long, over which the former uses bandwidth efficient modulation, large packets, and low target of BER probability but the latter uses energy efficient modulation, short packets, and high target of BER probability.

[70] highlights a direct communication link design between WSN and space-based communications using a signal transmission Collaborative Beamforming (CB) technique. The link budget results show that the number of sensor nodes required for a direct link is reduced with a low satellites altitude due to reduction in path losses,

which in turn improves power consumption and QoS. Multiple-Input Multiple-Output, (MIMO) antennas could improve results, however, it needs further consideration in design to compromise power consumption. In [36] the authors cover performance analysis on WSN integration between aerial platforms and satellites. Results indicate that an aerial platform's wireless sensors are preferred as their shortest path loss compares favourably to satellites, and their LoS connectivity compares favourably to terrestrial systems, which contributes in enhancing BER and improving power consumption from ground sensors.

A dynamic algorithm is proposed in [25] using an ATG channel model in disaster scenarios to optimise the position of a LAP and minimize path loss which in turns lead to improved RSS and reduced power consumption. This is being achieved by moving the LAP position between multiple points within a coverage area. Simulation results show a 10dB power consumption gain per user saved in case of applying Poisson distribution. In [71] researchers investigate the performance of WSN via aerial platforms for various applications. Their simulation considers the deployment of sensors in both ad-hoc and cluster scenarios. Results shows that it minimises path loss that in turn could lead to minimising power consumption at the receiver's end.

1.1.5 Operational Frequency and Interference

The frequency band is one of many factors that affect signal propagation. Other factors include transmitter and receiver antenna heights and antenna gains. Authors in [13, 26, 66] argue that the design of propagation models is experimentally driven, hence, the parameters chosen often vary widely but operational frequency seems to be a common choice in consideration of terrain morphology, interference avoidance, and RSS and throughput enhancement. Frequency allocation for terrestrial wireless systems is limited at low frequency bands upto a few GHz, which might decrease bandwidth. Therefore, additional BSs may be needed to meet the exponential growth in multimedia data traffic, which in turn may cause interference.

In contrast, higher frequency bands assigned for space-based communication systems, e.g. 28 to 47 GHz, offer access to wider bandwidths, yet they are more vulnerable to signal degradation, as radio signals get absorbed by atmospheric rain, snow or ice (rain fade) [47, 72-75]. A comprehensive survey in [43] reports many relevant challenges, and highlights key future perspectives. The review reports on the

added-value of IoT services using WiFi, WiMAX, and LTE technologies. However, their selection depends on application types and the operational environment.

The ITU's International Mobile Telecommunications-Advanced (IMT-Advanced) standard for 4G offers access to various telecommunication services and supports mobile applications for heterogeneous wireless environments that offer various frequency bands that can support the performance and high QoS requirements for multimedia applications, and high data rates to user and service requirements. The ITU has long been considering technologies that meet the criteria of the standard: LTE, WiMAX, and WiFi as Figure 1.6 shows [76-82].

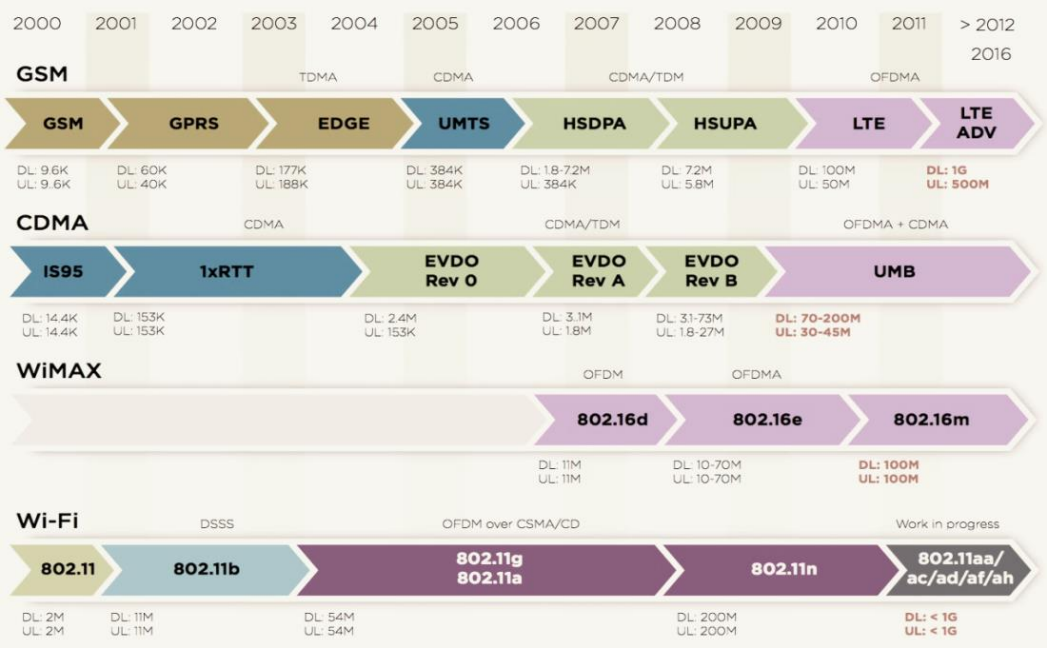

Figure 1.6: Progress evolution paths for LTE, WiMAX, and WiFi technologies

Both WiMAX and LTE assume an all-IP network approach, use Orthogonal Frequency-Division Multiple Access (OFDMA) in the DL, support Time-Division Duplex (TDD) and Frequency-Division Duplex (FDD), support different bandwidths, use both smart antenna and MIMO technology, provide QoS support, use similar modulation techniques such as Quadrature Phase Shift Keying (QPSK) and Quadrature amplitude modulation (QAM) 16QAM, and 64QAM in both the DL and UL [76-82]. However, they are quite different in their evolution, frequency bands, industry support, and deployment models. The peak data rate in LTE-A (release 12 and 13) is 1Gb/s in DL and 500Mb/s in UL with a coverage range of up to100 km. WiMAX release 2 can offer peak data rates of 350Mb/s in the DL, and 200 Mb/s in the UL with a coverage range of up to 50 km [76-82].

The existing unlicensed WiFi 802.11aa frequency bands are mainly 2.4 GHz and 5GHz. However, 802.11ad runs on 60GHz band and offers 10 times increase in throughput per stream, and a high speed in data transfer with MIMO support. This emerging technology “Gigabit WiFi” (WiGiG) whose speeds can reach 1Gbit/s, is by far the fastest WiFi version to date. Further, the next generation of 802.11ah standard known as “WiFi HaLow”, which is the new modification for longer forms of WiFi communication is set to reach several kilometres. This technology would support long distance IoT communications and business or industrial applications [83, 84].

According to a CISCO study the monthly global mobile data traffic is estimated to grow at around 24.3 exabytes by 2019, which is three times the current traffic, as Figure 1.7 illustrates [85]. Therefore, the Third Generation Partnership Project (3GPP) has introduced new technologies, e.g. LTE-A and WiMAX, with MIMO as a response to enhance capacity, mitigate interferences, extend coverage, and provide high throughput [86]. Moreover, Fifth Generation (5G) is widely anticipated to offer a data rate which could reach up to 10Gb/s. Thus, frequency band harmonization is essential to accommodate more users, and respond to the global mobile data demands. However, avoiding harmful interference between receivers is a challenge in need of consideration [85].

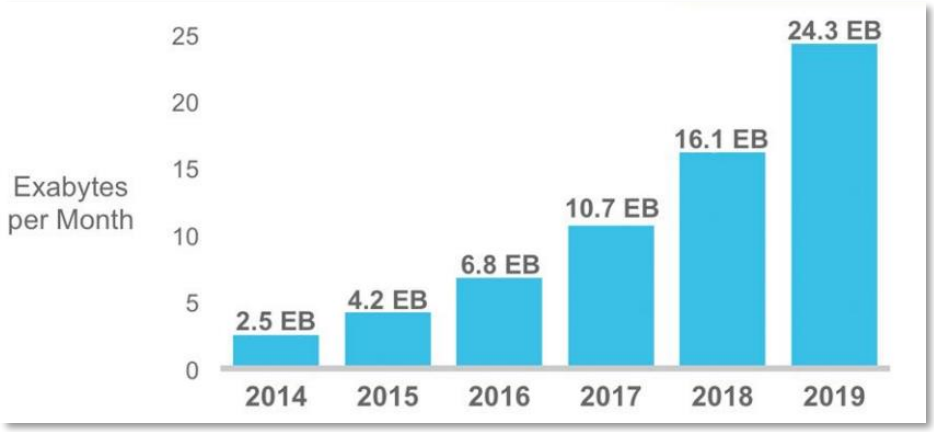

Figure 1.7: Cisco forecasts on monthly global mobile data traffic upto 2019

In aerial platform technology, WiFi [4, 14, 15, 22, 26, 49, 87, 88], WiMAX [12, 26, 49, 87] and LTE [4, 14, 18, 19, 24, 26, 62, 87, 88] have been considered widely in the literature to serve various applications for better coverage whether in LoS or NLoS, increased capacity and less interference, however, opinions and decisions vary. For instance, Aerial Base Stations with Opportunistic Links for Unexpected & Temporary

Events (ABSOLUTE) is one of the most important LAP project worldwide that deploy LTE in their specifications. Google balloon projects base their design and telecommunications payloads on LTE technology to provide Internet access globally. However, authors in [12, 54, 89, 90] emphasize the advantages of WiMAX over LTE-A in supporting military operations in disaster relief environments where users' requirements change rapidly. WiFi is still a candidate in LAP deployment to increase connectivity for short distances. However, the main limitations to date are vulnerability to interference as it is unlicensed, and it does not serve longer distances. No considerations have been made yet in terms of WiGiG technology for any communication systems including LAPs, which is an open future research topic.

Authors in [88] investigate the challenges of existing wireless technologies, i.e WiMAX, WiFi, LTE, and ZigBee for enabling aerial drone platforms in Alpine environments, to support short term winter events and provide a viable solution in emergency and rescue situations in a hostile environment. Results support WiMAX as a suitable wireless technology for drone communications for number of reasons: Low interference, flexibility in installation, wide coverage area, high QoS and throughput. In [49] experimental results show that the unlicensed band WiFi suffers interference, whilst using WiMAX evades interference as a result of using different frequency bands. To note, some propagation models used low frequency band to allow signals for more distance, but that leads to low bandwidth and throughput obtained. Thus, it is trad-off that needs to be carefully considered.

In [91] authors focus on evaluating the coverage performance of a mobile WiMAX network on aerial platforms, by measuring various channel conditions including throughput, packet error rates, Round Trip Time (RTT) and jitter for different modulation and coding schemes. Results indicate that mobile WiMAX is auspicious due to its low RTT and jitter combined with low packet error rates. Furthermore, it has the advantage of a rapid setup of dedicated cells without a complex infrastructure, which is an attractive solution for security and emergency communications. Future work aims to validate this work experimentally using terrestrial mobile WiMAX BSs and aerial platform equipped with mobile WiMAX.

The survey in [43] claims that traditional Wi-Fi signals can propagates up to 0.15km, however, the propagation distance can be increased up to 25km by deploying the components in an aerial platform with high transmitting power and more LoS connectivity using directional antennas. It is reported that WiFi payloads on aerial platforms have a high feasibility of establishing multimedia communications with terrestrial users.

In [23] an ATG model is considered to locate the 3D position of a LAP in an area with different user and traffic profiles using a PSO algorithm. This work addresses the compromise between increasing LAP's altitude and transmission power on the one hand and the path loss and interference on the other hand. Results confirm that to minimise interference in areas with higher user and traffic density, LAPs should be sited in lower altitudes to mitigate interference for users served by other LAPs.

In [92] a novel self-organized method is considered based on gradient search to increase the LAP network capacity. The proposed method indicates that a LAP's location can be changed if needed in space and time to provide better capacity, which may reduce the number of LAPs required as well as minimizing cost. Results suggest that fine tuning LAP altitudes and transmission power can minimize interference and maximize QoS. However, the method requires updated local information about users and traffic profiles. Consideration has been given to the antenna type that affects the performance of propagation models since omni-directional antennas consume more energy, and limit frequency reuse, thus increasing interference and reducing capacity. Considering the use of either smart or MIMO antenna technology to improve performance is being suggested in the literature [93-96].

1.1.6 Antenna Specifications

Typical antennas, whether directional or omni-directional are large in size, consume more power, increase interference, and offer small coverage [72, 97]. In contrast, aerial platforms require small-sized antennas, consuming less power, whilst maintaining a high-performance level. The effect of MIMO and smart antennas on near space solar-powered platform performance and capacity is discussed in [38, 65, 93], [98-100], where it is being argued that the antenna gain need to be optimised, otherwise end-users may experience weak radio across distances running into several miles. The advantages of deploying these antennas include maximizing capacity, improving QoS,

extending coverage range, reducing transmission power and relaxing battery requirements, reducing radio signal fading as a result of diversity gain, and maximizing link budget as a result of smooth user tracking with main lobes and interference nulls.

The first type of smart antennas is switched-beam, which has a finite number of fixed predefined patterns or hybrid approaches. The second type is adaptive array, which has an infinite number of patterns which can be adjusted in real time. An adaptive array can also offer optimum gain though simultaneously identifying and distinguishing between desired signals and multi-paths thus minimizing the effect of interfering signals. MIMO antenna technology is very similar to smart antenna technology and is one of the most efficient leading innovations in wireless systems for maximum capacity, improved QoS and coverage range. Alamouti's scheme makes MIMO a subset or an extension of adaptive smart antennas [37,38, 65, 93], [98-100].

A report from Nortel Networks Corporation [101] shows that MIMO may increase capacity, yield high predictable performance, have the ability of upgrading via additional sector antennas, work well in all environments, offer mode switching to deliver users the best experience and performance stability in a smooth handover process. In the past few years operators such as Airspan, Netronics, Nokia, Siemens, and Huawei have included MIMO antennas in their network designs [98-104]. Furthermore, instead of combating multipath signals, MIMO attains spatial multiplexing which aims to increase throughput without increasing the required bandwidth by exploiting multipath [95,96].

The antenna type reported in [11] is directional, whereas in [2, 17, 18] an isotropic omni-directional antenna is used. In [4] a consideration of smart light-weight antennas requirements are emphasised that guarantee the best of wireless communication operations in antagonistic radio propagation environments using LAPs technology. In [9] an electronically switched beam antenna is suggested to steer the RF power to and from a certain direction, which in turn may mitigate interference on LAP coverage zones. In [105] a three-dimensional MIMO antenna is considered for an ATG propagation model in LAP location assistance. The model aims to exploit angles of departure (AoDs) of receivers, and solve the relation between a LAP's altitude and number of RF chains. Simulation results show that the proposed approach outperforms existing approaches, i.e. matching filter and basis expansion precoding, in addition to high accuracy AoD information when number of antennas increases.

Researchers in [87] investigate the performance of 4G LTE, and WiFi multimode base stations are installed on aerial stations to deliver coverage for first responders in emergency situations. Single Input Single Output (SISO) directional antennas are utilized in aerial platforms to provide either macrocell, microcell or picocell coverage. The impact of platform altitude and mobility on channel stability has been studied to provide more information about resilience and scalability. Results show that the performance of different link segments whether LTE or WiFi at varying aerial-station altitudes of 0.5km to 2km is quite high. However, packet delay increases as the number of parallel services increase. These issues are claimed to be optimised in future work, with special consideration for MIMO antennas.

In [26] it is proposed that MIMO antennas could increase connectivity to transmit data from underwater marines to shore via tethered LAP. In [24] a directional Helical lightweight antenna in a LTE-based tethered LAP is considered that aims to implement the ABSOLUTE LAP project to provide Internet access during or after emergency situations. The MIMO functionality is utilised in this trial using spatial multiplexing techniques to enhance the throughput of the system. The authors in [61] recommend that two directive antennas can be implemented to obtain higher gain connectivity via tethered LAP, which gives similar performance as a MIMO antenna. A directive lightweight antenna with a fixed beam is considered in [66] to improve system capacity on aerial platforms, and reduce energy consumption since the energy is focused only in a desired direction. It is further inferred that selecting frequency band and controlling antenna power can greatly help in minimizing interference. Additionally, smart antennas either steered or switched beam could provide better results [9, 49, 66].

The study in [106] considers antenna radiation pattern diversity for Wi-Fi receivers using an autonomous aerial robot. Experimental results show that combining different antenna radiation patterns leads to improvement in communications between the aerial robot and receivers. However, this combination of different radiation patterns requires more transmission power to recompense the losses, which subsequently leads to an increase of interference for near Wi-Fi users. Adaptive antenna and MIMO functionality of antenna gain diversity could enhance accuracy and may give better results.

1.2 LAP Evolution Worldwide

There have been large projects and trials on aerial platform technology around the globe. From Europe (e.g. EU HeliNet, European COST Action 297, British StratSat, ABSOLUTE), to North America (e.g. Sky stations, Lockheed Martin), Asia (e.g. Japanese Skynet, Saudi PSATRI, Korean ETRI), and international cooperation across many countries (e.g. CAPANINA, ABSOLUTE, Google's Loon). This subsection summarizes globally recognized projects and trials in industry [107-122].

1.2.1 The EU CAPANINA Project

This 3-year project with 13 global partner project which started in 2004 was funded by the European union (EU). The project aims to develop an affordable wireless communication services to a number of users with data rates of up to 120Mbps. The CAPANINA project, which trialled in 2004 for the first time in the UK used a low altitude tethered balloon at an altitude of 300m. A second trial was conducted in Sweden in 2005 using a stratospheric balloon at a 25km altitude. A third trial was carried out in 2007 in the U.S. by National Aeronautics and Space Administration (NASA). A stratospheric balloon provided broadband services with both Free Space Optics (FSOs) link at 1.25Gb/s, and an RF link at 11Mb/s constrained by the IEEE standard 802.11b [30, 31, 109].

1.2.2 The South Korean Project

The South Korean HAP project started in 2000. The Korean Electronics and Telecommunications Research Institute (ETRI), and Korean Aerospace Research Institute (KARI) agreed to cooperate and develop projects related to remote sensing and telecommunication services. This Asian project is widely considered as one of the highest-level research around the world. ETRI put much effort to get the 28/31GHz bands licensed for Asian countries. The project which has been executed in three phases aimed to develop an unmanned airship and ground control systems. A 50m unmanned airship was delivered during the first phase. During the second phase, a stratospheric system, including a communications relay with ground stations was delivered at an altitude of 20km. During the third phase, a full-scale 200m airship with a 1000kg payload was delivered to the stratosphere layer [30, 31, 110].

1.2.3 The British Projects

There are large number of UK researchers that cooperate internationally in aerial platforms projects such as COST 297, CAPANINA, HeliNet, StratXX, and most recently Google's Loon. A real example is Lindstrand Technologies Ltd (LTL), which is a UK-based company that has been designing, manufacturing and developing over 5,000 aerial platforms that operate in 48 countries [111]. LTL has several aerial platforms projects, such as Sky Station and HALE airship with cooperation with European Space Agency (ESA). In 2000 a UK ATG company designed an unmanned solar-powered airship 200m long called “StratSat”. Its purpose was to provide an affordable and safe geostationary telecommunication services option for both civilian and military applications. Two contributions were added to the aerial platforms technology by the British team. First, solar cells array was placed in top of an aerial platform, and engineered to be readjusted towards the daily sun angle by rotating the whole airship. Second, although these platforms use renewable technology (solar power), a diesel engine was included into the StratSat airships to increase its time in the stratospheric layer [30, 31, 110-112].

Another innovative British project in aerial platform technology emerged in 2010 in Bedford. The project aims to combine both airship and aircraft as a Hybrid Air Vehicle to maximize its civil and military applications to reach both. It is regarded as a next generation lighter-than-air craft, as it is fixable, adaptable, cost effective, not reliant on infrastructure, and capable of carrying a heavy payload. One of the project’s output is “Airlander”, which can land on water, ice, or indeed on any landing surface. The vehicle uses a combination of helium gas and aerodynamic motors, which are used both for taking off [113, 114].

1.2.4 The Sky Station Project

Sky Station is an American airship project, which was introduced in 1996 by Sky Stations International Inc. (SSI) with NASA cooperation. It is considered as the first commercial application for video telephony Internet services using aerial platform technology. The project aims to provide high-speed wireless Internet access and phone services for worldwide coverage. It planned to deploy 250 platforms, which could be kept geo-stationary at altitudes at 21km, and used 47/48GHz band to cover every metropolitan city in the world, which involved 80% of the world’s population in 2004. The data rates planned were at the time 2Mb/s in uplink and 10Mb/s for downlink.

The average solar powered airship was around 200m in length and 60m in diameter, and carried a heavy telecommunications payload. Although the project was never deployed due to the immaturity of the technology at that time, the project added invaluable addition to the aerial platforms technology by bringing many radio regulations from ITU-R [30, 31, 110, 115].

1.2.5 The Japanese Project

The National Institute of Information and Communications Technology (NICT) and Japan Aerospace Exploration Agency (JAXA) are the main two Japanese bodies that have been developing aerial platforms technology as a future communications infrastructure since 1998. Skynet is one of the collaboration's output, and is considered as one of the largest aerial platforms projects in the world. This project aims to provide broadband communication services at a 28/31GHz band to cover the whole of Japan using a combined network of 15 aerial platforms. In 2002, the Japanese joined forces with NASA in NASA's Pathfinder Plus. This venture trialled successfully in Hawaii by developing a solar-powered unmanned aircraft at altitudes of 20km [30, 31, 110, 116].

1.2.6 The STRATXX AG-X station Project

The Swiss STRATXX project started in 2005 with developing cutting-edge technologies in the aeronautical and near-space solar-powered airships. One of the main project motivations was to commercialise the novel applications of aerial platform technology for low-cost communications especially in regions that suffer from the lack of a communications infrastructure. The X-Station platform was anticipated to provide several services on their platform, such as TV and radio broadcasting, mobile telephony, VoIP, and remote sensing via day- and night local GPS cameras. By 2010, the project's team presented a high-strength ultra-light material which met the stratospheric airships requirements, with high ability to deploy a vastly responsive communication network after natural disasters within short amount of time. The X-Station could cover up to a 1,000km in diameter, and was equipped with a spot beam antenna for WiMAX, 4G and digital broadcasting. STRATXX is one of successful demonstrations of LAPs [30, 31, 110, 112].

1.2.7 The ABSOLUTE Project

This 3-year project was funded by the EU from October 2012 to September 2015. This project aimed to investigate the LTE-A capability to cover disaster situations, public safety and security, and other temporary events using LAP technology. This project

also was set to provide multi-service and secure connectivity for large coverage areas with high capacity, low-latency by relying on LTE-A technology. The ABSOLUTE project is widely recognized as the progenitor of LAPs technology for wireless communication purposes, as large number of wireless communication aspects enormously introduced and developed, such as channel modelling, interference mitigation, handover management, propagation models, resource allocation, cognitive radios, ad hoc network planning [1, 14, 65, 117].

1.2.8 The Google Loons Project

The Google project is the latest in aerial platform technology introduced for commercial usage. It aims to provide high-speed Internet all over the world at an economical cost in response to the fact that over half of the world's population do not yet have Internet access. Google's balloons were officially announced in June 2011 as a network of balloons roaming on the stratosphere layer at nearly 20km above the Earth's surface to connect people in remote areas, bridge coverage gaps, and provide disaster relief. Google's stratospheric balloons use both wind layers, and intelligent software algorithms to steer the balloons to the right direction. At such an altitude, a balloon has antennas that can beam 4G LTE cellular signals to homes and phones within 100km in diameter, whereas users have special multiple antennas to be connected wirelessly. The balloon's electronic components are powered via an array of solar panels [107].

The first Google trial took place in 2013 in Canterbury, New Zealand, where 30 balloons lunched in a single week and 50 users got connected to the balloons. In March 2015, a new record break was achieved, whereby a Google Balloon spent over 6.5 months at 21km roaming the globe 9 times, and providing LTE connection with speeds of up to 10Mb/s. At the current time, Google's balloons provide networking in some parts of Brazil, New Zealand, Australia, and Latin America. In 2016, a Google Loon manager revealed that in Sri Lanka a Google Loon supported around 3 million mobile Internet connections, and over half a million fixed line internet subscribers out of the 20 million population. However, the main issue facing such a project is how to sustain the connectivity amongst the balloons and the ground receivers, as the balloons are continuously roaming. Another challenge is that many countries are refusing to cooperate with Google to allow its services to be available in their countries for both security and financial reasons 118-120].

1.2.9 The Lockheed Martin Project

Since 1928, Lockheed Martin has been working on wide range of aerospace, defence, and security advanced programmes for military and civilian applications. The Martin's programmes contributed significantly in developing aerial platforms systems globally. In 2009, a U.S. DARPA commissioned Lockheed Martin to construct a high-altitude airship to function as a radar in order to track objects from a distance of 300km. A further trail in 2011 resulted in an unmanned High-Altitude Long Endurance Defence (HALE-D) airship launched to keep American soldiers safer via high-tech communication systems and remote sensors. During these projects, many cutting-edge aerial platforms features have been engineered and developed, such as antenna and propagations, communications links, launch and landing methods, varied range missile warning, solar array electricity generation, and controlled vehicle recovery to a remote un-populated area [30, 31, 121].

1.2.10 The Saudi Arabian Project

In 2014, the Royal Saudi Ministry of Defense begun funding a $500m 10-year project in aerial plftorm and dron technolgy. The project host is Prince Sultan Advanced Technology Research Institute (PSATRI) in the captital city of KSA. One of the project outcomes is a tethered platform that aims to measure the resistance and performance of a highly elevated tethered platform to achieve three main objectives: First, sustainability of the aerial system under different weather conditions, second, remote sensing measurement for security and emergency applications, third, aerial imaging and live streaming. The last trial and experiment was conducted in February 2017, where primary data for this experiment have been collected by interviewing two of the experiment members [122, 123].

Table 1.2 presents a comparative review between terrestrial, aerial both (LAP and HAP), and satellite communication systems across many aspects drawn from the literature review.

Table 1.2: Comparative review of terrestrial, aerial and satellite communication systems

Issue	**Terrestrial**	**LAP**	**HAP**	**Satellite**
Altitude above ground	Up to 250m	0.1-5km	17-25km	750-36000km
Propagation delay	Varies	Very low	Low	High in GEO
Frequency band	Few GHz	1, 2, 4, 6,12-18, 27-40GHz	28−31 and 47/48GHz	1, 2, 4, 6, 12-18, 27-40GHz
Power supply	Electricity	Propellers, solar panels	Propellers, solar panels	Fuel, and Solar panels
Power consumption	High	Low	Low	High
Lifetime	Long term	Up to 5 years	Up to 5 years	up to 15 years
Capacity	Low due to attenuation by terrain and/or obstacles	High due to low altitude but low attenuation and delay	High due to low altitude but low attenuation and delay	Low especially with GEOs due to large path loss at high altitude
Propagation model	Empirical models	FSL, and few empirical models	FSL	FSL
Elevation angles	Not applicable	Medium	High	High
Coverage	Few km per BS	Up to 100km per Platform	Up to 400km per Platform	GEO: Large regions MEO/LEO: Global >500km
Geographical coverage	Land and coastline	Land and sea	Land and sea	Land and sea
Cell diameter	100m-2km	0.5-5km	1-10km	50-500km
Isolated area coverage	Higher energy consumption	Covered easily	Covered easily	Needs higher gain antenna
Shadowing from terrains	Causes coverage gaps; needs additional equipment	Problematic at low elevation angles	Problematic at low elevation angles	Problematic at low elevation angles
HO complexity	High	Low	Low	Medium in MEO/LEO
Deployment timing	In stages	Minimum of one platform	Minimum of one platform	MEO/LEO: In stages GEO: 1 stand-alone
Complexity	Operating in rural areas	When facing strong wind	Station-keeping	Complex MEOs and LEOs movement
Incremental deployment	BS scalability, but high financial cost and energy consumption	Unlimited capacity thru re-sizing spot-beam and/or platform scalability	Unlimited capacity thru re-sizing spot-beam and/or platform scalability	Unlimited capacity thru satellite scalability

Disaster relief	Vulnerable when disasters struck	Quick and Easy service provision	Quick and Easy service provision	Service provision
Short-term large-scale events	Costly - High number of BSs	Cost-effective	Cost-effective	Costly - High manufacturing and launching
Maintenance	Complexity rises with number of BSs	Less complex	Financially and operationally less complex	Financially and operationally complex
Environmental	Friendly	Friendly	Friendly	Non-friendly

1.3 Related Review Windup

As the prevalence and significance of wireless networks continuously grow, the necessity for advanced methods of modelling and computing wireless signal propagation grow too. Propagation models are valued tools and algorithms for the prediction of signal propagation loss between the transmitter and receiver in locations where the wireless communication systems network is to be deployed. This section aims to highlight the issues that evolve from the above discussion that relate to last mile connectivity and to identify unresolved issues or consider suggestions as Table 1.3 shows. It then uses this to review the research gaps and report own research motivations that have been used to pursue this doctoral research. The review of related literature reveals several research dimensions on aerial plftorms:

- Channel modelling and propagation models
- Ad Hoc network planning
- Relationship between payload and power consumption
- Radio and frequency band allocation
- Cutting-edge technologies on test such as MIMO, smart antenna, LTE-A, and WiFi
- Application support by LAPs
- Optimal LAP altitudes
- Bridging the digital gap brought by the lack of a telecommunication infrastructure

Table 1.3: Related review windup

Areas	***Issues***		***Approaches***
	Addressed	***Unresolved / Suggestions***	
Propagation Models	• Wide channel modelling for outdoors [2,9] • Two ATG propagation types, LoS and NLoS [17-26]	• Shadowing effect only considered by some [9] • Full link budget needs to be considered in various environments	***ATG models***
	• Few outdoor empirical models for LAPs [11-16] • Mathematical models drawn from experiments in various environments [11-16] • Wireless network planning [11-16]	• Limited LAP altitudes [11-16] • Additional empirical models need to be considered	***Empirical models***
Coverage and LAP Altitude	• Optimum LAP altitude calculation using RSS, MAPL, ITU's statistics on urban and atmospheric effects [9,12,40] • Enhancing RSS and coverage by increasing LAP altitude, transmission power, utilization, or deploying multi-tethered platform topology [4,12,42] • Helical directional or omnidirectional antennas for RF channel modelling to improve RSS and LAP coverage [22,49]	• Trade-off between LAP altitude and RSS and interference in urban environments [15] • Rise in interference as number of LAPs rise in an area [23] • Updating of urban ITU statistics needs to be considered [21] • Interference management between deployed multi-LAPs [30] • Limited LAP altitudes in empirical models [11-16] • Large size of directional or omnidirectional antennas, power consumption, and increased interference [49]	***RSS***
Antenna Specifications	• Widespread calculation of LAP coverage footprint • Achieving better connectivity at low elevation angles with directive antenna [29-33]	• Some elevation angles are unsuitable for all environments • Lack of consideration of elevation angle in empirical models due to low transmission altitude • Trade-off between low elevation angles, path loss, coverage • MIMO antennas for high elevation angles may yield better LoS connectivity, reduced path loss and extended coverage	***Elevation Angle***
	• Some consideration of smart/ MIMO antenna impact on improving link budget performance and minimizing interference [38, 65, 93]	• Smart switched beam antenna needs to be considered, although it is difficult to mount on small LAPs [66] • Advanced MIMO antennas that may improve performance [66]	***Smart Antenna***

Power Consumption	• Resource allocation techniques based on game theory that minimize power consumption [19] • Dynamic techniques that calculate optimal LAP location, minimize path loss, improve RSS, reduce power consumption [67-70]	• Trade-off between throughput and power consumption to guarantee fairness amongst users [19] • Optimisation of path loss to minimize transmitting power, and reduce power consumption [36]	***Software***
	• Direction of antenna reduces power consumption [66] • Antennas that serve various frequency bands • Hardware that may reduce power consumption such as batteries, thin solar panels, or propellers [51,63,64]	• Antenna direction reduces RSS as altitude rises [16] • MIMO antenna gain diversity may enhance accuracy and reduce power consumption [106] • Some antennas are unsuitable for mounting on small LAPs [66]	***Hardware***
Operation Frequency and Interference	• WiFi [4,14,22,26,49,87, 88], WiMAX [12,26,49,87], and LTE [4,14,18,19,24,26,62,87,88] technologies are widely considered for LAPs in relation to application types, operational environment and duration and the LAP's onboard communication payloads and power supply	• Vulnerability to interference because of its use of unlicensed band • Limited coverage • Increase in transmission power may increase coverage, but also increases power consumption and interference • Lack of consideration of WiFi HaLow due its immaturity	***WiFi***
		• Large installation and operational costs • Less coverage and data rate than LTE	***WiMAX***
		• Emergency or security applications may lead to network congestion and interference in comparison to WiMAX	***LTE***

We have drawn a series of issues that reportedly may improve the deployment of LAPs as aerial BSs and have also highlighted some main limitations which need to be addressed. The rest of this subsection outlines our research motivations in pursuing this doctoral research. These are drawn from the research gaps identified in Table 1.3:

- The *first research motivation* is to adapt ATG and other empirical propagation models for LAP to consider the elevation angle. The empirical propagation models reported in the literature are limited by the antenna height that is representative of the LAP altitude. Hence, we aim to choose empirical propagation models that consider high antenna and yield wide coverage in various terrains with strong RSS.
- The *second research motivation* is to optimise a propagation model for last-mile connectivity using LAPs. The current situation for optimizing link budget parameters is via what is called “trial and error approach”. Thus, the optimisation avenue pursued is that of machine learning using predictions obtained with the selected propagation models. Such a machine learning approach should yield a set of optimal link budget parameters that would define a model that optimises path loss and RSS and minimizes transmission power and power consumption.
- The *third research motivation* is to consider one of MIMO antennas functionality along with the rest of parameters, i.e. RSS, SINR, throughput, coverage at various LAP altitudes and urban, suburban, rural environments. This should increase signal quality and coverage, minimize interference and power consumption, and manage multipath. The MIMO functionality offers the advantage of diversity gain which is a notable shift from existing propagation models.

1.4 Research Aim and Objectives

The aim of this doctoral research is to optimise a propagation model for last-mile connectivity using LAP technology. Hence, to achieve the research aim, the following research objectives need to be pursued:

O1. Identification of parameters affecting last mile connectivity when deploying LAPs
O2. Selection of propagation models that are suitable for deploying LAPs as BS
O3. Adoption of the elevation angle parameter in the selected propagation models
O4. Evolution of an optimal propagation model using machine learning
O5. Implementation and deployment of the optimised model in two proofs-of-concept
O6. Validation of the optimised model’s predictions

Table 1.4 maps the research objectives against their deliverables.

Table 1.4: Research objectives and their deliverables

Objectives	Deliverables
O1	Parameters that effect last mile connectivity when deploying LAP as an aerial BS in urban, suburban, and rural environments: elevation angle, LAP altitude, coverage area, power consumption, operation frequency, and antenna
O2	Four representative simulated propagation models that include all or most of the last mile connectivity parameters identified in O1: ITU-R P.529-3, Okumura, Hata-Davidson, and ATG
O3	Adapted propagation models chosen in O2 to include elevation angle in predicting coverage footprint and simulating these in MATLAB
O4	Optimal propagation model for last-mile connectivity evolved in MATLAB using machine learning and the predictions of O3
O5	Implementation and deployment of the optimal propagation model evolved in O4 in two proof-of-concept applications: a WSN, and a cellular structure
O6	Validation of the optimal propagation model, first, against the adapted propagation models of O3 and then against those reported in the literature

1.5 Research Methods

The research method used in this research is a fusion of several methods. This multimethod ranges from defining challenges, through to model design to testing the proposed model deployment through to the development of a "proof-of-concept" [125-131]. Table 1.5 below demonstrates the resulting multimethod research method where each approach maps on one or more of the research objectives detailed on Table 1.4 above.

Table 1.5: Research methods deployed in pursue of research objectives

Research Method	Objective
Action Research	O1, O2, O3
Machine Learning	O4
Prototyping	O5
Lab Experiment	O6

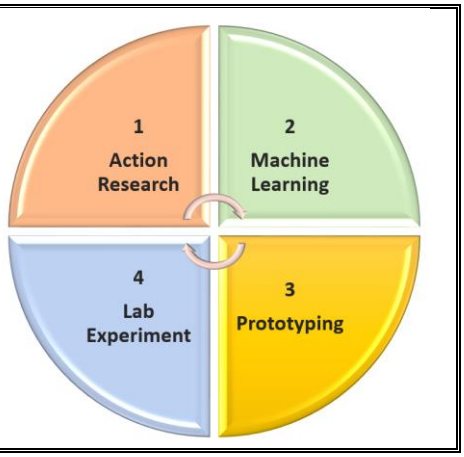

The first method, Action Research (AR), has been deployed in pursue of O1, O2, and O3. AR aims to build knowledge, and practical action by engaging in a cyclic process that interchanges between action and critical analysis with continuous adjustments, to extend the understanding of considered action. This commences with observations reported in literature on last mile connectivity using LAPs as an aerial BS across different terrains. This has helped with LAP specification in terms of transmitter altitude, coverage range, and frequency band and identification of propagation models that meet those LAP specifications. In turn, this has helped with identifying research gaps in all these. During the development that ensued the propagation models adopted were simulated in MATLAB to obtain early-stage prediction results and adapt these in helping to evolve an optimised propagation model during the deployment of the second method [125, 126].

The second method, Machine learning (ML), has been deployed in pursue of O4. There is no generic propagation model which can suit every environment and provide accurate predictions other than those models which have been custom-designed for that. Thus, the ML optimisation considered which uses computational methods to learn from random input data and an adaptive algorithm that improve the performance as the number of samples available for learning increases. This has helped with formulating a Neural Network (NN) framework that evolves an optimised propagation model by taking as inputs the adapted propagation models produced during the AR phase but at several LAP altitudes and across different urban, suburban, and rural environments and then clustering the results into Self-Organizing Maps (SOMs). The aim of the optimised model is to achieve a wider wireless coverage and improved QoS [127, 128].

The third method, Prototyping, has been deployed in pursue of O5. This has helped with the implementation and deployment of the optimised model in the two proof-of-concept applications. The two applications have been implemented using Rapid Application Development (RAD) tools in MATLAB. This method has provided further opportunities in data interpretation and validation of the optimised propagation model [129, 130].

The fourth method, the Lab Experiment (LE), has been deployed in pursue of O6. Simulations of the optimised and non-optimised propagation models have been mathematically modelled in MATLAB across different environments and LAP altitudes. Their predictions have been compared first against each other using Feed Forward Fitting Tool that uses the Levenberg-Marquardt backpropagation algorithm, and then against predictions reported in the literature. These have helped with validating the evolved optimal values of the model parameters [131, 132].

1.6 Thesis Outline

Chapter 2 discusses the design of an optimal propagation model for last-mile connectivity using LAPs. This starts by choosing among existing propagation models those that are representative of their respective types. Then, adapting these models by adding the elevation angle to predict the performance of link budget parameters. It then evolves using Machine Learning an optimised propagation model framework for last-mile connectivity with LAPs.

Chapter 3 discusses the implementation of the design from chapter 2. Firstly, it reports on the MATLAB implementation of four adapted propagation models from chapter 2. Secondly, it reports on the evolution of the optimised propagation model using NN-SOM, and assessment of its performance using the NN Feed Forward Fitting Tool. It also reports on the deployment of the optimised propagation model in a WSN, and a cellular structure across a range of different environments in KSA.

Chapter 4 compares the prediction results of the optimised model against those of the four adapted propagation models implemented in chapter 3 and then against some of those reported in the literature. The chapter concludes by validating the performance of the optimised model in two proof-of-concept applications.

Chapter 5 summarises the thesis and research contributions and makes suggestions for further research and development.

Chapter 2 : Optimisation of a Propagation Model

This chapter discusses the design of an optimal propagation model. At first it presents empirical and deterministic propagation models and then selects four propagation models that meet LAP requirements. It then adapts the selected models by adding the elevation angle to predict the performance of link budget parameters. Finally, it evolves an optimised propagation model for LAP last-mile connectivity using a Machine Learning (ML) technique.

2.1 Selecting Representative Propagation Models

Several competing propagation models have been proposed over the years but whilst they collectively raise many shortcomings such as limited altitude up to few tens of meters, lack of cover across different environments, low perdition accuracy they also exhibit several advantages. Therefore, here a reduction approach is considered in order to narrow down poprogation models from tens to four specific models that meet the LAP requirements. There are several common parameters across propagation models that effect the overall performance, such as antenna gain, transmission power, and loss. Other factors include: (f) Frequency of operation, (d) Distance between transmitter and receiver (coverage), (h_t) Transmitter antenna height (LAP altitude), (h_r) Receiver antenna height, and Terrain type.

Hence, the reduction approach is based on firstly, classifying models based on their type (Stochastic, deterministic, and Empirical), and secondly transmitter height, which represent LAP altitude up to (0.1km, 1km, 2.5km, 5km), as Figure 2.1 shows. The models are representative models of their respective types along with their main parameters of maximum transmission distance, transmitter and receiver antenna heights and high range of frequency band [7, 8, 19, 132-142]. Four propagation models, which are representatives of their types, have been selected since they exhibit advantages in relation to high altitude, wide coverage range, adaption across different terrains. In addition, all four have been extensively deployed in the past and as a result their correction factors have evolved over the years to yield extremely accurate results which makes the development and evaluation aspects of this research very precise. The four models are: ITU-R P.529-3, Okumura, Hata-Davidson, and ATG.

Although the propagation models shown in Figure 2.1 are representative models of their respective groups, none of the propagation models that involve an h_t of less than 0.1km are considered as the LAP altitude ranges between 0.1km and 5km above ground. ITU-RP.1546 offers an advantage of high h_t and wide coverage range but it offers low perdition accuracy. Empirical Propagation Model-73 (EPM-73) also offers an advantage of high h_t but it does not cover urban environments. Out of these models, a set of representative propagation models are selected that offer an advantage of high h_t, and wide coverage range ≥ 100 km. In addition to the high functionality and adaptivity of working in various terrains and environments with the merit of correction factors associated with them.

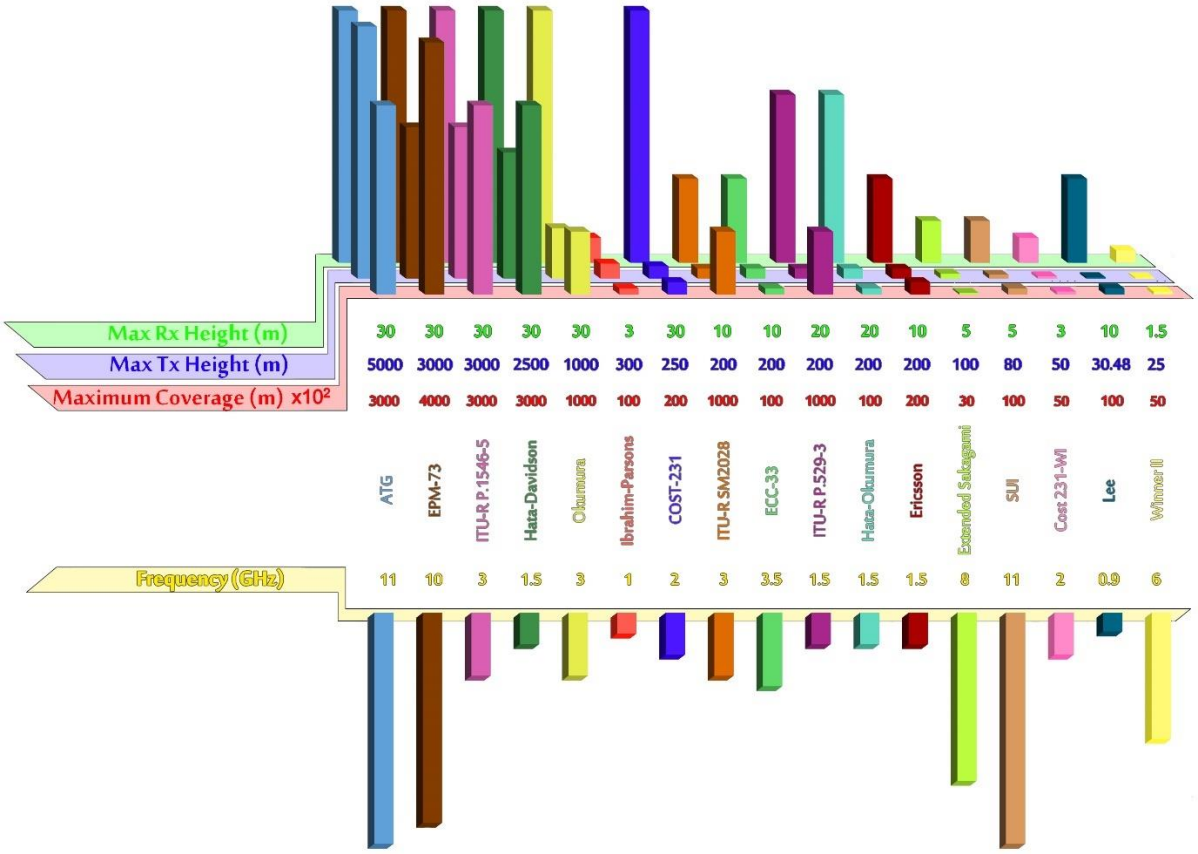

Figure 2.1: The selected Propagation Models for Last Mile Connectivity for LAPs

Four propagation models have been selected namely ITU-R P.529-3, Okumura, Hata-Davidson, and ATG, as Table 2.1 below shows. All four selected models have the merit of correction factors associated with them that thus yield high accuracy results [132-142].

Table 2.1: The four selected propagation models

Model	h_t [km]		h_r [km]		f [GHz]		d [km]		Terrain		
-	min	max	min	max	min	max	min	max	-	-	-
ITU-R P.529-3	0.03	0.2	0.001	0.02	0.15	1.5	0.1	100	U	S	R
Okumura	0.03	1	0.001	0.01	0.1	3	0.1	100	U	S	R
Hata-Davidson	0.03	2.5	0.001	0.02	0.15	1.5	0.1	300	U	S	R
ATG	0.01	5	0.001	0.03	0.3	11	0.1	300	U	S	R
U:Urban **S:**Suburban **R:**Rural											

2.1.1 ITU-R P.529-3 Propagation Model

This model is representative of propagation models for altitudes less than 1km. This model is an extended Hata model that defines path loss for urban, suburban and rural environments. The modified model was introduced to improve on the range limitation in the Hata model and cover distances of up to 100 km using a frequency range of up to 1.5GHz with correction factors [132-142].

Calculation of path loss P_L – Case 1: Urban area

$$\mathrm{P_L} = 69.55 + 26.16\log(\mathrm{f}) - 13.82\log(\mathrm{h_t}) - \mathrm{a(h_r)} + [44.9 - 6.55\log(\mathrm{h_t})] \times [\log(\mathrm{d})]^{\mathrm{b}} \quad (1)$$

$$\mathrm{a(h_r)} = 1.11\log(\mathrm{f}) - 0.7(\mathrm{h_r}) - [1.56\log(\mathrm{f}) - 0.8] \quad (2)$$

$$\mathrm{b} = 1 \quad \text{for } \mathrm{d} \leq 20\mathrm{km}$$

$$\mathrm{b} = 1 + (0.14 + 1.87\times10^{-4}(\mathrm{f}) + 1.07\times 10^{-3}(\mathrm{h_t}')\left(\log\left(\frac{\mathrm{d}}{20}\right)\right)^{0.8} \text{ for } 20\mathrm{km} < \mathrm{d} < 100\mathrm{km} \quad (3)$$

$$\mathrm{h_t}' = \frac{\mathrm{h_t}}{[1+(7\times10^{-6})\times(\mathrm{h_t})^2]^{\frac{1}{2}}} \quad (4)$$

Calculation of path loss P_L – Case 2: suburban area

$$\mathrm{P_L} = \mathrm{P_{L(urban)}} - 2[\log\left(\frac{\mathrm{f}}{28}\right)]^2 - 5.4 \quad (5)$$

Calculation of path loss P_L – Case 3: rural areas

$$\mathrm{P_L} = \mathrm{P_{L(urban)}} - 4.78[\log(\mathrm{f})]^2 + 18.33\log(\mathrm{f}) - 40.49 \quad (6)$$

Where $\mathrm{P_L}$: Path Loss (dB), f: Carrier Frequency (GHz), $\mathrm{h_t}$: Transmitter Antenna Height (km), $\mathrm{h_r}$: Receiver Antenna Height (km), and d: Distance of Transmission (km), $\mathrm{a(h_r)}$: Antenna Correction Factor.

2.1.2 Okumura Propagation Model

This is a classic empirical model and it is among the simplest and best models in terms of accuracy in predicting the path loss for early cellular systems especially in built-up areas with a dense and tall structure. This model can be used to calculate path loss in urban, sub-urban and rural areas using a frequency range of up to 3GHz with correction factors.

Calculation of path loss $\mathrm{P_L}$

$$\mathrm{P_L} = \mathrm{L_f} + \mathrm{Amn}\,(\mathrm{f}, \mathrm{d}) - \mathrm{G}(\mathrm{h_t}) - \mathrm{G}(\mathrm{h_r}) - \mathrm{G_{area}} \quad (7)$$

$$\mathrm{L_f} = 32.44 + 20\log(\mathrm{f}) + 20\log(\mathrm{d}) \quad (8)$$

$$\mathrm{G}(\mathrm{h_t}) = 20\log(\mathrm{h_t}/0.2),\ 0.01\mathrm{km} < \mathrm{h_t} < 1\mathrm{km} \quad (9)$$

$$\mathrm{G}(\mathrm{h_r}) = 10\log(\mathrm{h_r}/3),\ \mathrm{h_r} \leq 3\mathrm{m} \quad (10)$$

$$\mathrm{G}(\mathrm{h_r}) = 20\log(\mathrm{h_r}/3),\ 10 > \mathrm{h_r} > 3\mathrm{m} \quad (11)$$

Where: $\mathrm{P_L}$: Path Loss (dB), Lf: Free Space Path Loss (dB), $\mathrm{Amn}\ (f,\ d)$: Median Attenuation Relative to Free Space (dB), d: Distance of Transmission (km), f: Carrier Frequency (GHz), $\mathrm{G}(\mathrm{h_t})$: Transmitter Antenna Height Gain Factor (dB), $\mathrm{G}(\mathrm{h_t})$: Receiver Antenna Height Gain Factor (dB), $\mathrm{h_t}$: Transmitter Antenna Height (km), $\mathrm{h_r}$: Receiver Antenna Height (km), $\mathrm{G_{area}}$: Gain due to Type of Environment (dB). In order to predict $\mathrm{P_L}$ using Okumura's model, Lf between the points of interest is first predicted and then the value of $\mathrm{Amn}\ (\mathrm{f}, \mathrm{d})$ is added to it along with the type of terrain correction factor. The values of Amn and $\mathrm{G_{area}}$ are predicted empirically as Figure 2.2 shows.

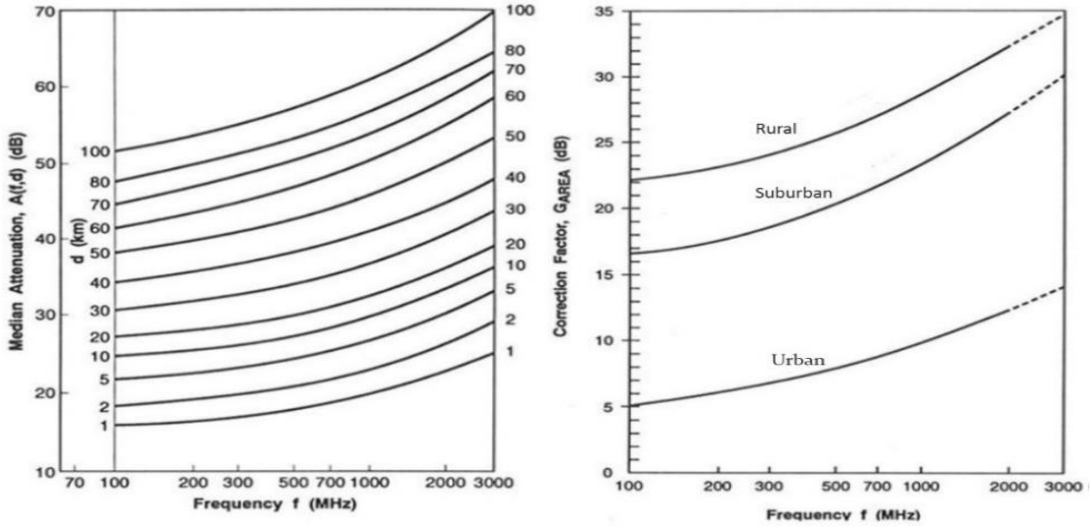

Figure 2.2: Empirical plots of Okumura model [29]

2.1.3 Hata-Davidson Propagation Model

This model consists of six correction factors including links of up to 300km and high transmitter antennas of up to 2.5km. This extends the model using a frequency range of up to 2GHz with correction factors for urban, suburban and rural areas.

Calculation of path loss $\mathbf{P_L}$

$$\mathrm{P_L HD} = \mathrm{P_L Hata} + \mathrm{A}\,(\mathrm{h_t}, \mathrm{d}) - \mathrm{S_1(d)} - \mathrm{S_2}(\mathrm{h_t}, \mathrm{d}) - \mathrm{S_3(f)} - \mathrm{S_4}(\mathrm{f}, \mathrm{d}) \quad (12)$$

$$\mathrm{P_L Hata} = 69.55 + 26.16\log(\mathrm{f}) - 13.82\log(\mathrm{h_t}) - \mathrm{a}(\mathrm{h_r}) + [44.9 - 6.55\log(\mathrm{h_t})]\log(\mathrm{d}) \quad (13)$$

Calculation of path loss $\mathbf{P_L}$ – Case 1: for urban area

$$\mathrm{a}(\mathrm{h_r}) = (3.2[\log(11.75\ \mathrm{x}\ \mathrm{h_r})]^2) - 4.9 \quad (14)$$

Calculation of path loss $\mathbf{P_L}$ – Case 2: for suburban or rural areas

$$\mathrm{a}(\mathrm{h_r}) = (1.1\log(\mathrm{f}) - 0.7)(\mathrm{h_r}) - (1.56\log(\mathrm{f}) - 0.8) \quad (15)$$

Where $\mathrm{P_L HD}$: Path Loss of Hata-Davidson (dB), $\mathrm{P_L Hata}$: Path Loss of Hata Model (dB), $\mathrm{a}(h_r)$: Correction Factor for mobile antenna height, f: Carrier Frequency (GHz), h_t: Transmitter Antenna Height (km), $\mathrm{h_r}$: Receiver Antenna Height (km), d: Distance of Transmission (km), A, $\mathrm{S_1}$: factors that extends distance to 300 km, $\mathrm{S_2}$: correction factor for height $\mathrm{h_t}$ of base station antenna extending the value of $\mathrm{h_t}$ to 2.5km, $\mathrm{S_3}$, $\mathrm{S_4}$: correction factors that extend frequency to 1.5GHz, as Table 2.2 shows.

Table 2.2: Distance and correction factors for Hata-Davidson

Distance $\boldsymbol{d}$(km)	A ($\boldsymbol{h_t}$,$\boldsymbol{d}$) (km)	S1 ($\boldsymbol{d}$) (km)
$\boldsymbol{d}$ < 20	0	0
20< $\boldsymbol{d}$ < 64.38	0.62137 (d -20)[0.5 + 0.15 log(h_t/121.92)]	0
64.38< $\boldsymbol{d}$ < 300	0.62137 (d -20)[0.5 + 0.15 log(h_t/121.92)]	0.174(d-64.38)
S2 ($\boldsymbol{h_t}$,$\boldsymbol{d}$)	0.00784|log(9.98/d)|(h_t-0.3) for h_t> 0.3km	
S3 ($\boldsymbol{f}$)	f / 250log(1.5GHz/ f)	
S4 ($\boldsymbol{f}$, $\boldsymbol{d}$)	[0.112log(1.5GHz/ f)](d-64.38) for d > 64.38km	

2.1.4 ATG Propagation Model

The model considers path loss, shadowing (large-scale fading), and small-scale fading, where each occurs either in LoS or NLoS. Each of these is also considered separately with different probabilities as function of environment type, buildings height and density. NLoS occurs as a result of the shadowing effect and reflection of signals from interfering obstacles which in turn leads to an additional path loss especially with increasing distance from the BS in urban environments. Small-scale fading is

neglected and because of that the path loss and shadowing effects of LOS and NLOS components are much higher.

In ATG the path-loss is greatly dependent on the elevation angle, which aims at achieving LoS most of the time. The ITU has suggested a standardized model for different environments based on three main parameters. 1) Ratio of built-up land area to the total land area (dimensionless); 2) Mean number of buildings per unit area (buildings/km^2), 3) Scale that describes the building height distribution according to Rayleigh's probability density function. Table 2.3 summarizes selected ITU-R empirical parameters as *a, b, c, d*, and *e* for different environments being simulated as LoS probability for a wide range of elevation angles.

Table 2.3: Selected ITU-R parameters for different environments

Environment	***a***	***b***	***c***	***d***	***e***
Urban	187.3	0	0	82.10	1.478
Suburban	120	0	0	24.30	1.229
Rural	101.6	0	0	3.25	1.241

A common method to model ATG propagation is to consider LoS and NLoS along with their probability of occurrence.

Calculation of the total path loss $\mathbf{P_L}$

$$\mathrm{PL_T} = \rho_{\mathrm{LoS}} \times \mathrm{PL_{LoS}} + \rho_{\mathrm{NLoS}} \times \mathrm{PL_{NLoS}} \quad (16)$$

The probability of having LoS connections at an elevation angle of θ is given by:

$$\rho_{\mathrm{LoS}} = \mathrm{a} - \frac{\mathrm{a-b}}{1+[\frac{\theta-\mathrm{c}}{\mathrm{d}}]^{\mathrm{e}}} \quad (17)$$

$$\rho_{\mathrm{NLoS}} = 1 - \mathrm{P_{LoS}} \quad (18)$$

The path loss for LoS and NLoS are:

$$\mathrm{PL_{LoS}\,(dB)} = 20\log\frac{4\,\pi\,(\mathrm{f})(\mathrm{d})}{\mathrm{c}} + \eta_{\mathrm{LoS}} \quad (19)$$

$$\mathrm{PL_{NLoS}\,(dB)} = 20\log\frac{4\,\pi\,(\mathrm{f})(\mathrm{d})}{\mathrm{c}} + \eta_{\mathrm{NLoS}} \quad (20)$$

Where a, b, c, d and e are ITU-R parameters for the three types of environments as shown on Table 2.3, θ: Elevation Angle in degrees depends on environment type, f: Frequency (GHz), d: Distance of Transmission (km), η_{LoS}, η_{NLoS}: average additional loss to free space depending on environment type.

2.2 Adapting the Selected Propagation Models

When providing coverage of a large area, it becomes increasingly necessary to consider the earth's curvature and radius. Therefore, one of our key research contribution is to adapt the four selected propagation models to additionally consider the elevation angle in predicting the coverage footprint at various LAP altitudes. Such a prediction that considers a LAP's quasi-stationary condition at a specific altitude requires calculation of the distance between a LAP and a ground receiver and additionally of the distance between the LAP and a projection point onto the ground and the earth surface curvature and radius.

This adaptation does not only offer LoS service connectivity and coverage but also Out-of-Sight (OoS) service to receivers that would normally experience outage or low connectivity as a result of their distance, the earth's curvature, or terrain morphology. This adaptation improves the coverage range, RSS and QoS. The distance D of the selected propagation models is computed based on elevation angle θ as follows:

$$\cos\theta = \frac{E_r}{E_r+H} \tag{21}$$

$$\theta = \cos^{-1}\frac{E_r}{E_r+H} \tag{22}$$

$$D = \theta . E_r \tag{23}$$

$$D = 2\,E_r[\cos^{-1}\left(\frac{E_r}{E_r+H} * \cos(\theta)\right) - \theta] \tag{24}$$

Figure 2.3 shows the trigonometric geometry for a LAP, whereby given a LAP's altitude H, E_r is the Earth's radius at 6378 km, and θ is the elevation angle from a user's location.

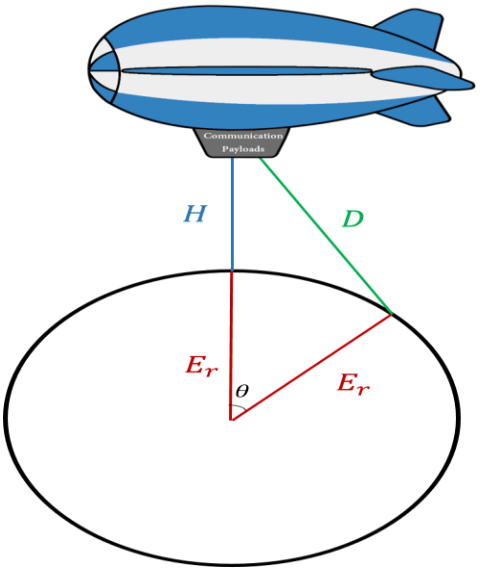

Figure 2.3: Trigonometric geometry for a LAP

The literature offers various considerations and assumptions with regards to selecting an appropriate elevation angle that suits an environment. Figure 2.4 depicts the geometry of threshold elevation angles proposed here for urban, suburban, and rural environments respectively, 15°, 10°, 5°, where the LAP is in a quasi-stationary position.

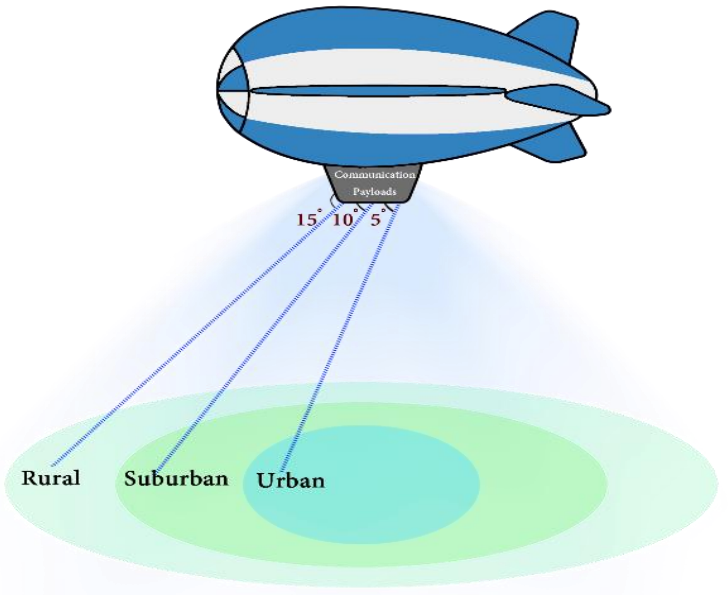

Figure 2.4: The geometry of threshold elevation angles for urban, suburban, and rural

The adapted propagation models aim to predict the performance of fuller range of link budget parameters, PL, RSS, SNIR, throughput, optimum altitude and coverage. PL is computed based using each propagation model formula. Then, calculation of the rest of the link budget parameters is based on PL predictions. At first, a threshold value for PL, MAPL, needs to be calculated for both UL and DL with the smallest value of the two set as path loss threshold. Thus, MAPL can be calculated as follows:

Down Link Threshold

$$MAPL = EIRP + R_s + \mathrm{G(h_t)} - losses \quad (25)$$

$$EIRP = P_t + \mathrm{G(h_r)} - Losses \quad (26)$$

Up Link Threshold

$$MAPL = EIRP + R_s + \mathrm{G(h_r)} - losses \quad (27)$$

$$EIRP = P_t + \mathrm{G(h_t)} - Losses \quad (28)$$

Where *EIRP* is Effective Isotropic Radiated Power, R_s: Receiver sensitivity, $\mathrm{G(h_t)}$: Transmitter antenna gain, $\mathrm{G(h_r)}$: Receiver antenna gain, and *L*: Losses including feeder, cable, body, interference and fade margin [4,11, 143-146].

Each of the four selected models predicts values for five parameters: path loss, RSS, SINR, throughput, and footprint coverage. Calculating path loss is useful for monitoring system performance, network planning and coverage to achieve good reception. RSS helps to estimate the coverage range when the signal weakens as the receiver moves away from the transmitter. RSS depends on path loss, transmitter and receiver height and gain and environment factors [4,11]. The SINR is used to measure the quality of a wireless link and bit error ratio. Throughput is one of performance indicators, which decreases with path loss, distance, and shadowing. RSS depends on transmitter power ($\mathrm{P_t}$), path loss ($\mathrm{P_L}$), transmitter antenna gains $\mathrm{G(h_t)}$, receiver antenna gains $\mathrm{G(h_r)}$ as well as (L) connector and cable loss.

SNIR is RSS (dB) over N: Noise figure (dB) plus I: Interference (dB). The literature reveals that there is no formula with which to calculate the exact throughput based on P_L and SINR. However, an approximated prediction can be made using Shannon's formula. Thus, throughput (C) can be predicted in bits per second (b/s) as a function of bandwidth (BW) in MHz and SINR as linear power ratio not dB. Furthermore, the optimum LAP altitude and coverage footprint can be derived from the path loss and RSS results. Coverage footprint in all four models is based on an elevation angle from a user's location which is a significant departure from current empirical models [143-146]. The values of these parameters can be predicted as follows:

$$\mathrm{RSS} = \mathrm{P_t} + \mathrm{G(h_t)} + \mathrm{G(h_r)} - \mathrm{P_L} - \mathrm{L} \tag{29}$$

$$\mathrm{SINR\ (dB)} = \frac{\mathrm{RSS}}{\mathrm{N+I}} \tag{30}$$

$$\mathrm{C} = \mathrm{B} \times \log(1 + \mathrm{SNIR}) \tag{31}$$

In order to give a brief description of the propagation models' algorithm, a flowchart is given in Figure 2.5; where PL, RSS, SINR, throughput, and coverage is calculated at each chosen altitude across different environments.

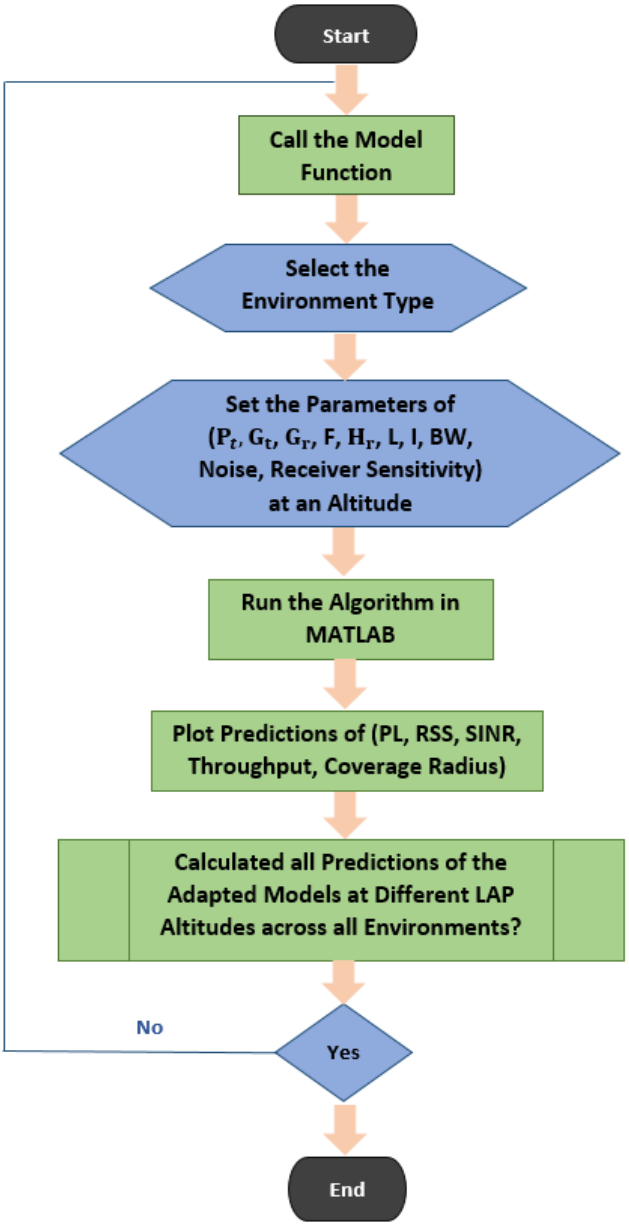

Figure 2.5: Flowchart of the propagation models' algorithms

2.3 Optimizing a Propagation Model

ML techniques and algorithms are used for data analytics to obtain valuable information from complex and large data that allow making a smart decision. The learning concept is based on learning from the internal pattern of the data, where data can adjust their internal parameters accordingly. The optimisation phase here aims to highlight the architecture of the optimisation framework that achieves wider wireless coverage and better QoS for network planning for last-mile connectivity using LAPs. The ML technique deployed here for evolution of an optimal set of parameters for a propagation model is NN-SOM alongside its NN Feed Forward Fitting Tool, as Figure 2.6 shows [147].

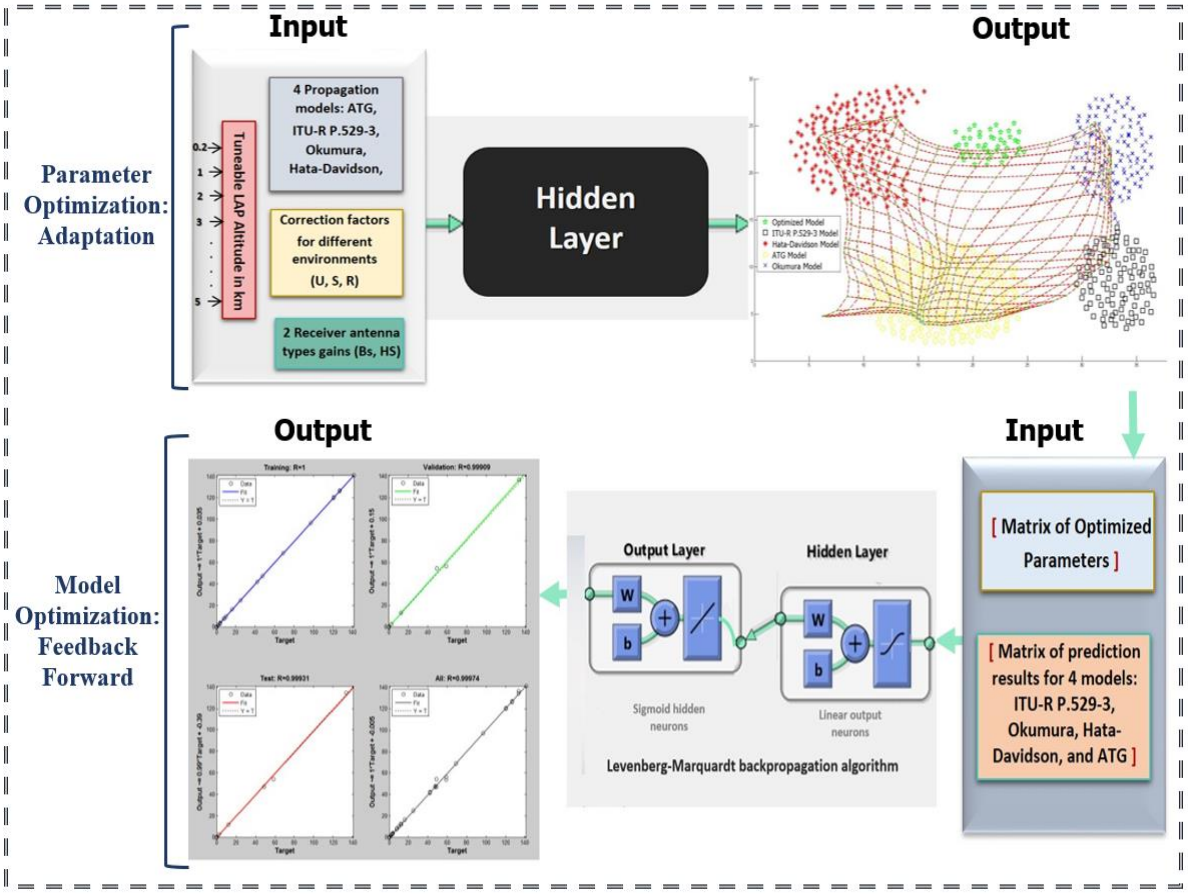

Figure 2.6: Machine Learning Optimisation Framework using Neural Nets

2.3.1 Optimisation with NN-SOM

The first step in the optimisation framework takes inputs of adapted propagation models at several LAP altitudes process them using NN-SOM that cluster the parameters after deploying minimax technique which can be checked in range of scenarios across urban, suburban, and rural environments. The NN-SOM technique is an unsupervised learning algorithm that trains the NN to evolve an optimised model for each selected altitude. NN broadly consist of three layers namely a) input layer, b) hidden layer, c) output layer [147-153]. At every LAP altitude considered in the evolved optimised model, there is set of predications results given as input. This includes PL, RSS, SINR, throughput, and coverage radius for every one of the four adapted propagation models in different environments, and antenna gains as Figure 2.7 shows.

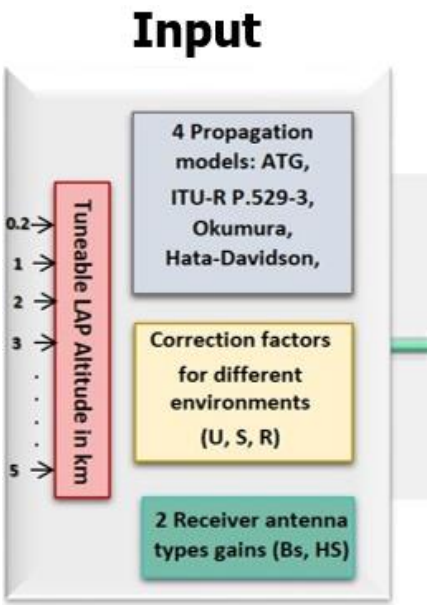

Figure 2.7: Inputs to the evolved optimised model to NN-SOM

The NN-SOM is a pattern recognition process that maps input to output layers via hidden process layer. The networks are trained to predict optimum output values based on the three basic elements of a neuron: synaptic weights, summing function, and activation function. The NN hidden layer is black box. Although a black box does not mean that the internal processing of the model is sheltered from being interpreted, it means that the resulting parameters or patterns are generated by random weights and minimax functions of the entered parameters [147-153]. The NN-SOM algorithm runs over two phases: Learning and Adaptive. The flowchart on Figure 2.8 describes the operations which aim to evolve an optimised a propagation model.

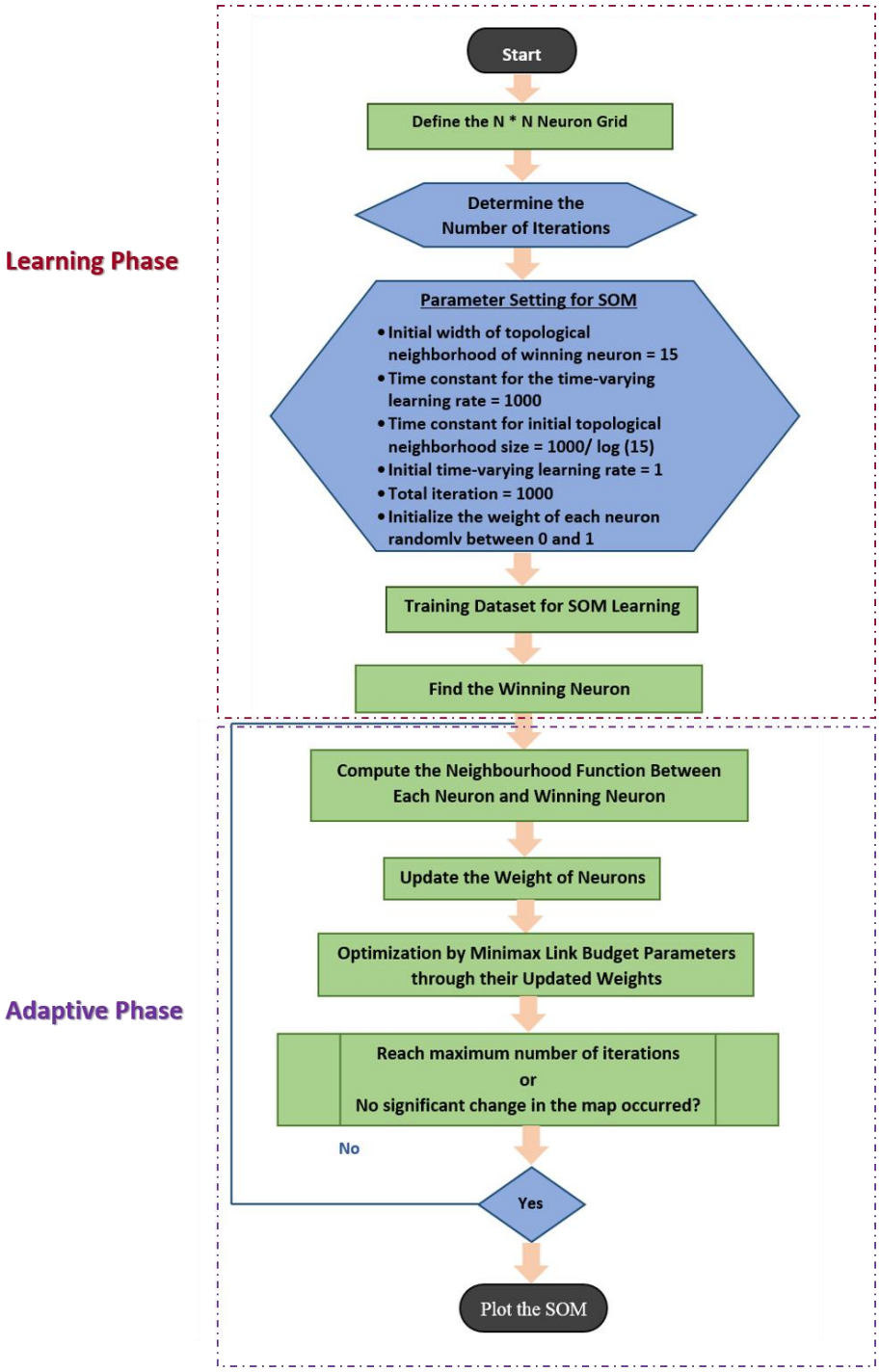

Figure 2.8: Flowchart of the NN-SOM Optimisation

2.3.1.1 Learning Phase

The learning phase commences with initializing, as per equation 32, each neuron's weight, w_i, with a random value between 0 and 1, the learning rate $\eta(n)$ to 1, and the maximum number of iterations, $n\,max$, to 1000. $\eta(n)$ is a training parameter that controls the size of the weight vector during the learning phase of NN-SOM.

$$w_1 = [w_{j1} \dots \dots w_{jm}]\mathrm{T} \quad (32)$$

$\eta(n)$ = 1

$n\ max$ = 1000

We adapt an unsupervised NN approach which is typical of Kohonen's NN-SOM, for which no labelled training data is required during the learning process; instead it learns from input data [150]. Following initialization, a stimulus, i.e. a random representative input sample from the data set, x, is presented to the network for training, as per equation 33.

$$x = [x_1 \dots \dots x_m]\mathrm{T} \tag{33}$$

All inputs (x) used for training the network are sourced from inputs of adapted propagation models at several LAP altitudes. The learning phase then proceeds with the definition of the topological map, M_A, using a lattice of neurons, A, as per equation 34.

$$\mathrm{M}_A = \begin{cases} \Psi_{A\to X} : X \to A; & x \in X \to s(x) \in A \\ \Psi_{X\to A} : A \to X; & i \in A \to w_i \in X_i \end{cases} \tag{34}$$

$x_U = [\text{Predictions of urban evirements at adapted propagation models at several LAP altitudes}]$

$x_S = [\text{Predictions of suburban evirements at adapted propagation models at several LAP altitudes}]$

$x_R = [\text{Prediction of rural evirements at adapted propagation models at several LAP altitudes}]$

The map, $\mathrm{M}_A = \Psi_{A\to X}, \Psi_{X\to A}$, defines concurrently two mappings, from an input vector $x \in X$ to a neuron $\mathrm{i} \in A$, and an inverse mapping from neuron $i \in A$ to a weight vector $w_i \in X$. Finally, with each input pattern all neurons attempt to compute the Best Matching Unit (BMU) by calculating the Euclidean distance between the input vector and the weights of each neuron. The shortest distance between a matching winning neuron and the input data x is declared as the BMU as per equation 35, where m denotes the dimension of the input pattern, $d_{j,i}$ denotes the distance between two neurons i and j.

$$d_{w,x} = \sqrt{\sum_{m=1}^{n}\left(x_m - w_{jm}\right)^2} \tag{35}$$

2.3.1.2 Adaptive Phase

The adaptive phase involves updating of synaptic weight vectors of winning neuron and neighbors as per equations 36 and 37, where $\boldsymbol{h_{j,i}}$ denotes a function of topological neighborhood to measure how close the neurons **i** and **j** are, σ is the effective width of the neighborhood which decreases with each iteration, σ_0 is the initial value of σ, and $\boldsymbol{\tau}$

is the time constant defining the slope of the graph. The winner neuron updates itself and its neighbor neurons with the patterns of the input dataset using synaptic weight adjustments as per equation 38, where $w_j(n)$ stops the weight from going to infinity. Topological ordering of clusters to detect rapidly both different and similar clusters gets underway and over the course of this phase, the algorithm converges to the most suitable clusters. The neighborhood function is a Gaussian [147-153].

In equation 39, each minimax parameter is optimised through its updated synaptic weight $w_j(n+1)$, whereby it attempts to optimise the values of the vector, minimizing PL, maintaining SINR, and maximizing RSS, Throughput, and Radius. M_j refers to each of the four propagation models and MOP refers to optimised model at each altitude at a specific environment. After each cycle, the parameters are recomputed, and new vectors are put on the converged map. Finally, the process is repeated through Equations 32-39 up to the maximum number of iterations (n), or no significant change in the map has occurred.

$$h_{j,i} = exp^{(\frac{-{d_{j,i}}^2}{2\sigma^2})} \tag{36}$$

$$\sigma(n) = \sigma_0 exp^{(\frac{-n}{\tau})} \quad , \quad \sigma_0 = 5 \tag{37}$$

$$w_j(n+1) = w_j(n) + \eta(n)\, h_{j,i(x)}(n)(x - w_j(n)) \tag{38}$$

$$\text{MOP} = \left[w_j(n+1) * \text{Mj}_{\min}(\text{PL}),\ w_j(n+1) * \text{Mj}_{\max}(\text{RSS}),\ w_j(n+1) * \text{Mj}_{\min<>\max}(\text{SINR}),\right.$$
$$\left. w_j(n+1) * \text{Mj}_{\max}(\text{Throughput}),\ w_j(n+1) * \text{Mj}_{\max}(\text{Radius})\right] \tag{39}$$

Generally, the NN-SOM has a two-dimensional lattice of neurons and each neuron is considered as a cluster. All neurons attempt each input pattern, where the selected one from the input pattern wins and gets activated. Further, the winner neuron updates itself and neighbour neurons to anticipate the distribution of the patterns in the input dataset, a process called “adaptation”. Comparable clusters then get side by side, a process called “topological ordering of clusters”, to support detecting both different and similar clusters rapidly. Figure 2.9 shows the output layer in the evolved optimised model. Although the number of clusters must be defined, defining the number of clusters can be solved by running the algorithm with varying numbers of clusters and selecting the most suitable clustering results based on the offered merits [148,152]. The learning process continues until the settings that are set by the user-defined parameters are achieved. The trained net is then used to classify the entire input.

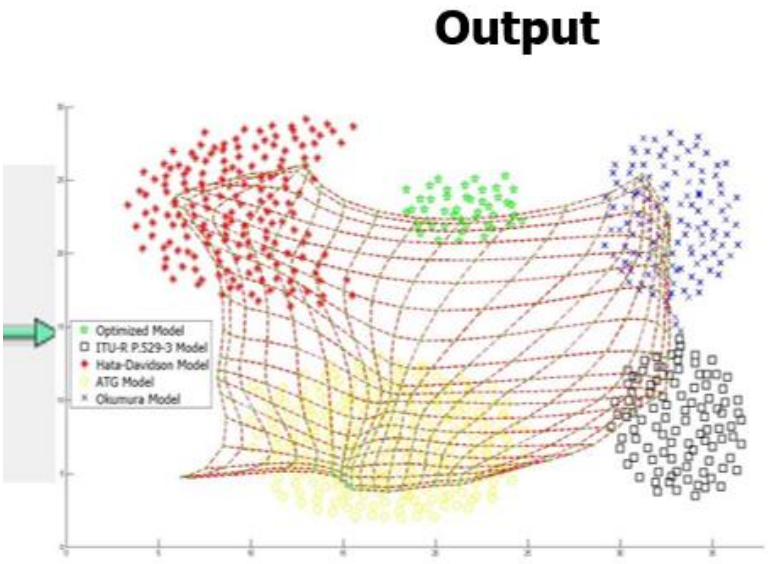

Figure 2.9: The output layer in the evolved optimised model

2.3.2 NN Feed Forward Fitting Tool Optimisation

The second step in optimisation deploys the Levenberg-Marquardt backpropagation algorithm using the NN Feed Forward Fitting Tool in MATLAB to evaluate the performance of the optimised set of parameters with the four simulated models. The NN fitting tool in MATLAB supports data selection, network creation and training, and network performance evaluation using Mean Square Error (MSE) and regression analysis. In the model optimisation stage, all output from the NN-SOM is entered as input to the NN Feed Forward Fitting Tool [152, 154-159]. The process of optimisation uses two matrixes, one populated with optimised model parameters and one populated with the parameters of the four adapted propagation models, as Figure 2.10 demonstrates.

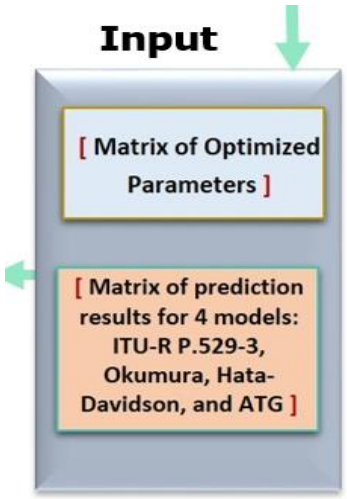

Figure 2.10: Input to the two-layer feedforward network

The NN design of a two-layer feedforward network consists of one hidden layer using a tan-sigmoid transfer function, and a linear neuron output layer, as Figure 2.11 below shows. This enables the network to learn of nonlinear and linear relations between input and output vectors. The linear transfer function, however, to the tan-sigmoid function, allows the network to produce values outside the -1 to + 1 range. NN suits multi-dimensional plotting problems well, given reliable data and adequate neurons in its hidden layer. Adjusting weights and biases during training of a network are considered to minimize a network performance function that uses the MSE, the correlation and average squared error between the network outputs and target outputs [152, 154-159].

Another design decision is the choice of the training function. The Levenberg-Marquardt backpropagation algorithm uses the Hessian matrix approximation of Newton's method, which is regarded as faster and more accurate near an error minimum. Thus, the scalar $\boldsymbol{\mu}$ decreases after each drop-in performance function, which means the performance function is continuously reduced at each iteration of the algorithm. The Hessian matrix can be approximated as:

$$H = JT^{J} \tag{40}$$

The gradient is calculated as:

$$g = J^{T} e \tag{41}$$

The Hessian matrix approximation of Newton's method is as:

$$xk + 1 = xk - [JT^{J}\mu J]^{-1} J^{T} e \tag{42}$$

Where $\boldsymbol{J}$ is a Jacobian matrix which consists of first values of the network errors in consideration of the assigned weights and biases and $\boldsymbol{e}$ is a vector of network errors. The Jacobian matrix can be computed via a backpropagation technique that is less complex than the Hessian matrix. The available input vectors and target vectors are randomly divided into three sets; training which makes offerings to the network while training, and in turn the network is tuned in response to errors, hence, calculating the gradient and updating the weights and biases; validation which measures network generalization and stops training when generalization halts improving; Testing which delivers an autonomous measure of performance during and after training, thus with no effect on training [152, 154-159].

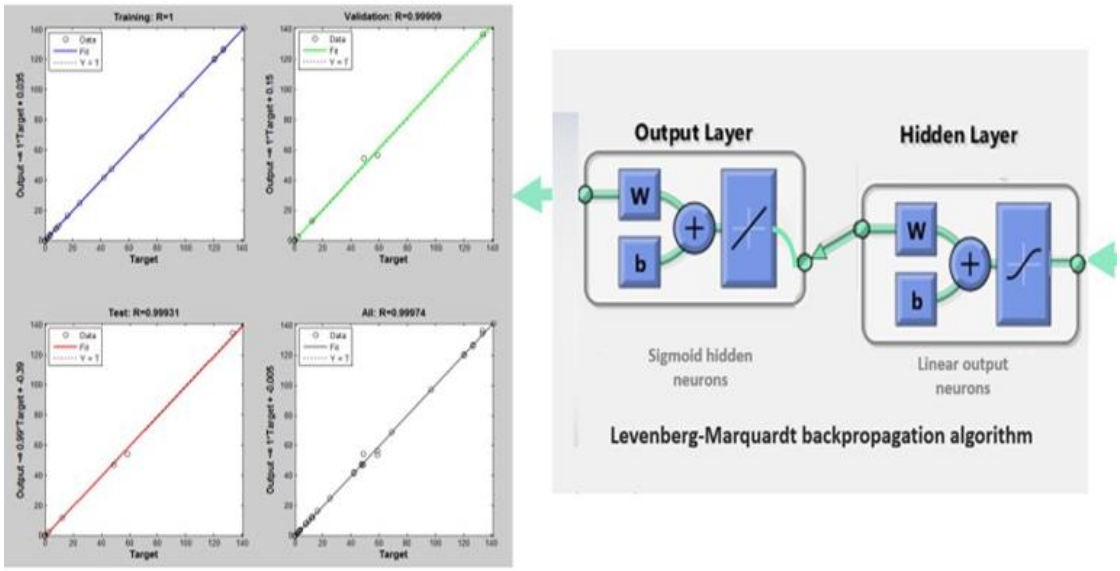

Figure 2.11: The Levenberg-Marquardt Backpropagation Algorithm

The flowchart in Figure 2.12 illustrates the steps of how the Levenberg-Marquardt algorithm of the NN fitting process occurs using MSE and regression analysis. This includes selecting data, creating and training a network, and evaluating performance.

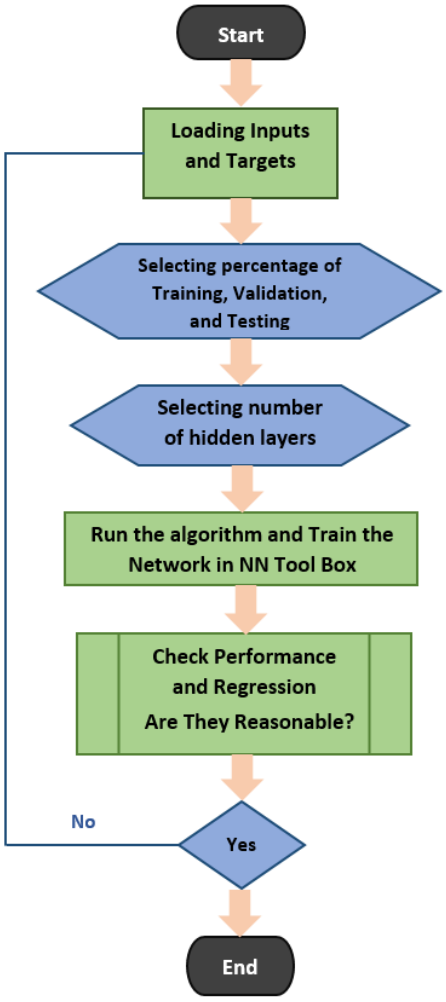

Figure 2.12: Flowchart of NN Feed Forward Fitting Tool Optimisation

2.4 Evolution Example

Table 2.4 shows a (4x5) matrix of four adapted propagation models with five link budget parameter predictions at a LAP altitude of 0.2km above ground in an urban environment that has been used as input to the optimisation framework to evolve an optimal set of parameters to an optimal propagation model.

Table 2.4: Matrix of four adapted propagation models

Model	Parameters				
	-PL (dB)	-RSS (dBm)	SINR (dB)	Throughput (Mb/S)	Radius (km)
ITU-R P.529-3	128.18	53.18	6.65	2.83	2
Okumura	114.70	39.70	4.97	4.65	2
Hata-Davidson	139.55	64.55	8.07	2.09	2
ATG	115.96	40.96	5.12	3.87	3

At first the NN-SOM defines the NN map and then trains the network using the predictions on the matrix of Table 2.4. Then, a minimax technique optimises each parameter using their evolving synaptic weight, i.e. minimize PL, maximize RSS, throughput and coverage radius whilst maintaining the SINR level. The adaptive process is repeated until either to a predefined number of iterations, or no significant change in the map has occurred. The final output is clustered on the map as per Figure 2.9 and the evolved set of optimal parameters populate the propagation model as shown on Table 2.5.

Table 2.5: Matrix of optimised model

Model	-PL (dB)	-RSS (dBm)	SINR (dB)	Throughput (Mb/S)	Radius (km)
Optimised	108.11	35.42	5.17	4.78	4

The Levenberg-Marquardt backpropagation algorithm uses the NN Feed Forward fitting to evaluate the performance of the optimised set of parameters in comparison to those of the four adapted models as shown on Figure 2.13. In this selected example, the numerical predictions of the optimised set of parameters show improvement across the five parameters of the link budget in comparison to the four adapted propagation models. Further and more detailed examples are presented in chapter 4.

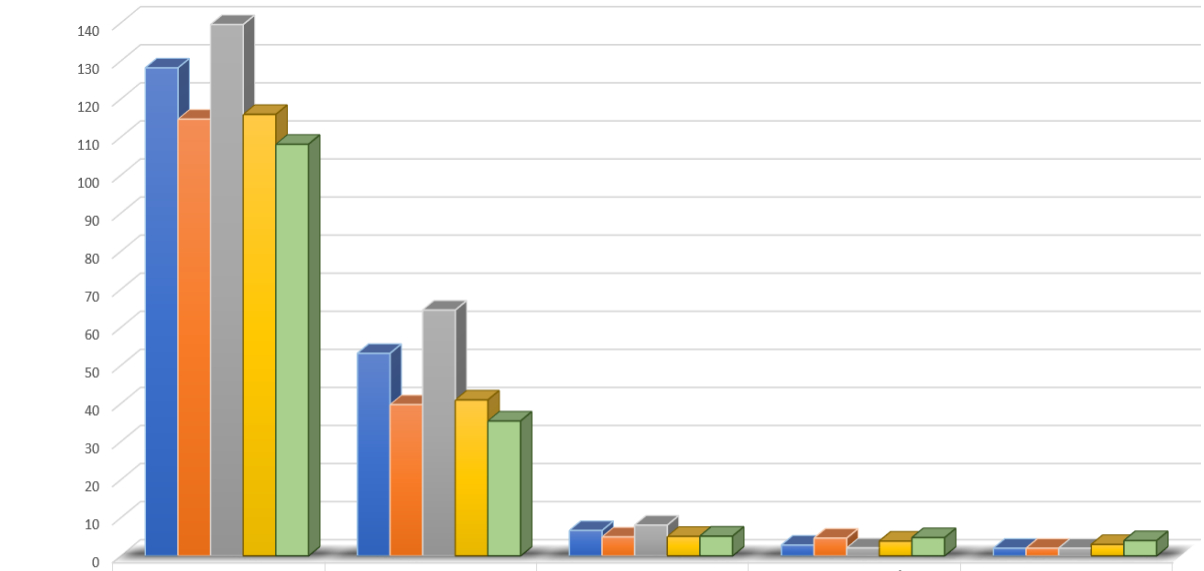

	PL (dB)	RSS (dBm)	SINR (dB)	Throughput (Mb/S)	Radius (km)
ITU-R P.529-3	128.18	53.18	6.65	2.83	2
Okumura	114.7	39.7	4.97	4.65	2
Hata-Davidson	139.55	64.55	8.07	2.09	2
ATG	115.96	40.96	5.12	3.87	3
Optimized	108.11	35.42	5.17	4.78	4

Figure 2.13: A comparison between the parameters in the optimal and adapted models

2.5 Summary

This chapter has discussed the framework that evolved the optimal propagation model for last-mile connectivity using LAPs. This has been achieved by first selecting and then adapting four representative propagation models and then using NN-SOM alongside its NN Feed Forward Fitting Tool to evolve the optimal propagation model. The process is concluded with an evolution example. The following chapter discusses the implementation of the four adapted propagation models and the evolution of the optimal propagation model and also presents reports on the deployment of the optimised propagation model in a WSN as well as in a cellular structure across a range of different environments in KSA.

Chapter 3 : Implementation of Propagation Model Optimisation

This chapter details the implementation of the chapter 2. It details the MATLAB implementation of the four adapted propagation models, the optimisation of a propagation model using NN-SOM, and the assessment of the evolved model performance using the NN Feed Forward Fitting Tool. It concludes with reporting on the deployment of the optimised propagation model in a WSN, and a cellular structure across a range of different environments in KSA. Figure 3.1 gives an overview of implementation and deployment of a LAP as an aerial BS to serve the last mile connectivity to terrestrial users. It, also, shows a propagation model with two path loss components: FSPL, and an additive path loss due to shadowing effects.

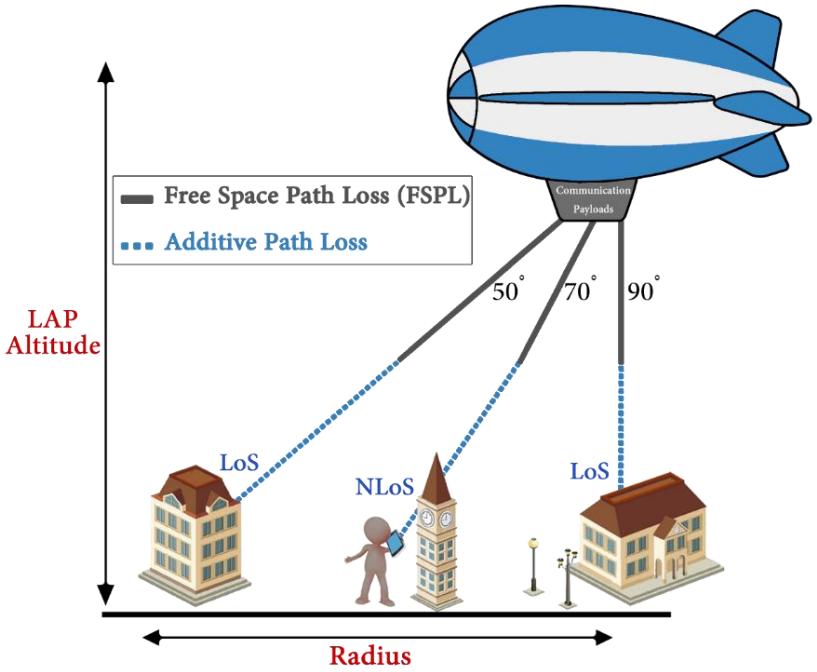

Figure 3.1: Deploying a LAP as an aerial BS to serve last mile connectivity

Figure 3.2 maps the design of chapter 2 to the implementation, as three phases. Phase 1 maps the process of calibration of PL with each of the four adapted propagation models to its MATLAB code and checks the MAPL threshold. Phase 2 maps the process of determining the link budget parameters with each propagation model to its MATLAB code. Phase 3 maps the evolution of the optimised propagation model using two NN optimisation techniques to their MATLAB code. The algorithms for each phase are presented on Tables 3.2, 3.3, 3.4, 3.6, and 3.8 as well as demonstrated on Figures 3.3 to 3.7.

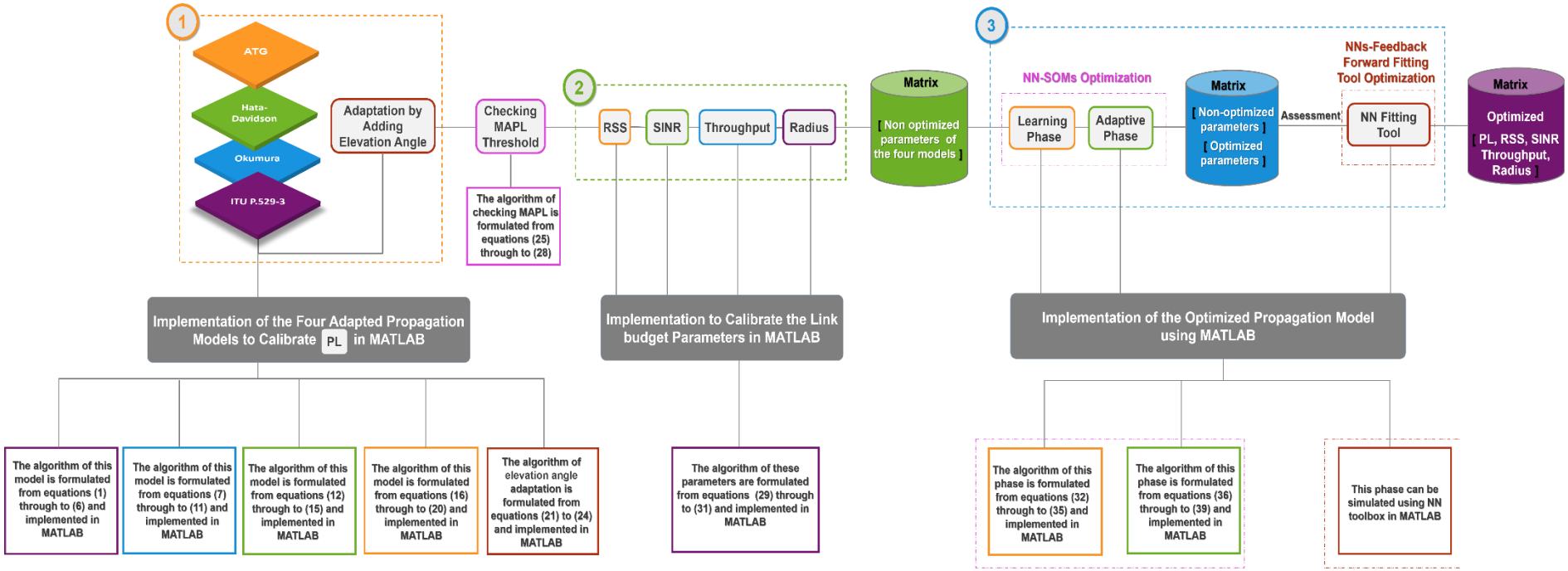

Figure 3.2: Mapping the design to its implementation

3.1 Implementation of the Adapted Propagation Models

The four adapted propagation models have been simulated under the same conditions using MATLAB. Our simulations have produced predictions over a wide range of LAP altitudes across all terrains and with due consideration to a fuller range of link budget parameters using WiMAX MIMO antenna specifications. Alongside the adoption of MIMO functionality antennas, and elevation this yields an extended coverage range, multipath management opportunities, and interference mitigation. Table 3.1 shows the simulation parameters that relate to MIMO antenna specifications as used by Airspan's 3.5GHz WiMAX [160]. Table 3.2 maps their formal definition with equations (1) through to (31) to the MATLAB implementation of each of the adapted propagation models. Execution of the algorithm starts at a LAP altitude of 0.2 km in an urban environment with BS antenna gain. This is then repeated for Handset (HS) antenna gain at different LAP altitudes and environments. Overall this is executed 96 times to predict the full range of link budget parameters [147].

Table 3.1: Simulation parameters specification

Parameters	Value
Frequency band [GHz]	3.5
Bandwidth [MHz]	10
Modulation type	QPSK
Noise figure [dBm]	6
Elevation angel for Urban	15°
Elevation angel for Suburban	10°
Elevation angel for Rural	5°
Transmitter side	
Transmitter Power [dBm]	40
Transmitter Antenna Gain [dBi]	17
Diversity gain [dBi]	6
Transmitter Rx Sensitivity [dBm]	-88.9
Interference margin loss [dB]	3
Connector loss [dB]	0.3
LAP altitude (km)	0.2, 1, 2.5, 5
Receiver side	
Receiver Power [dBm]	27
Receiver Antenna Gain [dBi] (stations)	15
Receiver Antenna Gain [dBi] (handset)	2
Diversity gain [dBi]	3
Receiver Rx Sensitivity [dBm]	-90.9
Interference margin loss [dB]	3
Connector loss [dB]	0.1
Body loss [dB]	0
Receiver antenna height (m)	1, 5

Table 3.2: Formal definition to MATLAB Implementation of each adapted propagation model

Implementation of ITU-R P.529-3 propagation model

Calculation of path loss P_L – Case 1: Urban area

$$P_L = 69.55 + 26.16\log(f) - 13.82\log(h_t) - a(h_r) + [44.9 - 6.55\log(h_t)] \times [\log(d)]^b \quad (1)$$

$$a(h_r) = 1.11\log(f) - 0.7(h_r) - [1.56\log(f) - 0.8] \quad (2)$$

$$b = 1 \quad \text{for } d \le 20{,}000 \text{ m}$$

$$b = 1 + (0.14 + 1.87 \times 10^{-4}(f) + 1.07 \times 10^{-3}(h_t')\left(\log\left(\frac{d}{20{,}000}\right)\right)^{0.8} \quad \text{for } 20{,}000 \text{ m} < d < 100{,}000 \text{ m} \quad (3)$$

$$h_t' = \frac{h_t}{[1+(7\times10^{-6})\times(h_t)^2]^{\frac{1}{2}}} \quad (4)$$

Calculation of path loss P_L – Case 2: suburban area

$$P_L = P_{L(\text{urban})} - 2[\log\left(\frac{f}{28}\right)]^2 - 5.4 \quad (5)$$

Calculation of path loss P_L – Case 3: rural areas

$$P_L = P_{L(\text{urban})} - 4.78[\log(f)]^2 + 18.33\log(f) - 40.49 \quad (6)$$

```
ahr =(1.1*(log10(f))-0.7)* hr - (1.56*(log10(f))-0.8);
ht_1 = (ht/(1+(7*10^-6) *ht^2 ))^(1/2);

if d <= 20
    b = 1;
else
    b = 1+(0.14+1.87* 10^(-4) *f + 1.07*10^(-3) * ht_1)* (log10(d/20))^0.8;
end

PLu=69.55+26.16*log10(f)-13.82*log10(ht)-ahr+(44.9-6.55*log10(ht))*(log10(d))^b;

switch area_type
    case 'urban'
        path_loss = PLu;
    case 'suburban'
        path_loss = PLu - (2*(log10(f/28))^2)-5.4;
    case 'rural'
        path_loss = PLu-4.78*(log10(f))^2+18.33*log10(f)-40.49;
```

Implementation of Okumura propagation model

Calculation of path loss P_L

$$P_L = L_f + Amn(f,d) - G(h_t) - G(h_r) - G_{area} \quad (7)$$

$$L_f = 32.44 + 20\log(f) + 20\log(d) \quad (8)$$

$$G(h_t) = 20\log(h_t/0.2),\ 0.01\text{km} < h_t < 1\text{km} \quad (9)$$

$$G(h_r) = 10\log(h_r/3),\ h_r \le 3\text{m} \quad (10)$$

$$G(h_r) = 20\log(h_r/3),\ 10 > h_r > 3\text{m} \quad (11)$$

The values of Amn and G_{area} are predicted empirically in relation to the type of terrain correction factor

```
Ght = 20*log(ht/200);           % Transimtter Antenna Height Gain Factor
if(hr<3)                        % Reciver Antenna Height Gain Factor
    Ghr = 20*log(hr/3);
else
    Ghr = 10*log(hr/3);
end

Lf = 32.44+20*log10(f)+20*log10(d);      % Free Space Propagation Loss
switch area_type
    case 'urban'
        Garea=13;
    case 'suburban'
        Garea = 29;
    case 'rural'
        Garea = 35;
end
path_loss = Lf+Amu-Ght-Ghr-Garea;
```

Implementation of Hata-Davidson propagation model

Calculation of path loss P_L

$$P_LHD = P_LHata + A(h_t,d) - S_1(d) - S_2(h_t,d) - S_3(f) - S_4(f,d) \quad (12)$$

where:

$$P_LHata = 69.55 + 26.16\log(f) - 13.82\log(h_t) - a(h_r) + [44.9 - 6.55\log(h_t)]\log(d) \quad (13)$$

Calculation of path loss P_L – Case 1: for urban area

$$a(h_r) = (3.2[\log(11.75 \times h_r)]^2) - 4.9 \quad (14)$$

Calculation of path loss P_L – Case 2: for suburban or rural areas

$$a(h_r) = (1.1\log(f) - 0.7)(h_r) - (1.56\log(f) - 0.8) \quad (15)$$

A, S_1, S_2, S_3, S_4 are correction factors in relation to the type of terrain and distance

```
if d < 20
    S1 = 0;
    A = 0;

elseif d>=20 && d<=64
        A = 0.62137 * (d - 20) * (0.5 + 0.15 * log10(ht/121.92));
        S1 = 0;

else d>=65 && d<=300
    A = 0.62137 * (d - 20) * (0.5 + 0.15 * log10(ht/121.92));
    S1 = 0.174*(d - 64.38);
end


if ht > 300
    S2 = 0.00784 * abs(log10(9.98 /d)) * (ht - 300);
else
    S2 = 0;
end

S3 = (f / 250)*log10(1500/f);

if d > 64.38
    S4 = (0.112 * log10(1500/f))*(d - 64.38);
else
    S4 = 0;
end

switch area_type
    case 'urban'
        a_hr = 3.2*(log10(11.75 * hr))^ 2 - 4.97;
    case 'suburban'
        a_hr = (1.1*log10(f) - 0.7) * hr - (1.56*log10(f) - 0.8);
    case 'rural'
        a_hr = (1.1*log10(f) - 0.7) * hr - (1.56*log10(f) - 0.8);
end

PL_Hata = 69.55 + 26.16 * log10(f) - 13.82*log10(ht) - a_hr + (44.9 - 6.55 * log10(ht)) * log10(d);
path_loss = PL_Hata + A - S1 - S2 - S3 - S4;
```

Implementation of ATG propagation model

Calculation of the total path loss P_L

$$PL_T = \rho_{LoS} \times PL_{LoS} + \rho_{NLoS} \times PL_{NLoS} \quad (16)$$

The probability of having LoS connections at an elevation angle of θ is given by:

$$\rho_{LoS} = a - \frac{a-b}{1+[\frac{\theta-c}{d}]^e} \quad (17)$$

$$\rho_{NLoS} = 1 - P_{LoS} \quad (18)$$

The path loss for LoS and NLoS are:

$$PL_{LoS}\,(dB) = 20\log\frac{4\pi(f)(d)}{c} + \eta_{LoS} \quad (19)$$

$$PL_{NLoS}\,(dB) = 20\log\frac{4\pi(f)(d)}{c} + \eta_{NLoS} \quad (20)$$

a, b, c, d and *e* are ITU parameters in relation to the three types of environments

```
% The probability of having LoS connections at an elevation angle
R_LoS= (a-((a-b)/(1+((theta-c)/d)^e)))/100;

% The probability of having NLoS connections at an elevation angle
R_NLoS= 1- R_LoS;

% The path loss for LoS and NLoS are:
PL_LoS  = 20 * log10(dist)+ 20 * log10(f)+ 20 * log10(4*3.141/c_l)+EtaLoS;
PL_NLoS = 20 * log10(dist)+ 20 * log10(f)+ 20 * log10(4*3.141/c_l)+EtaNLoS;

% The total path loss

path_loss= R_LoS*PL_LoS+ R_NLoS*PL_NLoS;
end
```

Implementation of Elevation Angle Adaptation

$$\cos\theta = \frac{E_r}{E_r+H} \quad (21)$$

$$\theta = \cos^{-1}\frac{E_r}{E_r+H} \quad (22)$$

$$D = \theta.E_r \quad (23)$$

$$D = 2\,E_r[\cos^{-1}\left(\frac{E_r}{E_r+H} * \cos(\theta)\right) - \theta] \quad (24)$$

```
%Earth Radius
Er = 6378;

% elevation angles for urban=15°, suburban=10°, and rural=5°
for theta=15

% Altitude
for H=1

 %The distance D of the four propagation models is computed based on elevation angle θ as follows
D = 2*Er*((acosd((Er/(Er+H))*cosd(theta))-theta))
end
end
```

Implementation of MAPL Threshold

Down Link Threshold

$$MAPL = EIRP + R_s + G(h_t) - losses \quad (25)$$

$$EIRP = P_t + G(h_r) - Losses \quad (26)$$

Up Link Threshold

$$MAPL = EIRP + R_s + G(h_r) - losses \quad (27)$$

$$EIRP = P_t + G(h_t) - Losses \quad (28)$$

The MAPL threshold value needs to be calculated for both UL and DL with the smallest value of the two set as path loss threshold.

```
%Down Link Threshold
MAPL_D = [EIRP_D + Rs + GT - L];

EIRP_D= [PT + GR - L];

%Up Link Threshold
MAPL_U = [EIRP_U + Rs + GR - L];

EIRP_U= [PT + GT - L];
```

Implementation of Link Budget Parameters

$$RSS = P_t + G(h_t) + G(h_r) - P_L - L \quad (29)$$

$$SNIR\,(dB) = \frac{RSS}{N+I} \quad (30)$$

$$C = B \times \log(1 + SNIR) \quad (31)$$

PL is estimated in relation to distance

```
PL = Model_type1;
RSS = PT + GT + GR - PL - L;
SNIR = RSS / (N + I);
THROUGHPUT = B * log2(1 + (10^(SNIR/10)));

for d = 1:1:100
    PL = Model_type1;
    RSS = [RSS (PT + GT + GR - PL(end) - L)];
    SNIR = [SNIR (RSS(end) / (N + I))];
    THROUGHPUT = [THROUGHPUT (B * log2(1+(10^(SNIR(end)/10))))];
end
```

3.2 Implementation of the Optimised Propagation Model

The NN-SOM has been used alongside its NN Feed Forward Fitting Tool to evolve an optimal set of parameters in a propagation model. The optimisation process takes as input the four adapted propagation model predictions at several LAP altitudes process and after using minimax it clusters the parameters using NN-SOM. It then deploys the Levenberg-Marquardt backpropagation algorithm using the NN Feed Forward Fitting Tool to evaluate the performance of the optimised set of parameters against those of the four adapted models.

3.2.1 Implementation of the NN-SOM

The implementation uses a minimax technique and visualizes the cluster results, so that the resulting patterns are open to interpretation. The NN-SOM algorithm runs over the Learning and Adaptive phases formally defined by equations (34) through to (39). Each run takes approximately 2h to converge. Table 3.3 maps the formal definition of the optimised model to its MATLAB Implementation that yields optimised propagation model parameter predictions across various LAP altitudes and environments when executed. The adapted unsupervised NN approach is typical of Kohonen's NN-SOM for which no labelled training data is required during the learning process but instead it learns from input data. All input ($\mathbf{x}$) used for training the network is sourced from the adapted propagation models' predictions which have been collected at several LAP altitudes across three terrains urban, suburban, and rural for both BS and HS antennas.

PL is minimised to achieve a high level of reception but with the smallest attenuated signal not exceeding the MAPL, i.e. [-146.5 dB … -133.5 dB], for BS and HS respectively. RSS is maximised to achieve a wider wireless connectivity, and to avoid service degradation and/or interruption. SINR is maintained between 4dBi and 19dBi. A threshold for RSS and SINR for both BS and HS antennas depends on modulation methods and receiver sensitivity as in the WiMAX link budget specification of Table 3.1. The RSS value is kept below -91dBm [161, 162]. Throughput and coverage radius are both maximised to achieve higher data rates and wider connectivity.

Table 3.3: Formal definition to MATLAB Implementation of the optimised model

Formal Definition	MATLAB code
Defining the SOM Architecture	
$w_1 = [w_{j1} \dots \dots w_{jm}]\mathrm{T}$ (32) $x = [x_1 \dots \dots x_m]\mathrm{T}$ (33) $\mathrm{M}_A = \begin{cases} \Psi_{A\to X} : X \to A; & x \in X \to s(x) \in A \\ \Psi_{X\to A} : A \to X; & i \in A \to w_i \in X_i \end{cases}$ (34)	16 %% ========== Define the SOM Architecture ========== 17 % Determine the number of rows and columns in the self-organizing map 18 somRow = 20; 19 somCol = 20; 20 21 % Number of iteration for convergence 22 Iteration = 1000; 23 24 %%========== Parameter Setting For SOM ========== 25 % Initial size of topological neighbourhood of the winning neuron 26 width_Initial = 15; 27 28 % Time constant for initial topological neighbourhood size 29 t_width = Iteration/log(width_Initial); 30 31 % Initial time-varying learning rate 32 learningRate_Initial = 1; 33 34 % Time constant for the time-varying learning rate 35 t_learningRate = Iteration;

Computing the Neighbourhood

$$d_{w,x} = \sqrt{\sum_{m=1}^{n} (x_m - w_{jm})^2} \quad (35)$$

```
    neighbourhood_Function = zeros(somRow, somCol);

    for r = 1:somRow
       for c = 1:somCol
           if (r == win_Row) && (c == win_Col)
               % neighborhood function for winning neuron
               neighbourhood_Function(r,c) = 1;
           else
               % % neighborhood function for other neurons
               distance = (win_Row - r)^2+(win_Col - c)^2;
               neighbourhood_Function(r,c) = exp(-distance/(2*width_Variance));
```

Finding the Best Match

$$h_{j,i} = exp^{\left(\frac{-d_{j,i}^2}{2\sigma^2}\right)} \quad (36)$$

$$\sigma(n) = \sigma_0 exp^{\left(\frac{-n}{\tau}\right)}, \quad \sigma_0 = 5 \quad (37)$$

```
function [euclidean_Distance, i] = findBestMatch( train_data, somMap, somRow,...
                                   somCol, dataRow, dataCol )
% This function finds the best matched code vector (Winning neuron) based
% on the input image
%
    % Initialize matrix for storing the Euclidean distance between the input
    % vector and each neuron
    euclidean_Distance = zeros(somRow, somCol);

    i = randi([1 dataRow]);

    for r = 1:somRow
        for c = 1:somCol
            V = train_data(i,:) - reshape(somMap(r,c,:),1,dataCol);
            euclidean_Distance(r,c) = sqrt(V*V');
        end
```

Updating the Weights

$$w_j(n+1) = w_j(n) + \eta(n)\, h_{j,i(x)}(n)(x - w_j(n)) \quad (38)$$

```
function WeightVectorUpdated = updateWeight(  train_data, somMap, somRow, ...
                    somCol, dataCol, index, learningRate, neighborhood)
% This function update the weight of all the neurons depending on the
% distance between winning neuron and other neuron

   WeightVectorUpdated = zeros(somRow, somCol, dataCol);

   for r = 1: somRow
      for c = 1:somCol

          % Reshape the dimension of the current weight vector
          currentWeightVector = reshape(somMap(r,c,:),1,dataCol);

          % Update the weight vector for each neuron
WeightVectorUpdated(r,c,:) = currentWeightVector + learningRate*neighborhood(r,c)*(train_data(index,:)-currentWeightVector);

      end
```

MiniMaxing Parameters

$$M_{opt} = \left[w_j(n+1) * \mathrm{Mj}_{\min}(\mathrm{PL}),\ w_j(n+1) * \mathrm{Mj}_{\max}(\mathrm{RSS}),\ w_j(n+1) * \mathrm{Mj}_{\min<>\max}(\mathrm{SINR}),\ w_j(n+1) * \mathrm{Mj}_{\max}(\mathrm{Throughput}),\ w_j(n+1) * \mathrm{Mj}_{\max}(\mathrm{Radius})\right] \quad (39)$$

```
    %% ================== Check parameter limits (upper and lower bounds) ==

    param1=PL;
    param2=RSS;
    param3=SINR;
    param4=Throughput;
    param5=Radius;

        case 1
        if (param1*(updateWeight) < 146.5 )
          param11 = param1*(updateWeight);
        end
       case 2
        if (param2*(updateWeight) < 91 )
          param22 = param2*(updateWeight);
        end
      case 3
        if ( param3*(updateWeight) > 4 && param3*(updateWeight) < 19 )
          param33 = param3*(updateWeight);
        end
      case 4
        param44 = param4*(updateWeight);
      case 5
        param55 = param4*(updateWeight);
  end
```

3.2.2 Implementation of the NN Feed Forward

The output of the NN-SOM and the predictions obtained from the four simulated models are used as input to NN Feed Forward fitting tool. The optimisation process uses the Levenberg-Marquardt backpropagation algorithm alongside the NN Feed Forward Fitting Tool to evaluate the performance of the evolved set of parameters against those of the four simulated models. The network learns of nonlinear and linear relations between input and output vectors. The linear transfer to the tansigmoid function allows the network to produce values outside the range of [-1 … + 1]. NN suits multi-dimensional plotting problems assuming reliable data and adequate neurons in its hidden layer. Figure 3.3 shows the formal definition of the NN Feed Forward Tool. Figures 3.4 through to 3.7 depict its implementation using the NN MATLAB toolbox.

The Hessian matrix can be approximated as:

$$H = JT^J \tag{40}$$

The gradient is calculated as:

$$g = J^T e \tag{41}$$

The Hessian matrix approximation of Newton's method is as:

$$xk + 1 = xk - [JT^J \mu J]^{-1} J^T e \tag{42}$$

Figure 3.3: Formal definition of the NN Feed Forward

Figures 3.4 and 3.5 show the percentage of Training, Validation, and Testing, as well as assigning the optimum number of hidden layers needing to be adjusted several times in order to obtain optimal performance and regression. Figures 3.6 and 3.7 show training and evaluation. Validation uses regression plotting to determine the optimal number of iterations during which validation produces a minimal value. After initial training of the NN model, the performance changes after each training iteration. This training set and validation set decreases continuously to the point where overfitting happens, and thus the error rate increases. Understanding the NN training performance, Regression plots, and Error Histogram plot for Training data can give additional verification of network performance.

Figure 3.8 visualises the final output matrices of Figure 3.2. The blue cylinder depicts a matrix of non-optimised and evolved optimised model parameters clustered in groups by the NN-SOM. The purple cylinder depicts a matrix of optimised parameters following their evaluation using MSE and regression analysis.

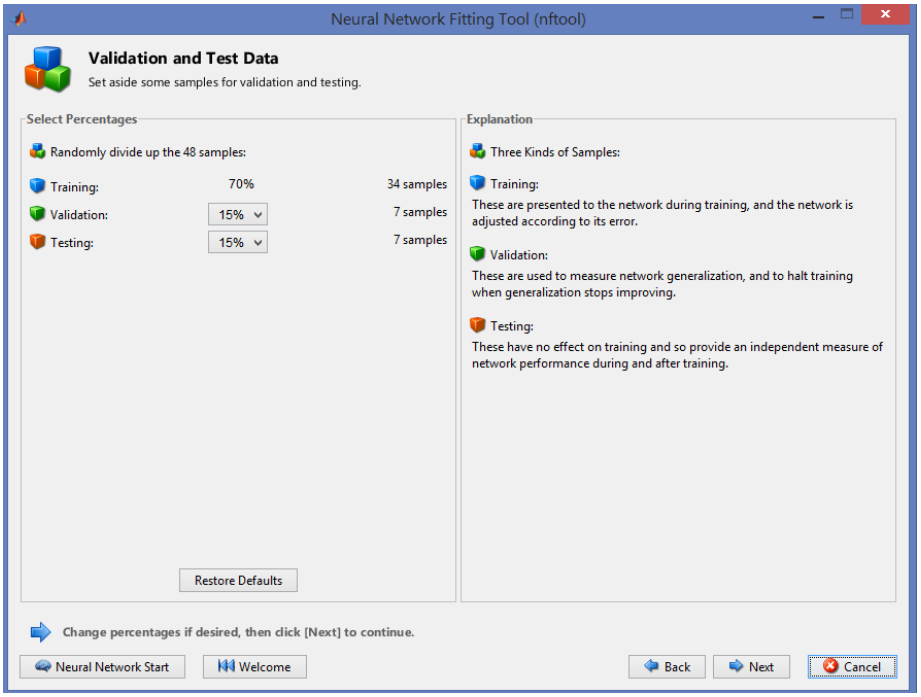

Figure 3.4: Input and target vectors settings using the MATLAB NN fitting tool

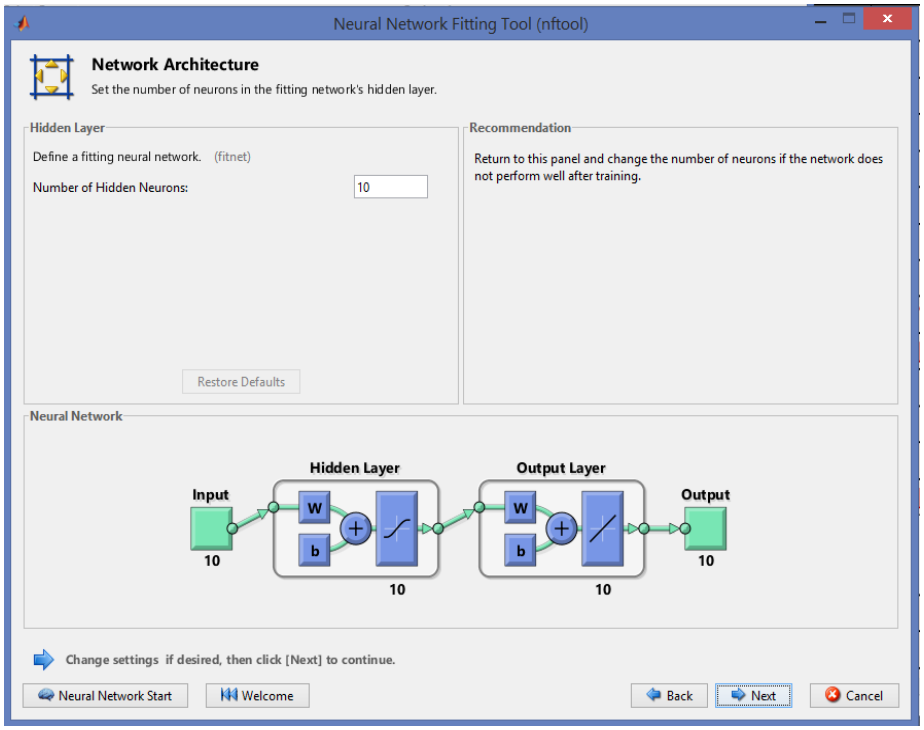

Figure 3.5: Defining optimum number of Neurons using the MATLAB NN fitting tool

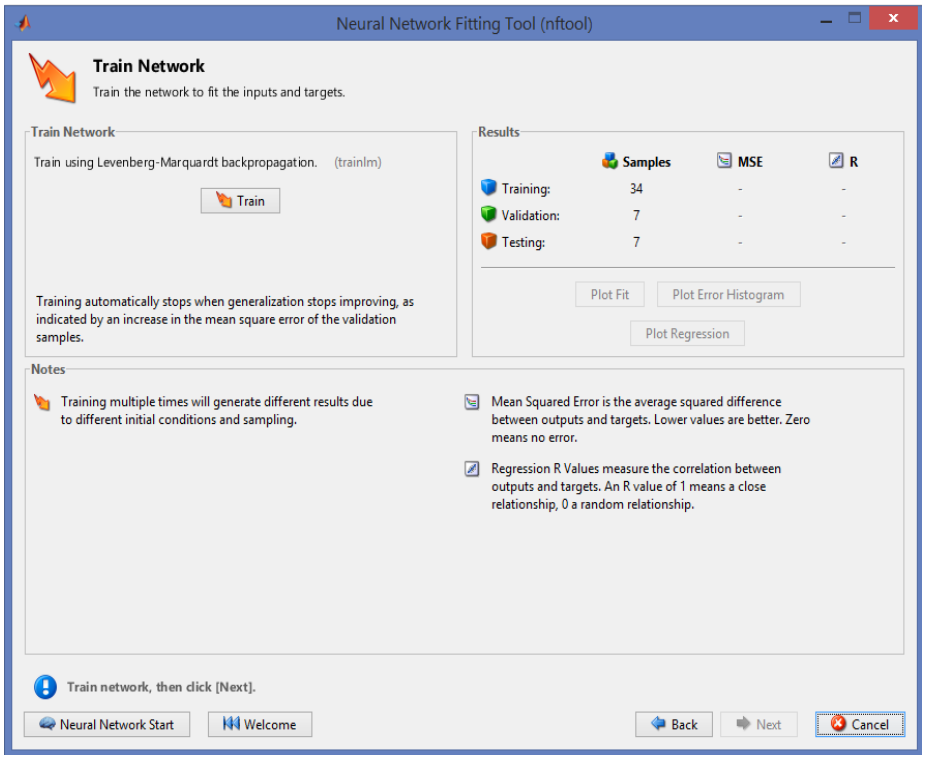

Figure 3.6: Training and measuring MSE using the MATLAB NN fitting tool

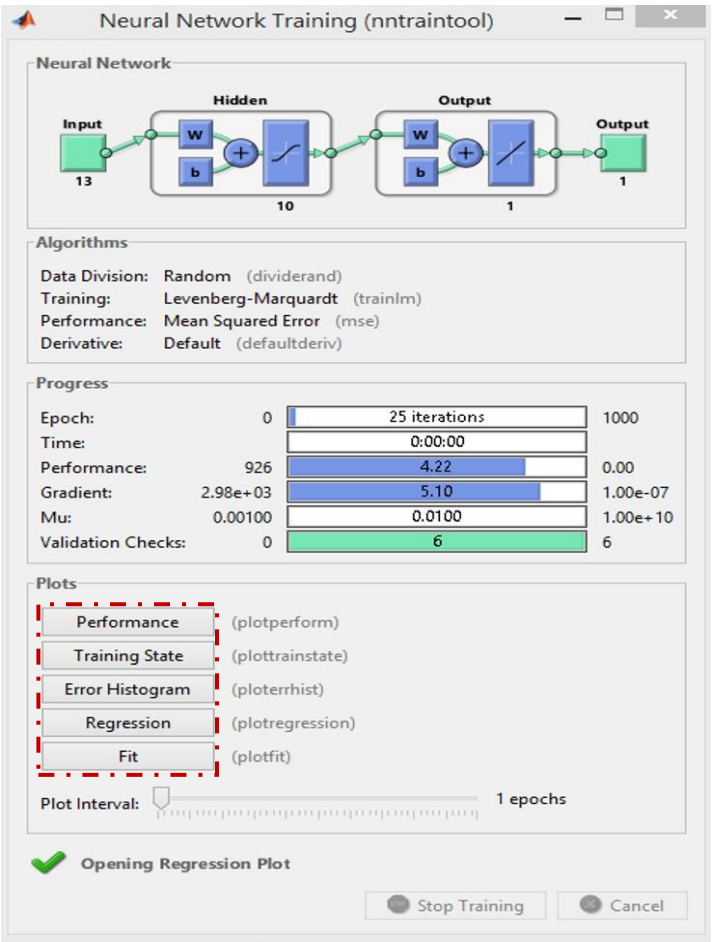

Figure 3.7: Evaluating parameter performance using the MATLAB NN fitting tool

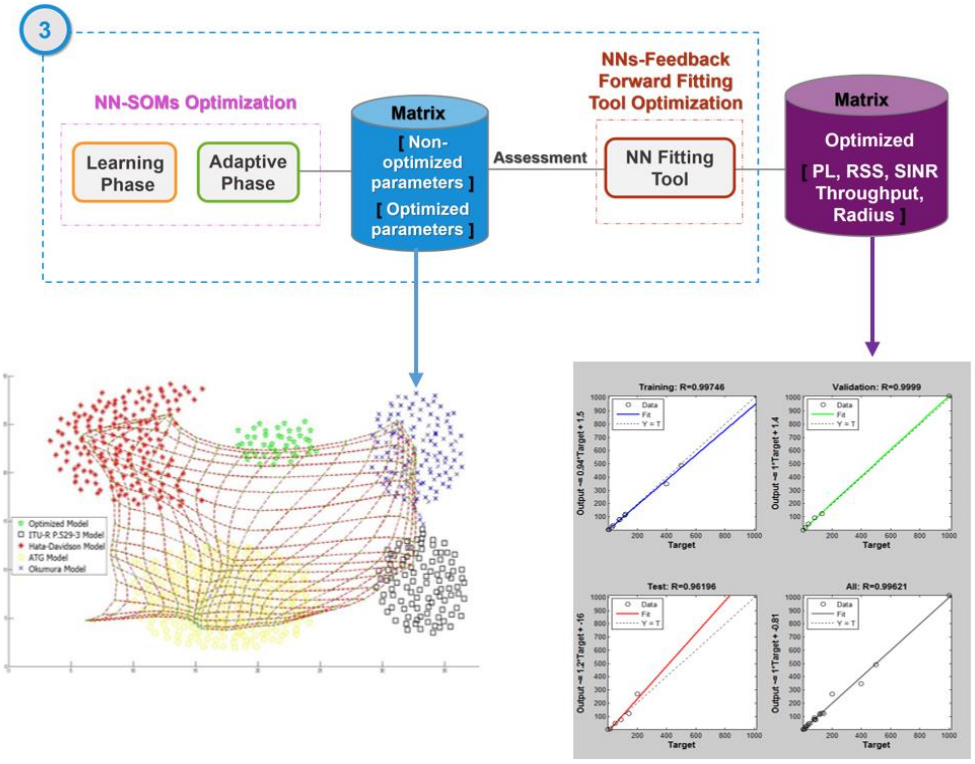

Figure 3.8: Visualisation of final output matrices

3.3 Optimised Model Deployment

In this section, we present the deployment of the optimised model in a WSN in which energy per bit to noise power spectral density ratio (Eb/No) and the BER performance of an AWGN channel are compared against that of the non-optimised models. We then present the deployment of the optimised model in a cellular structure design in which one of the Grade of Service (GoS) parameters the Probability of Blocking (P_B) performance is compared against that of the non-optimised models across various KSA environments.

3.3.1 WSN Deployment

The deployment showcases the usefulness of developing an optimised propagation model not only for telecommunications in general, but also for WSNs that serve cutting-edge technologies in applications such as disaster relief, security, surveillance, traffic control, and IoT. Such an Ad Hoc network may contain several remote sensors that collect ground segment data as Figure. 3.9 illustrates [67-71].

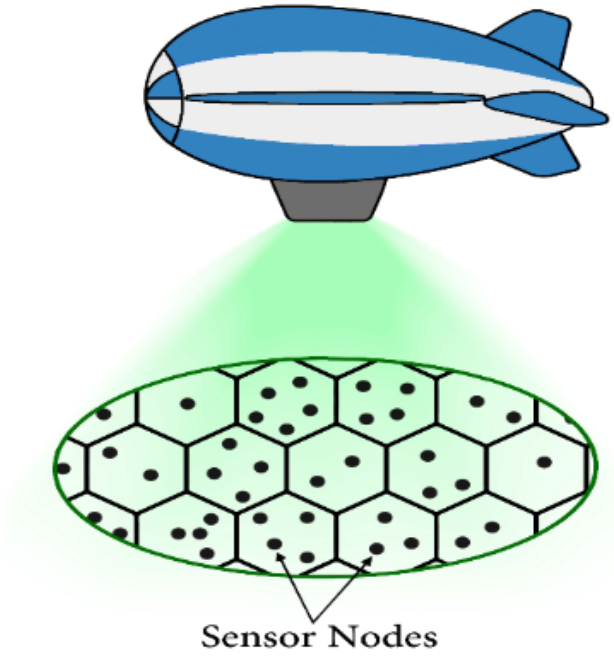

Figure 3.9: LAP-WSNs architecture

The link quality between a LAP sink and ground sensors relies on many factors such as elevation angle between the LAP and the sensors, operation frequency, transmission power, transmit and receive antenna gains, RSS, atmospheric conditions, bit rate and link distance. The NN-optimised model may address two WSN issues: channel impairments because of high path losses and fading problems, lifetime because of battery, propagation path loss, and antennas type. Therefore, an initial consideration of an optimised propagation model promises not only to extend the coverage range and reduce fading, but also to optimise power consumption without using sensor power enhancements or external power sources because of the low propagation path loss and high RSS. The performance of wireless Ad Hoc networks may be analysed by considering their two main QoS indicators: the Eb/No and the BER which highlight the performance of different digital modulation schemes. These indicators are considered in the link budget in order to set QoS guarantees for the applications they serve. The proposed algorithms for WSN are shown on Figure 3.10 which flowcharts the calculation steps.

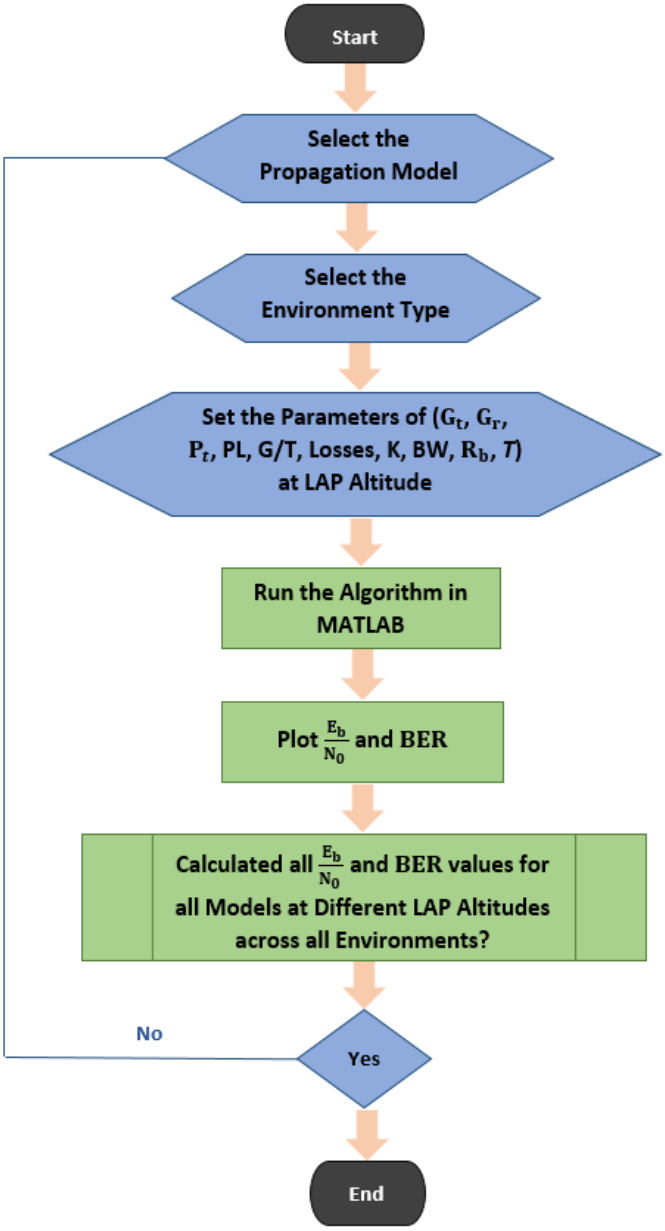

Figure 3.10: Flowchart of the WSN calculation

Setting the EIRP parameter values and path loss $\mathbf{P_L}$ from the initial four propagation models and the optimised model [163-166], the Eb/No can be expressed (in dBm) as:

$$\frac{E_b}{N_0} = \frac{C}{N} + 10\log BW - 10\log R_b \quad (43)$$

$$\frac{C}{N} = EIRP - P_L - A_R + \left(\frac{G}{T}\right) - 10\log\frac{K\,Bw}{0.001} \quad (44)$$

$$EIRP = P_t + G_t + G_r - L \quad (45)$$

$$\frac{G}{T} = G_r - 10\log T \quad (46)$$

Where C/N is carrier power measured in dB, BW is bandwidth measured in Hz, $\mathrm{R_b}$ is the data rate of WiMAX for specific QPSK modulation and bandwidth value set at 6.048 Mb/s. EIRP is measured in dBm, transmitter power ($\mathrm{P_t}$), transmitter antenna gains ($\mathrm{G_t}$), receiver antenna gains ($\mathrm{G_r}$) as well as (L) connector and cable loss, A_R is rain attenuation and atmospheric gas attenuation which are negligible, K is Boltzmann's constant (1.38065×10^{-23}), 0.001 represents a normalization, G/T the ratio of the receive antenna gain to system noise temperature measured in dB0, T is an effective temperature in this model (310K). The link performance indicator for signal quality is BER/Probability of Error which in turn is directly related to Eb/No. Thus, we calculate the BER as a function of Eb/No for a QPSK modulation in an AWGN channel as:

$$\mathrm{BER} = \frac{1}{2} erfc \sqrt{\frac{\mathrm{E_b}}{\mathrm{N_0}}} \tag{47}$$

Where $erfc$ is a complementary error function that describes the cumulative probability curve of Gaussian distribution. The algorithm for measuring the performance of WSN can be sourced form equations (43) to (47), where the predictions of the optimised model and non-optimised models are considered as inputs to predict Eb/No and BER results for both large and small antenna gain using the "semilogy" function in MATLAB. Table 3.4 shows the implementation of the WSN to validate the optimised model against the non-optimised models in relation to Eb/No and BER.

Table 3.4: Implementation of the WSN in MATLAB

Formal Definition	MATLAB code
Calculate Eb/No	

$\frac{\mathrm{E_b}}{\mathrm{N_0}} = \frac{\mathrm{C}}{\mathrm{N}} + 10\log \mathrm{BW} - 10\log \mathrm{R_b}$ (43)
$\frac{\mathrm{C}}{\mathrm{N}} = \mathrm{EIRP} - \mathrm{P_L} - A_R + \left(\frac{\mathrm{G}}{\mathrm{T}}\right) - 10\log\frac{K\,Bw}{0.001}$ (44)
$\mathrm{EIRP} = \mathrm{P_t} + \mathrm{G_t} + \mathrm{G_r} - \mathrm{L}$ (45)
$\frac{\mathrm{G}}{\mathrm{T}} = \mathrm{G_r} - 10\log T$ (46)
	`EbN0=(c/n)+(10*log10(BW))-(10*log10(Rb));`
	
	`c/n=EIRP-PL-AR+(G/T)-(10*log10((K)/(BW)/0.001));`
	
	`EIRP= Pt+Gt+Gr-L;`
	
	`G/T=GR-(10*log10(T));`

Calculate BER	

$\mathrm{BER} = \frac{1}{2} erfc \sqrt{\frac{\mathrm{E_b}}{\mathrm{N_0}}}$ (47)	`EbN0_dB = 0.2:0.2:40;`
	`EbN0 = 10.^(EbN0_dB/10);`
	`BER = 1/2.*erfc(sqrt(EbN0));`
	`figure(1)`
	`subplot(5,1,5)`
	`semilogy(EbN0_dB,BER,'-.g*')`
	`grid on`

3.3.2 Cellular Design Deployment

Full deployment of wireless communications in some KSA regions still experiences a coverage gap. This is not directly related to economic costs but the geomorphology of these areas which are vast and rugged. This research aims to shade light on this by deploying the optimised model across several KSA environments. This is done by tailoring a cellular structure network using LAPs to achieve coverage of the entire country with the purpose of closing coverage gaps. Additionally, it covers events that could benefit from a LAP network topology. Two proposed cell planning configurations have been considered in the literature via aerial platforms to divide the coverage area into one or multiple cells. Each configuration has its own advantages and applications. Results show that the performance of multicell outweighs single cell configuration [71].

In this research, we have considered a multiple-cells configuration to enhance the capacity due to frequency reuse through the application of a regular patterns of cells. P_B is one of the GoS benchmarks that is used to set the desired performance of a trunked system based on the obtained predictions of the non-optimised and the optimised models [167, 168].

The proposed algorithm to construct a cellular cell requires tuning the parameters of the central cell radius, beam width and number of tiers [169-171]. The current population density and distribution have been obtained from the Saudi central department of statistics and information and additional information obtained from [172] and [173] has been considered in the design too. Taking these parameters into consideration may meet the demand or nature of the planned area in KSA, hence help achieve five main goals. First, increase system capacity by applying a frequency reuse technique. Second, define the appropriate cells location. Third, deliver a wireless service via an approximate number and size of cells based on people density and planned area's size. Fourth, solves issues of coverage gaps between cells or cells overlap. Fifth, offer energy saving resources. Figure 3.11 shows the footprint of a beam formed using smart antenna MIMO arrays installed on-board platforms. Figure 3.12 illustrates a coordinate system of cellular structure [169-171].

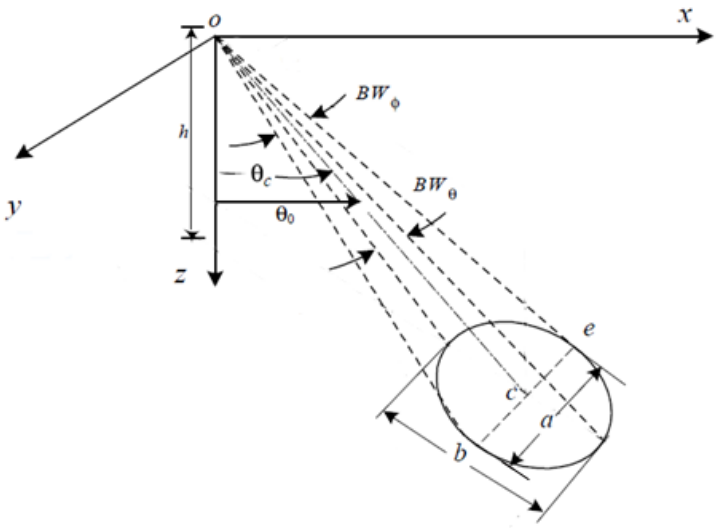

Figure 3.11: Aerial platforms cell footprint

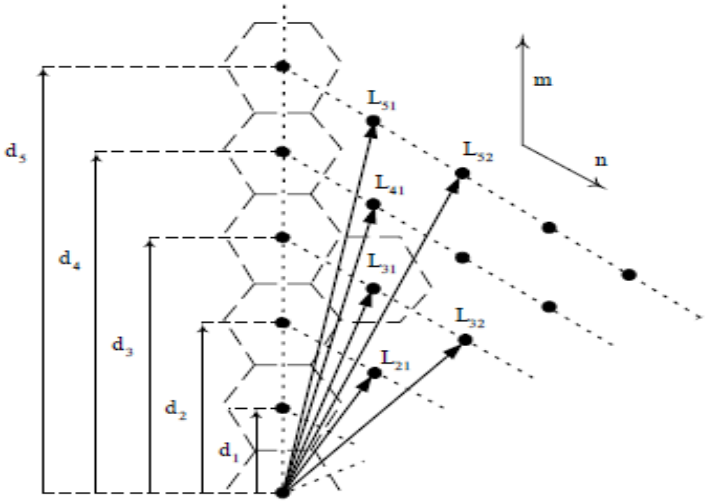

Figure 3.12: The co-ordinate system of cellular structure

The algorithm is sourced from equations (48) to (53) and the values of b, a, antenna beam widths, direction and platform altitude can be obtained as:

$$b = h\left(\tan\left(\theta o + \frac{BW\theta}{2}\right) - \tan\left(\theta o - \frac{BW\theta}{2}\right)\right) \quad (48)$$

$$a = 2h\ \sec(\theta c)\tan\left(\frac{BW\varphi}{2}\right) \quad (49)$$

$$\theta c = \tan^{-1}\left(\tan\left(\theta o - \frac{BW\theta}{2}\right) + \frac{b}{2h}\right) \quad (50)$$

$$Lmn = d1\sqrt{m^2 + n^2 - mn} \quad (51)$$

$$dm = ro\sqrt{3} \quad (52)$$

$$\alpha mn = \cos^{-1}\left(\frac{2m-n}{2\sqrt{m^2-mn+n^2}}\right) \quad (53)$$

Where *h* is the platform altitude in km, $\boldsymbol{\theta o}$ and $\boldsymbol{\theta c}$ are beams oriented towards a cell, $\boldsymbol{a}$ is a major axis and $\boldsymbol{b}$ is a minor axis, 3dB beam width in the elevation plane is

denoted by $\boldsymbol{BW\theta}$ and the azimuth plane is denoted by $\mathbf{BW\varphi}$. The hexagonal shape identifies the boundaries of the ground cell. In the cellular layout geometry, $\mathbf{m}$ and $\mathbf{n}$ denote cell coordinates. The radial distance $\mathbf{dm}$ represents a distance from the center cell that is below an LAP $\mathbf{Lmn}$ to the next cell by an azimuth angle $\boldsymbol{\alpha mn}$ that is measured from the vertical axis m. m and n are considered only in the first sector of the tier, whereas for other cells this is located by rotating the structure by 60◦ with the same central distance. $\mathbf{ro}$ is the central cell radius.

The flowchart on Figure 3.13 is used to display the tailoring of a cellular structure network using a LAP across different environments. By tuning the parameters of tailoring a cellular structure to meet the demand or nature of KSA, as well as considering the planned area's size and its population density as Table 3.5 demonstrates, we can design some patterns of cell structures, as representatives of their regions that have the same characteristics. Table 3.6 shows the MATLAB implementation of the cellular structure network via LAP, where the algorithm is sourced from equations (48) through to (53).

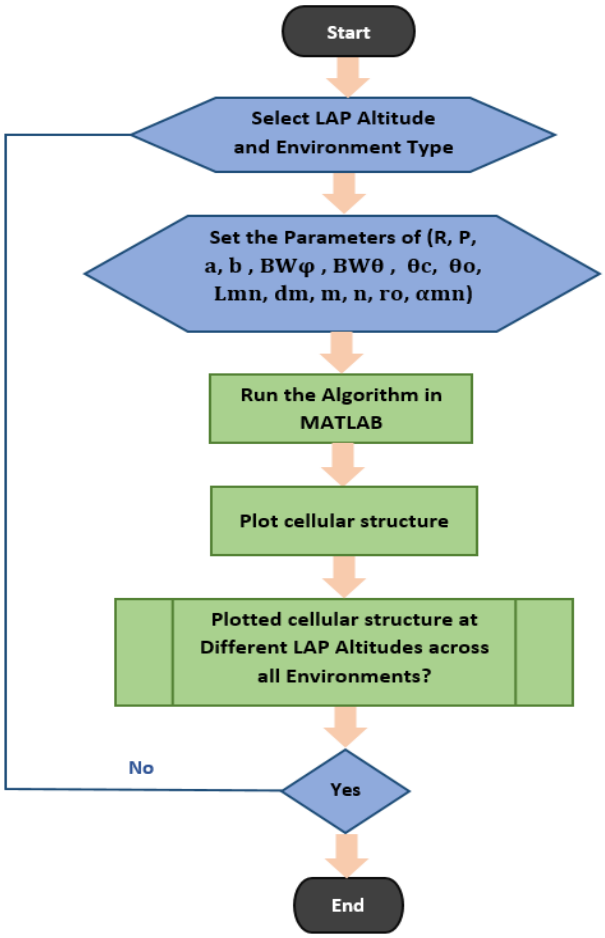

Figure 3.13: Flowchart of tailoring a cellular structure network using a LAP

Table 3.5: Saudi provinces area size and population number [174]

Region	Area	Population
Riyadh	380,000 km²	6,876.96
Makkah	164,000 km²	3,591.59
Madinah	589,000 km²	1,570.84
Qassem	65,000 km²	1,084.68
Eastern Region	710,000 km²	562.30
Hail	125,000 km²	440.14
Jizan	11,671 km²	410.44
Asser	80,000 km²	341.35
Baha	10,362 km²	236.32
Tabuk	108,000 km²	175.61
Najran	360,000 km²	138.52
Jawf	139,000 km²	125.59
Northern border	127,000 km²	116.90

Table 3.6: Implementation of cellular structure network via LAP using MATLAB

Formal Definition		MATLAB code
$b = h\,(\tan(\theta o + \frac{BW\theta}{2}) - \tan(\theta o - \frac{BW\theta}{2}))$	(48)	
$a = 2h\,\sec(\theta c)\tan(\frac{BW\varphi}{2})$	(49)	
$\theta c = \tan^{-1}(\tan(\theta o - \frac{BW\theta}{2}) + \frac{b}{2h})$	(50)	
$Lmn = d1\sqrt{m^2 + n^2 - mn}$	(51)	
$dm = ro\sqrt{3}$	(52)	
$\alpha mn = \cos^{-1}(\frac{2m-n}{2\sqrt{m^2-mn+n^2}})$	(53)	

```
% first tier parameters
ro=h*tan(BW/2);
d(1)=sqrt(3)*ro;
tho(1)=atan(d(1)/h);
b(1)=h*(tan(tho(1)+BW/2)-tan(tho(1)-BW/2));
tc(1)=atan(tan(tho(1)-BW/2)+b(1)/(2*h));
a(1)=2*h*sec(tc(1))*tan(Bf/2);
d(1)=0.25*sqrt(3)*(2*ro+b(1));
% Pointing indexing
theta1(1:6)=tho(1)*180/pi;
phio1(1:6)=0:60:300;
theta0=0;
phio0=0;
% Other tiers parameters
Tier=5;          % No. of tiers
```

This simulation runs at first with the value of the inner cell radius (*ro),* and the first sector of the first tier of the cellular structure is plotted. For the rest of the outer tiers, the algorithm updates the central distances with the new expected major and minor axis of the cell. Then, the rest of the cells in the same tier can be obtained by rotating the structure by multiples of 60◦ in the azimuth plane but with the same central distance. The algorithm updates the cell locations with their corresponding parameters as one changes the type of environment. The algorithm generates antenna pointing angles considering the uniformity of the radio coverage such as minimal coverage gaps and overlap. Table 3.7 shows a range of design configurations for MATLAB simulation.

Table 3.7: Simulation parameters of the cellular structure

Terrain	Central Cell Radius in (km)	Beamwidth in (°)	Tiers number
Urban	0.2	3.9	15
Suburban	1.5	5.7	13
Rural	3	10	8

The proposed cell configurations are evaluated in relation to a trunked mobile radio system which provides access to users on demand from an available number of channels. A small number of channels can accommodate a large but random number of users, due to the limited radio spectrum. GoS measures the ratio of users accessing a trunked system during the busiest hours. Thus, we consider P_B in evaluating the performance of the optimised against the adapted propagation models. The algorithm is defined with equations (54) through to (57):

$$(P_B) = \frac{A^C/C!}{\sum_{i=0}^{C} A^i/C!} \quad (54)$$

$$A_u = \lambda_T \, x \, H \quad (55)$$

$$A = U \, x \, A_u \quad (56)$$

$$A_c = AxR_n \quad (57)$$

Where P_B is the ratio of number of lost calls to total number of calls, C is a rounding number of channels multiplied by obtained RSS of a model. A is total traffic, H is call duration, and λ_T is rate of call arrival, U is number of users, A_u is call rate per user, A_c is carried traffic, R_n is number of cells [167, 168]. Table 3.8 shows the MATLAB implementation of the P_B via LAP.

Table 3.8: Simulation parameters for the implementation of the probability of blocking

Formal Definition	MATLAB code
$(P_B) = \frac{A^C/C!}{\sum_{i=0}^{C} A^i/C!}$ (54) $A_u = \lambda_T \, x \, H$ (55) $A = U \, x \, A_u$ (56) $A_c = AxR_n$ (57)	6 %Number of channel 7 C= 50; 8 RSS=[66, 53, 72, 54, 48]; %Runding RSS of Urban 9 10 N_C= C*RSS; 11 12 %Traffic intensity 13 T_tr = [0.1:0.1:100]; 14 15 %Erlang B equation 16 for i=1:length(N_C) 17 18 sum=0; 19 20 for k=0:N_C(i) 21 22 sum = sum + T_tr.^k/ factorial(k); %Loop for Part Using "k" variable 23 24 end 25 26 Pr_block (i,:) = T_tr.^N_C(i)./factorial(N_C(i))./sum;

Figure 3.14 shows the perceived network design of centralized LAPs over the KSA sky either to provide long or short term wireless services.

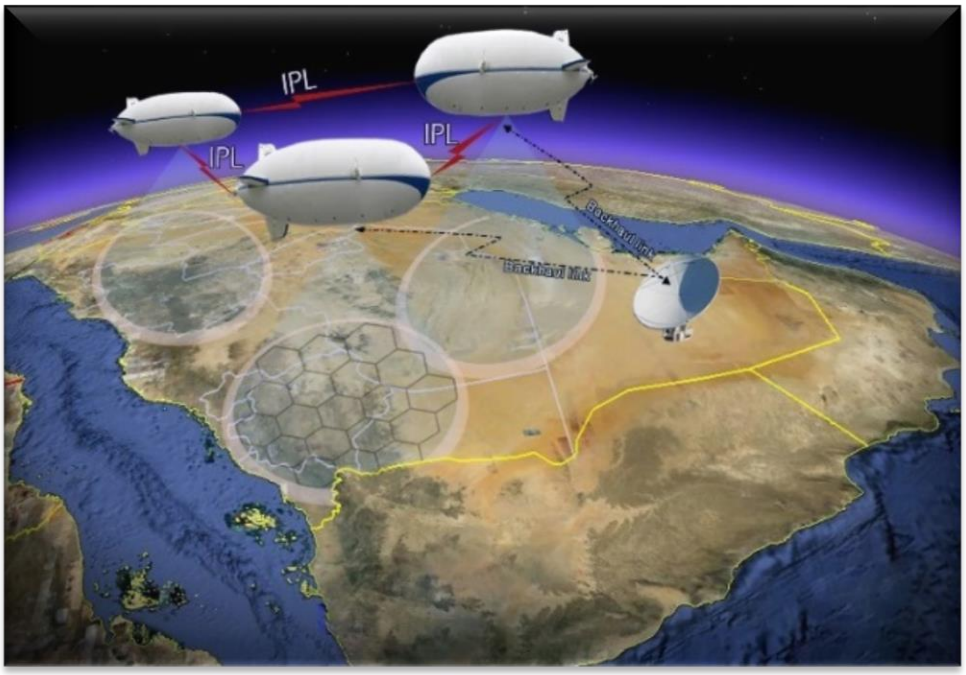

Figure 3.14: A network design of aerial platforms over the KSA sky

3.4 Summary

In this chapter, we have discussed the MATLAB implementation of the design proposed in the previous chapter. This has included the implementation of the four adapted propagation models, as well as the process of evolution of the optimised propagation model using NN-SOM alongside its NN Feed Forward fitting tool. This chapter has also reported on the deployment plan and MATLAB implementation of the optimised model in WSN, and a cellular structure network design across a range of environments in KSA. The following chapter compares the predictions obtained from the optimised model first against those obtained from the adapted propagation models and secondly against those reported in the literature. The performance of the optimised against the non-optimised models is also assessed in the WSN and cellular structure designs.

Chapter 4 : Evaluation of the Optimised Propagation Model

This chapter presents and compares the prediction results generated by both the non-optimised and the optimised propagation models. Follows, validates the predictions of both the non-optimised and optimised propagation models at first using the NN Feed Forward Fitting Tool and then against those reported in the literature. The chapter concludes the evaluation by assessing the performance of the optimised model in two proof-of-concept applications.

4.1 Prediction Results

4.1.1 Prediction Results: Non-Optimised Propagation Models

Simulating the propagation models and generating their predictions has been carried out in MATLAB at various LAP altitudes across different environments with due consideration to a fuller range of link budget parameters. Each of the four adapted model estimate values for five parameters: path loss, RSS, SINR, throughput, and coverage radius. The algorithms of these models have been formulated from equations 1 through to 31 and simulated under the same conditions using the antenna specification of Table 3.1. The simulations have considered two types of receivers based on antenna gains for BS, and HS, at different LAP altitudes that are representative of the transmitter antenna altitude $\boldsymbol{h_t}$. Simulated predictions are shown as line graphs on Figures 4.1 through to 4.12, and then numerically on Tables 4.1 through to 4.3, across urban, suburban, and rural environments, respectively.

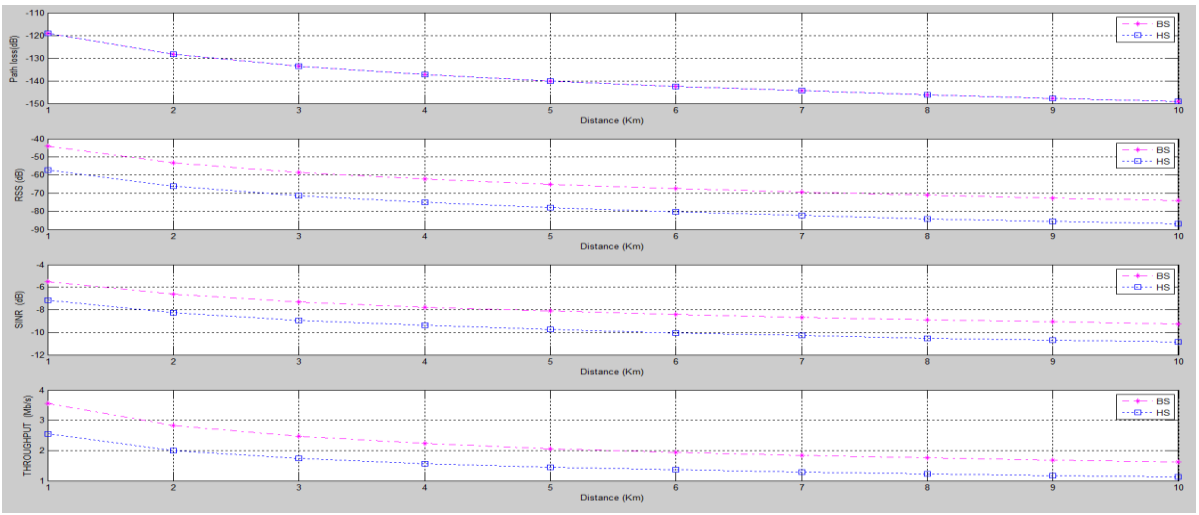

Figure 4.1: Prediction plots of ITU-R P.529-3 model, at 0.2 km LAP altitude, in an urban environment – BS and HS receivers

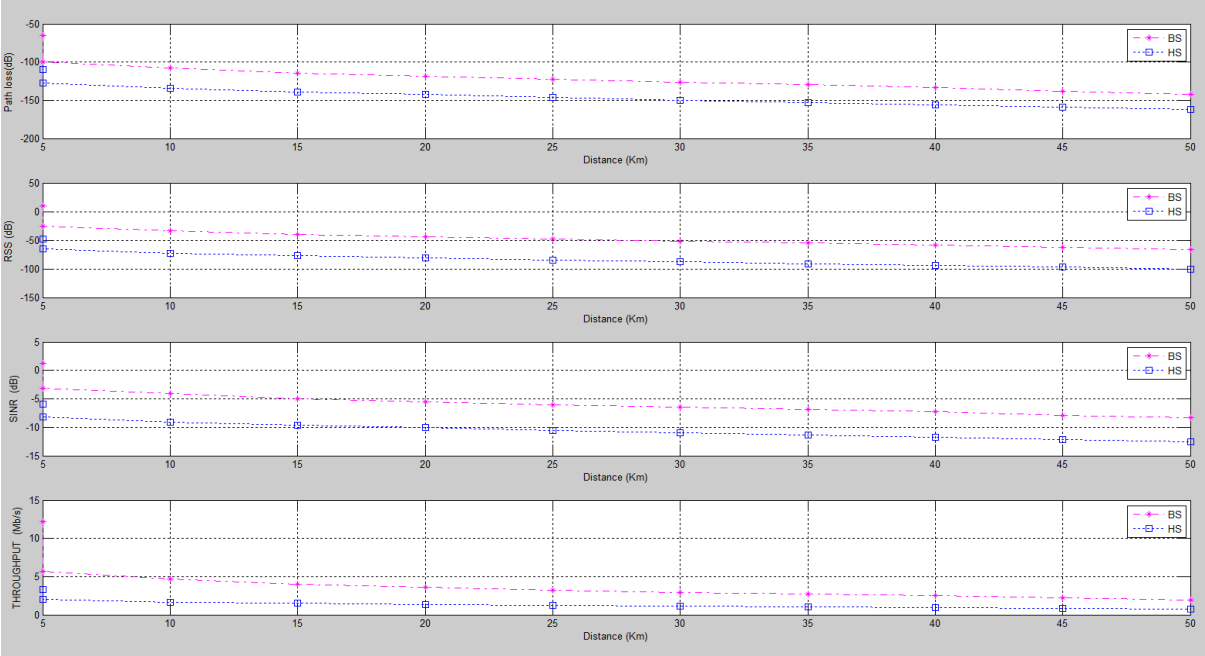

Figure 4.2: Prediction plots of Okumura model, at 1 km LAP altitude, in an urban environment – BS and HS receivers

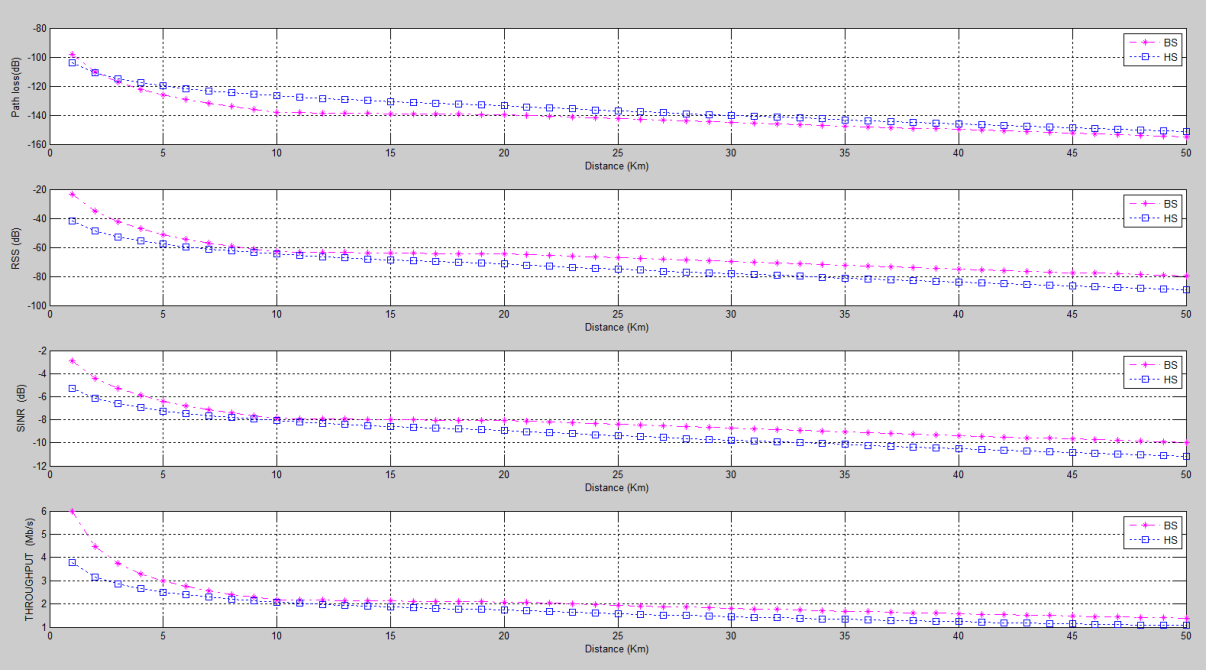

Figure 4.3: Prediction plots of Hata-Davidson model, at 2.5 km LAP altitude, in an urban environment – BS and HS receivers

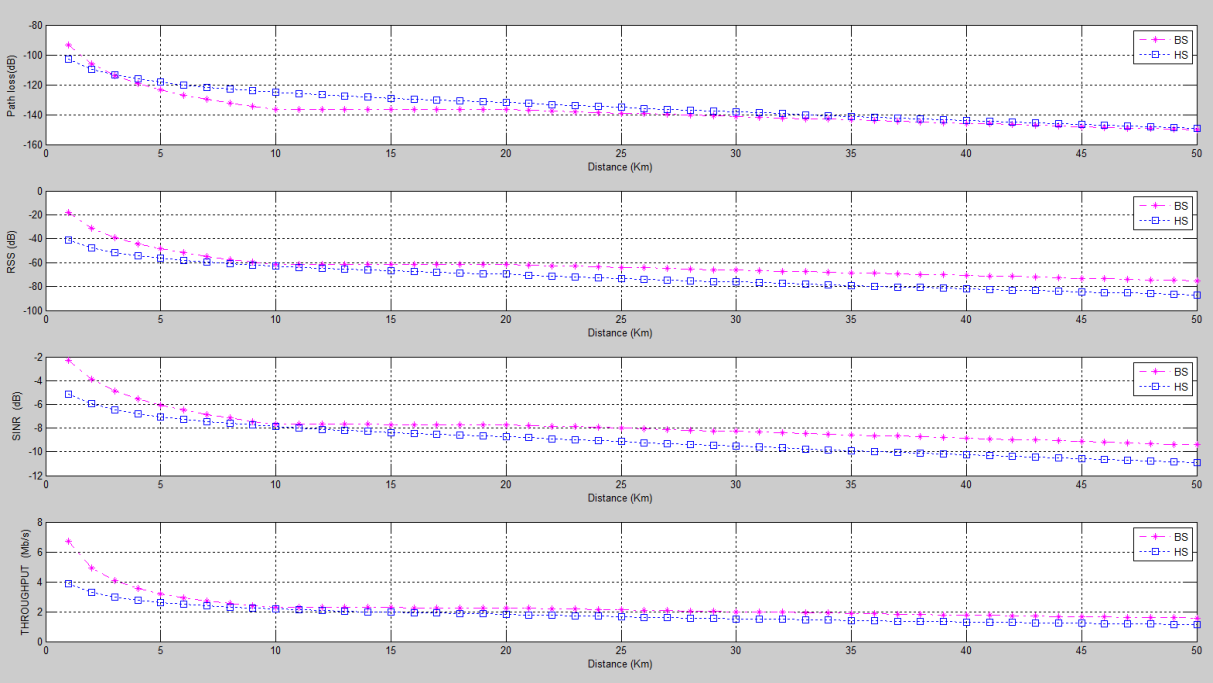

Figure 4.4: Prediction plots of ATG model, at 5 km LAP altitude, in an urban environment – BS and HS receivers

Table 4.1: Predictions in an urban environment

Model	-PL (dB)		-RSS (dBm)		SINR (dB)		Throughput (Mb/S)		Radius (km)	
	BS	HS	BS	HS	BS	HS	BS	HS	BS	HS
Altitude of 0.2 km										
ITU-R P.529-3	128.18	128.18	53.18	66.18	6.65	8.27	2.83	2	2	2
Okumura	114.70	114.70	39.70	52.70	4.97	6.58	4.65	3.13	2	2
Hata-Davidson	139.55	132.50	64.55	71.50	8.07	9	2.09	1.71	2	1.5
ATG	115.96	115.96	40.96	53.96	5.12	6.74	3.87	2.77	3	3
Altitude of 1 km										
ITU-R P.529-3	0	0	0	0	0	0	0	0	0	0
Okumura	115.54	115.54	40.54	52.89	5.94	6.89	3.70	2.87	8	8
Hata-Davidson	143.19	133.50	68.19	72.50	8.52	9.20	1.96	1.63	8	4
ATG	129.93	129.93	54.93	67.93	6.87	8.49	2.70	1.91	8	7
Altitude of 2.5 km										
ITU-R P.529-3	0	0	0	0	0	0	0	0	0	0
Okumura	0	0	0	0	0	0	0	0	0	0
Hata-Davidson	139.60	133.09	64.60	71.09	8.07	8.89	2.09	1.75	19.5	7.5
ATG	137.87	133.50	62.87	71.50	7.86	8.95	2.19	1.72	19	12.5
Altitude of 5 km										
ITU-R P.529-3	0	0	0	0	0	0	0	0	0	0
Okumura	0	0	0	0	0	0	0	0	0	0
Hata-Davidson	0	0	0	0	0	0	0	0	0	0
ATG	143.86	133.50	68.86	71.50	8.61	8.95	1.86	1.70	38	15.5

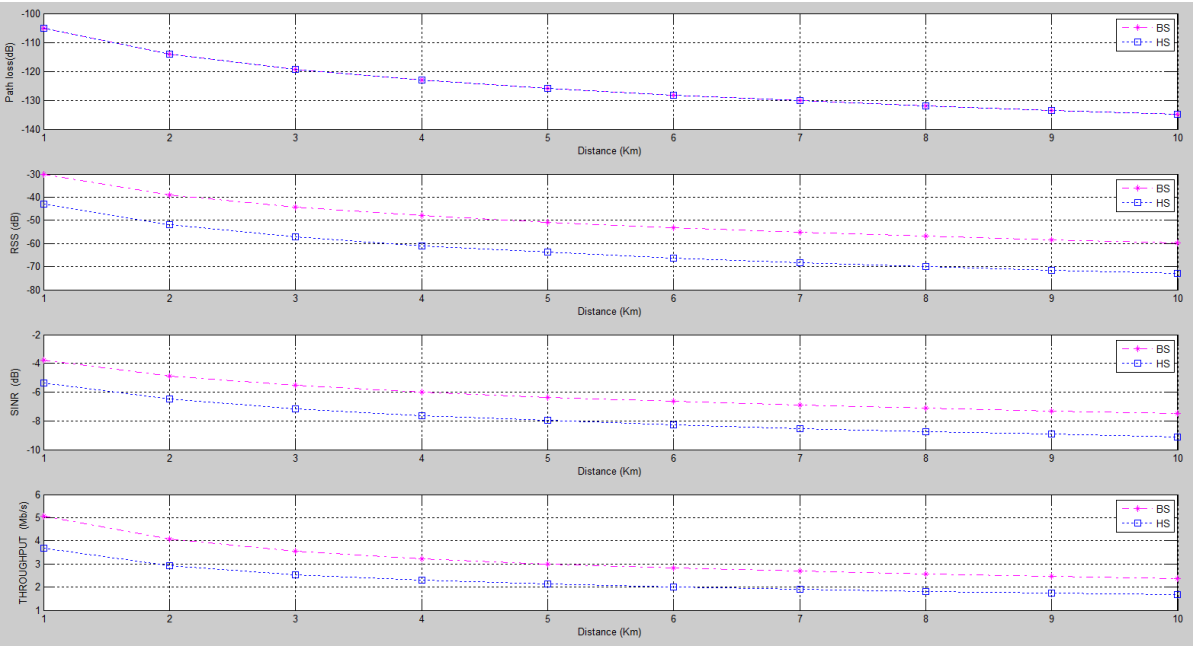

Figure 4.5: Prediction plots of ITU-R P.529-3 model, at 0.2 km LAP altitude, in a suburban environment – BS and HS receivers

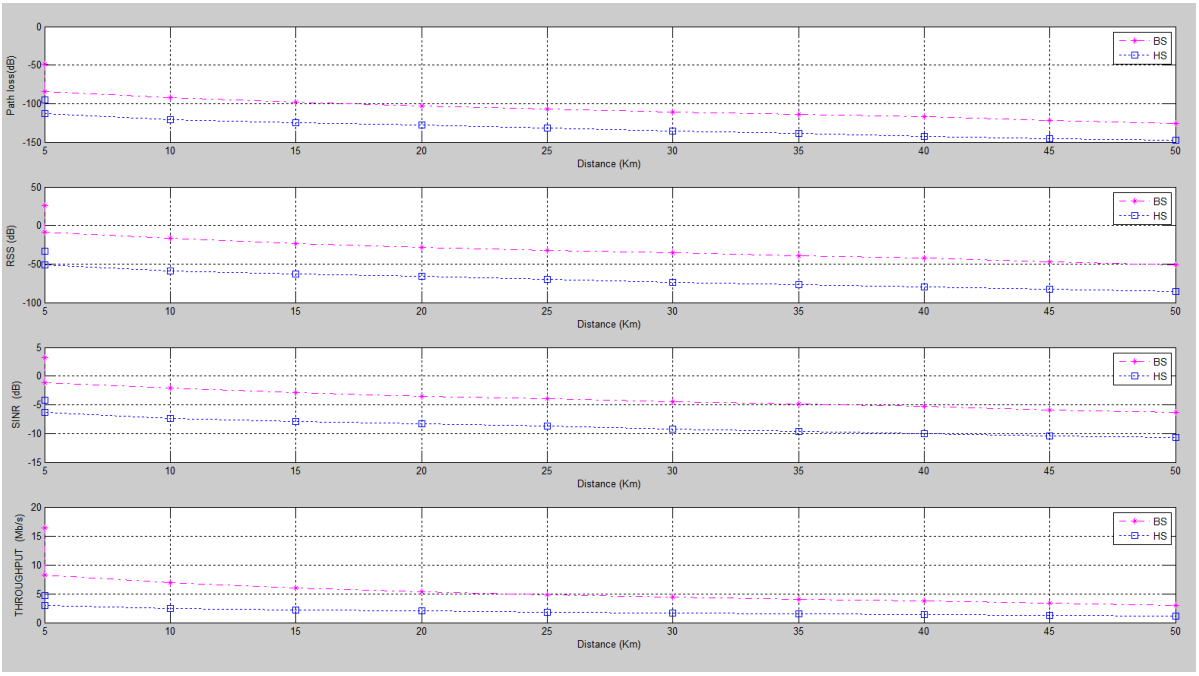

Figure 4.6: Prediction plots of Okumura model, at 1 km LAP altitude, in a suburban environment – BS and HS receivers

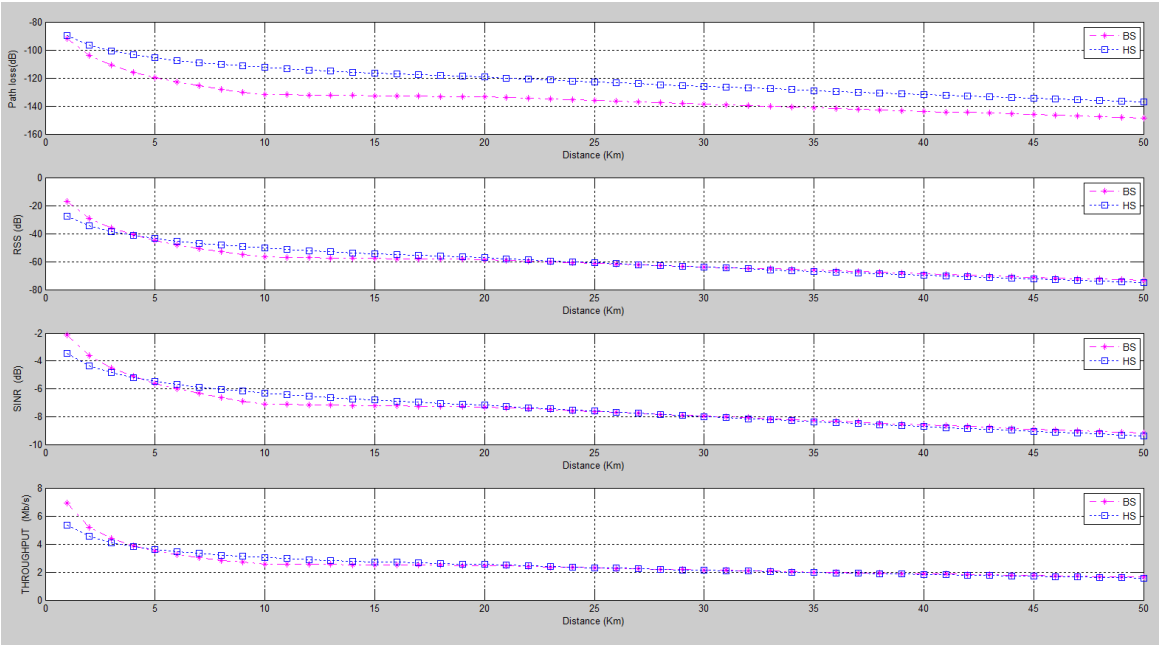

Figure 4.7: Prediction plots of Hata-Davidson model, at 2.5 km LAP altitude, in a suburban environment – BS and HS receivers

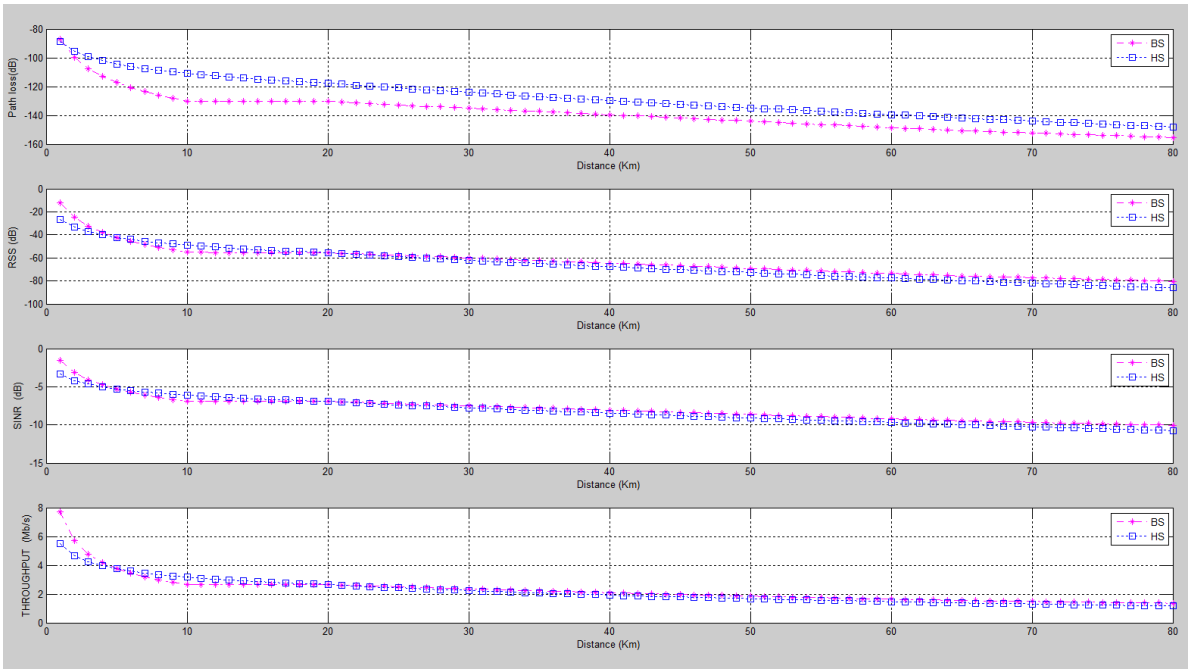

Figure 4.8: Prediction plots of ATG model, at 5 km LAP altitude, in a suburban environment – BS and HS receivers

Table 4.2: Predictions in a suburban environment

Model	-PL (dB)		-RSS (dBm)		SINR (dB)		Throughput (Mb/S)		Radius (km)	
	BS	HS	BS	HS	BS	HS	BS	HS	BS	HS
Altitude of 0.2 km										
ITU-R P.529-3	119.24	119.24	44.24	57.24	5.53	7.15	3.56	2.54	3	3
Okumura	98.70	98.70	23.70	36.70	3	4.59	4.30	4.65	4	3
Hata-Davidson	138.58	131.32	63.58	71.32	7.94	8.91	2.15	1.74	3	2
ATG	118.62	118.62	43.62	56.62	5.45	7.07	3.62	2.58	4	4
Altitude of 1 km										
ITU-R P.529-3	0	0	0	0	0	0	0	0	0	0
Okumura	100.03	100.03	28.5	39.5	4.22	4.05	3.60	1.08	14	10
Hata-Davidson	141.13	133.13	66.13	72.13	8.27	9.15	2	1.64	12	6
ATG	132.58	123.58	57.58	70.58	7.20	8.82	2.52	1.78	12	11
Altitude of 2.5 km										
ITU-R P.529-3	0	0	0	0	0	0	0	0	0	0
Okumura	0	0	0	0	0	0	0	0	0	0
Hata-Davidson	138.47	133.44	63.47	71.44	7.93	8.93	2.15	1.74	29.5	20
ATG	140.50	133.48	65.50	71.48	8.18	8.93	2.04	1.73	28	14.5
Altitude of 5 km										
ITU-R P.529-3	0	0	0	0	0	0	0	0	0	0
Okumura	0	0	0	0	0	0	0	0	0	0
Hata-Davidson	0	0	0	0	0	0	0	0	0	0
ATG	146.47	133.50	71.47	71.71	8.93	8.96	1.74	1.69	56	17.5

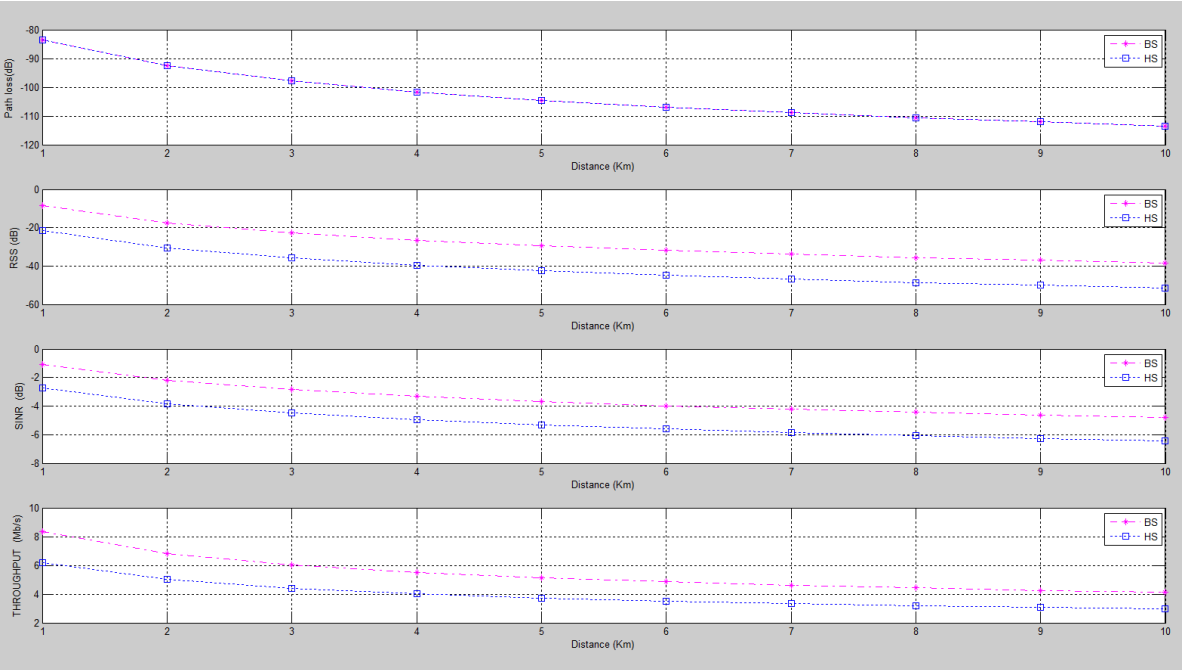

Figure 4.9: Prediction plots of ITU-R P.529-3 model, at 0.2 km LAP altitude, in a rural environment – BS and HS receivers

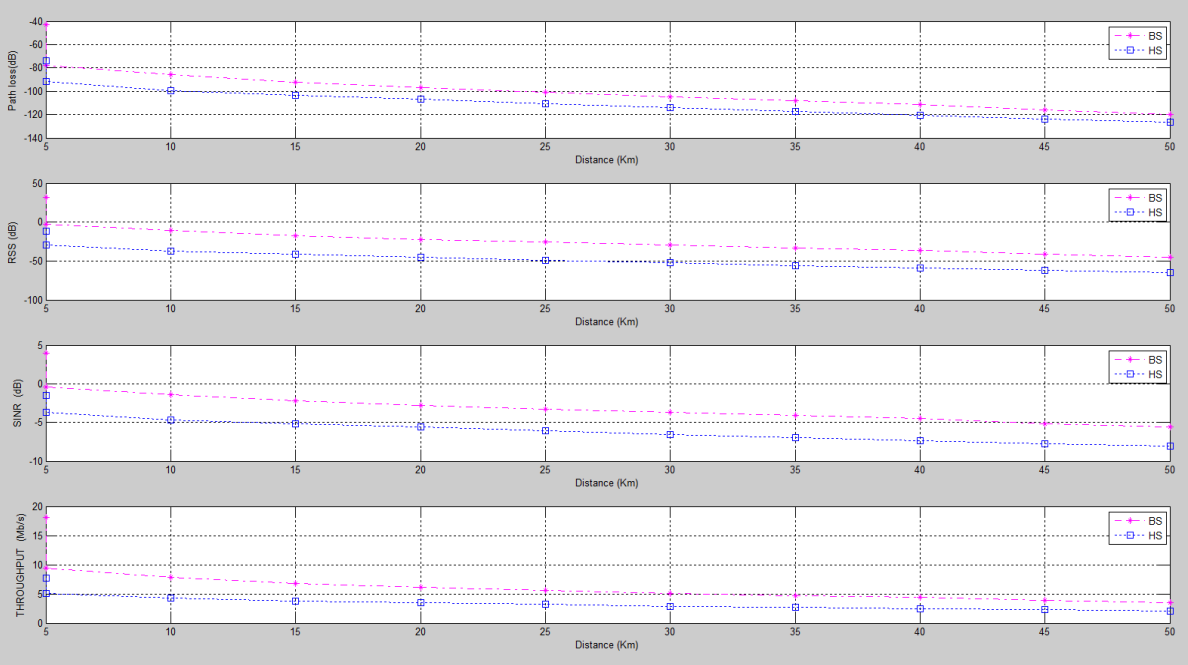

Figure 4.10: Prediction plots of Okumura model, at 1 km LAP altitude, in a rural environment – BS and HS receivers

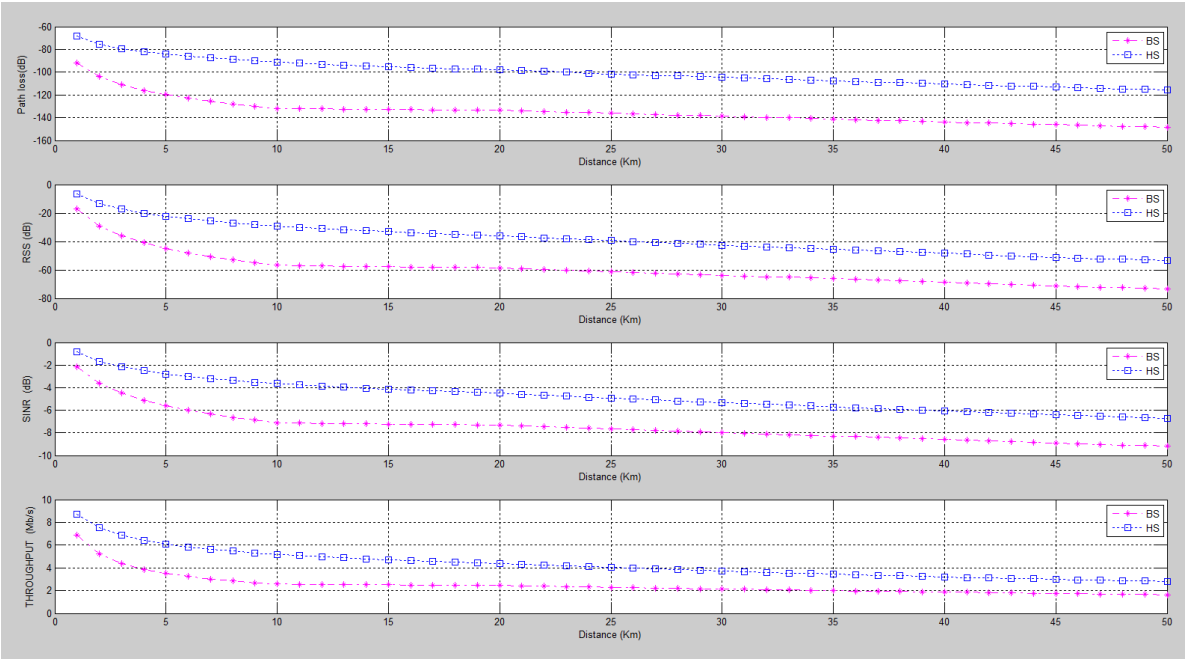

Figure 4.11: Prediction plots of Hata-Davidson model, at 2.5 km LAP altitude, in a rural environment – BS and HS receivers

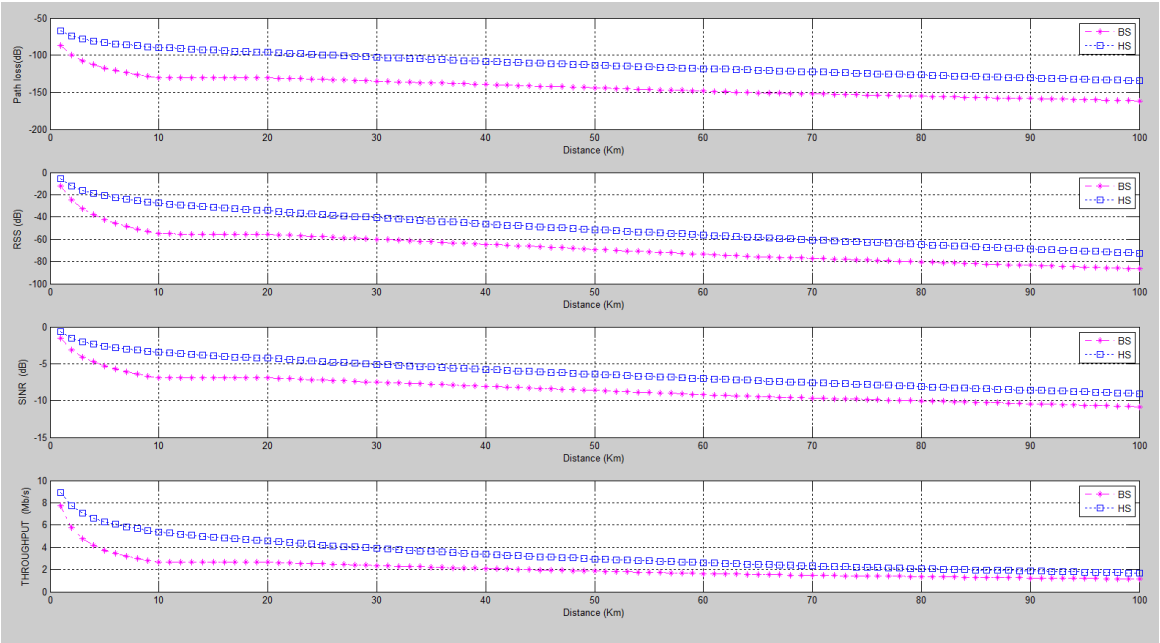

Figure 4.12: Prediction plots of ATG model, at 5 km LAP altitude, in a rural environment – BS and HS receivers

Table 4.3: Predictions in a rural environment

Model	-PL (dB)		-RSS (dBm)		SINR (dB)		Throughput (Mb/S)		Radius (km)	
	BS	HS	BS	HS	BS	HS	BS	HS	BS	HS
Altitude of 0.2 km										
ITU-R P.529-3	104.48	104.48	29.48	42.48	3.68	5.31	5.14	3.73	5	5
Okumura	110.19	110.19	35.19	48.19	4.39	6.02	3.47	3.22	5	5
Hata-Davidson	144.20	133.30	70.20	71.30	8.74	8.91	1.80	1.74	5	2
ATG	122.66	122.66	47.66	60.66	5.96	7.58	3.20	2.32	5	5
Altitude of 1 km										
ITU-R P.529-3	0	0	0	0	0	0	0	0	0	0
Okumura	123.10	123.10	38.10	52.10	5.85	7.87	3.01	3.16	22	20
Hata-Davidson	145.30	133.30	71.30	72.30	8.99	9.02	1.62	1.70	21	6.5
ATG	136.50	133.11	61.50	71.11	7.69	8.88	2.26	1.75	23	16
Altitude of 2.5 km										
ITU-R P.529-3	0	0	0	0	0	0	0	0	0	0
Okumura	0	0	0	0	0	0	0	0	0	0
Hata-Davidson	146.41	133.44	71.41	71.44	8.93	8.93	1.74	1.74	45	20
ATG	144.40	133.41	69.40	71.41	8.67	8.96	1.83	1.73	56	19
Altitude of 5 km										
ITU-R P.529-3	0	0	0	0	0	0	0	0	0	0
Okumura	0	0	0	0	0	0	0	0	0	0
Hata-Davidson	0	0	0	0	0	0	0	0	0	0
ATG	146.50	133.50	71.50	72.50	8.92	10	1.70	1.65	80	22.5

Tables 4.1 through to 4.3 offer predictions in relation to propagation PL, RSS, SINR, throughput, and coverage footprint at various LAP altitudes in various urban, suburban, and rural environments. PL predictions are used for monitoring system performance and coverage to achieve a certain level of reception thus, it is a key parameter in our

simulations. In all four models across all environments and altitudes, PL is below the MAPL, with the lowest PL predicted being that of the Okumura model followed by that of the ATG model. In ATG model, η_{LoS} ranges between 3 to 5dB, whereas η_{NLoS} ranges between 8 to 12dB [32, 139]. The range of PL floats between -104dB to -146.5dB, whereas PL increases with distance and/or geomorphology due to multipath, and or NLoS. With reference to the WiMAX link budget specification, the MAPL for a BS antenna with a gain of 23dB is -146.5dB, and for a HS antenna with a gain of 5dB is -133.5dB. MAPL values are taken as threshold for PL values, thus at a LAP altitude of 5km the ATG model reaches the MAPL for HS antennas across all environments, but for BS in rural only. PL in the Okumura model for both BS or HS is the same, since the receiver antenna gain is neglected. In urban environments, NLoS occurs because of the shadowing effect and reflection of signals from interfering obstacles which in turn leads to an additional PL especially with increasing distance.

RSS depends on PL, transmitter and receiver height, gain and environmental factors. Calculating this parameter helps to estimate the coverage range when the signal becomes weaker as the receiver moves the farthest away from the transmitter. In our simulations, RSS yields a reasonably good average across all four models, with the maximum RSS value varying between -85dBm to -91dBm [142, 162,176]. As RSS is linked to PL, the Okumura model achieves the best predicted result followed by the ATG model. The RSS for the HS antenna is less than the value of BS because of the antenna gain. Unsurprisingly, increasing the transmitter altitude and transmission power, increases both the coverage and RSS. Keeping transmission power constant at different transmitter altitudes yields varying levels of RSS. The predicted results show that exceeding transmitter altitude over the LAP altitude and beyond its maximum limit leads to intolerable errors especially in urban areas.

The SINR is widely used in wireless communications to measure the quality of a wireless link and bit error ratio. In our simulations, SINR averages between 4dB and 10dB across all models, with values below 4dB deemed unacceptable in consideration of WiMAX's SINR range of 4dB min to 19dB max. An SINR below 4dBi is considered inadequate, while one above 20dBi is regarded as wasted transmitter power. SINR values in BS are higher than those in HS across all environments and altitudes due to achieved RSS predictions. One observation is that SINR increases as LAP altitudes and/or distance increase but as we move towards rural SINR increases with distance.

The expected throughput is one of the indicators to evaluate the performance of propagation models. It decreases with path loss and increase in distance, and with shadowing. In our simulations, there is negative correlation where throughput decreases as LAP altitudes and/or distance increase in all area types. Overall, Okumura model yields the best predicted result in throughput across all environments followed by ATG model. Throughput values in BS are higher than those in HS across all environments and altitudes as they are directly linked to SINR results. The maximum throughput achieved is around 5.14Mbps in a rural environment at an altitude of 0.2km with the ITU-R P.529-3 model. The minimum is around 1.65Mbps in a rural environment at an altitude of 5km with the ATG model, due to a low PL.

Network coverage is affected both by transmitter and receiver antenna specifications, geomorphology, and minimum elevation angle. The radius increases with transmitter altitude, as well as with changing from an urban to a rural environment, due to a decrease in the elevation angle. Shadowing and reflection may lead to an increase in distance. Three factors that may additionally increase coverage include modulation methods, receiver sensitivity and transmission power. The radius averages between 2km and 80km across all models with the results supporting the designated elevation angle. Some of the models may stretch this further as they do not exceed their MAPL.

4.1.2 Prediction Results: Optimised Propagation Model

The predictions of the adapted models at several LAP altitudes have been used as input to a machine learning technique to evolve the optimised model. The ML technique deployed for evolution of an optimal set of parameters for a propagation model is NN-SOM which has been simulated in MATLAB using equations 32 through to 39 under the same conditions. During the learning phase, the evolved parameters are clustered in a SOM and during the adaptive phase an optimal set is evolved across urban, suburban, and rural environments using a minimax technique. Figures 4.13 through to 4.18 illustrate the optimal set of parameters evolved across urban, suburban, and rural terrains for both BS and HS antennas, whilst Tables 4.4 through to 4.6 report the numerical predictions of the optimised set as they appear in MATLAB.

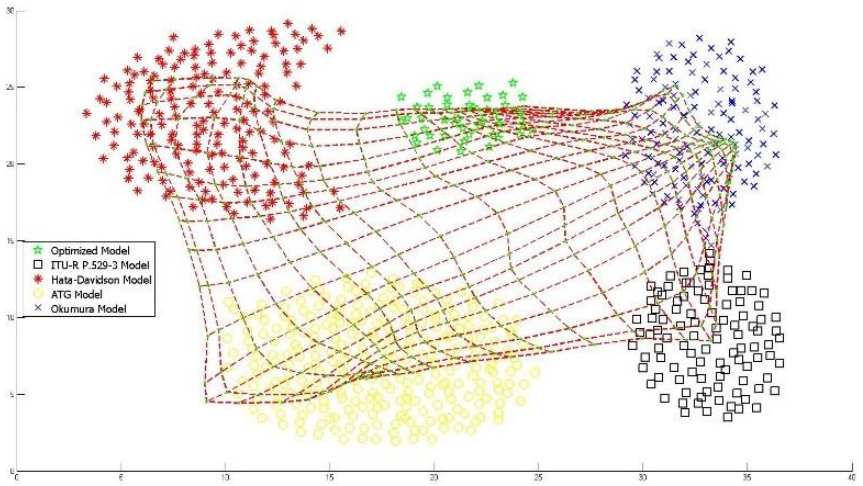

Figure 4.13: Parameter optimisation in an urban environment – BS

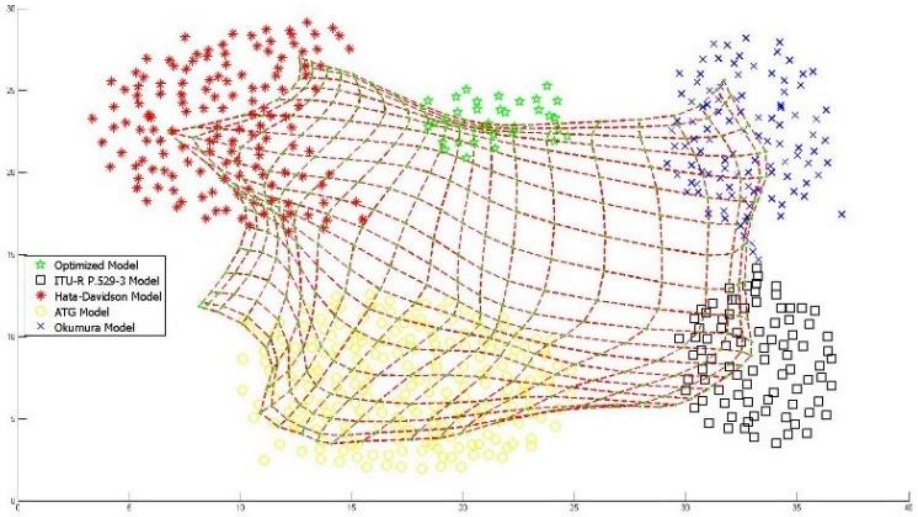

Figure 4.14: Parameter optimisation in an urban environment – HS

Table 4.4: Optimised predictions in an urban environment

Model	-PL (dB)	-RSS (dBm)	SINR (dB)	Throughput (Mb/S)	Radius (km)
Altitude of 0.2 km					
Optimised BS	108.11	35.42	5.17	4.78	4
Optimised HS	109	47.91	6.54	3.46	3
Altitude of 1 km					
Optimised BS	110.23	38.77	6.11	3.86	11
Optimised HS	111.20	47.39	6.97	2.93	9
Altitude of 2.5 km					
Optimised BS	130.53	57.30	7.18	2.34	22
Optimised HS	128.20	64.81	8	1.92	15
Altitude of 5 km					
Optimised BS	135.83	61.40	8.21	1.95	41
Optimised HS	129.40	68.54	8.84	1.77	19

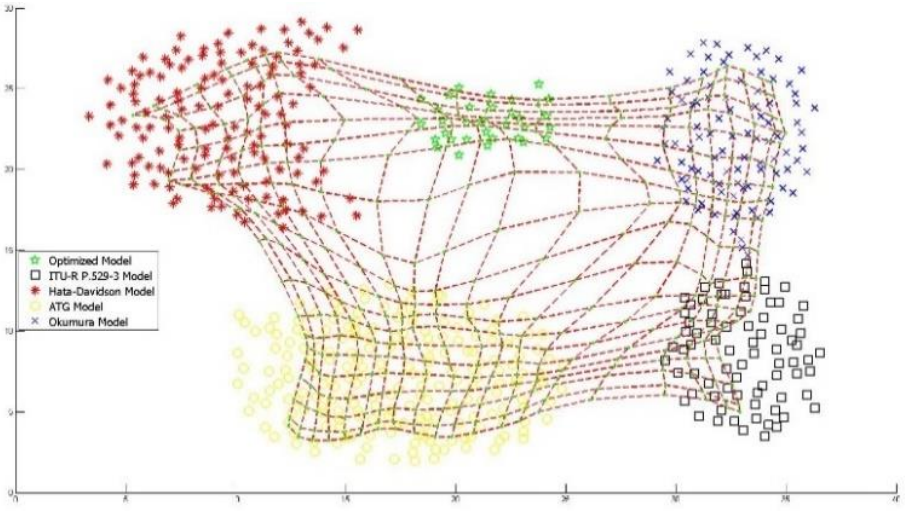

Figure 4.15: Parameter optimisation in a suburban environment – BS

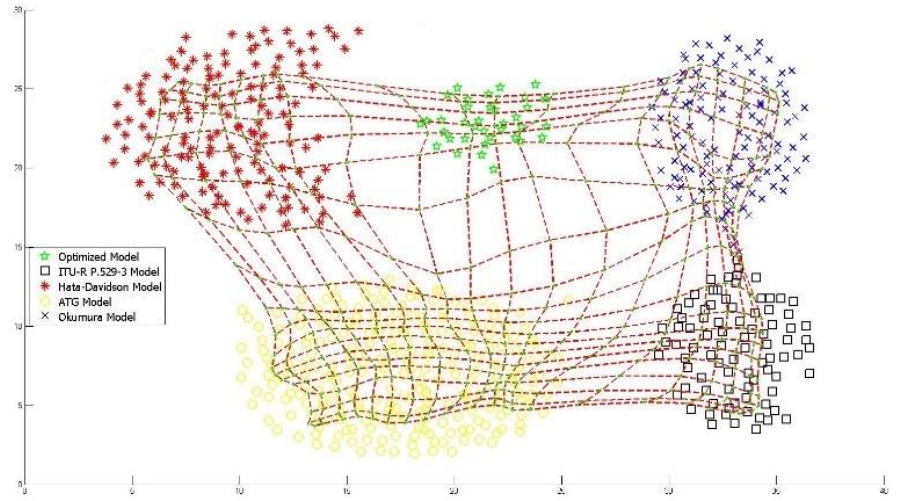

Figure 4.16: Parameter optimisation in a suburban environment – HS

Table 4.5: Optimised predictions in a suburban environment

Model	-PL (dB)	-RSS (dBm)	SINR (dB)	Throughput (Mb/S)	Radius (km)
Altitude of 0.2 km					
Optimised BS	94.68	21.53	5.11	4.41	6
Optimised HS	95.91	34.61	5.86	4.38	4
Altitude of 1 km					
Optimised BS	97.10	25.43	8.11	3.81	16
Optimised HS	98.06	36.12	6.96	1.94	12
Altitude of 2.5 km					
Optimised BS	130.16	57.70	7.61	2.29	32
Optimised BS	128.01	65.63	7.91	1.86	20
Altitude of 5 km					
Optimised BS	137.89	63.80	9.29	1.87	60
Optimised HS	130.66	68.15	10.74	1.69	24

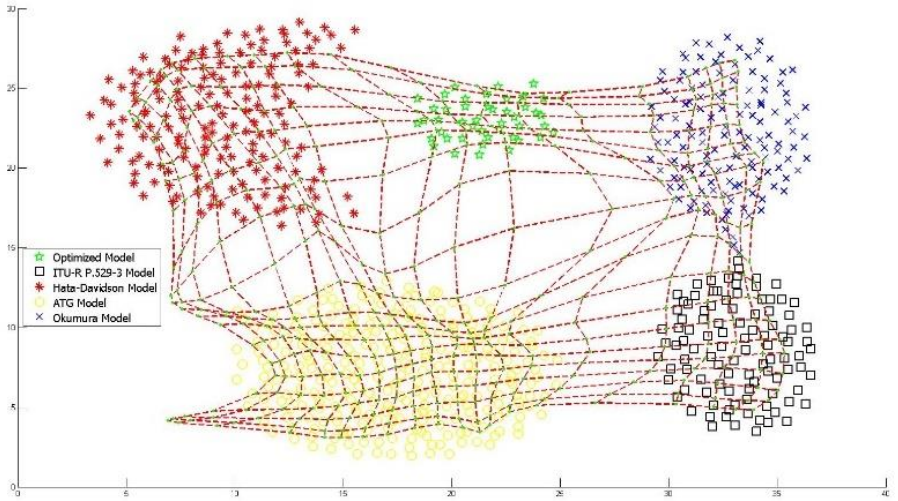

Figure 4.17: Parameter optimisation in a rural environment – BS

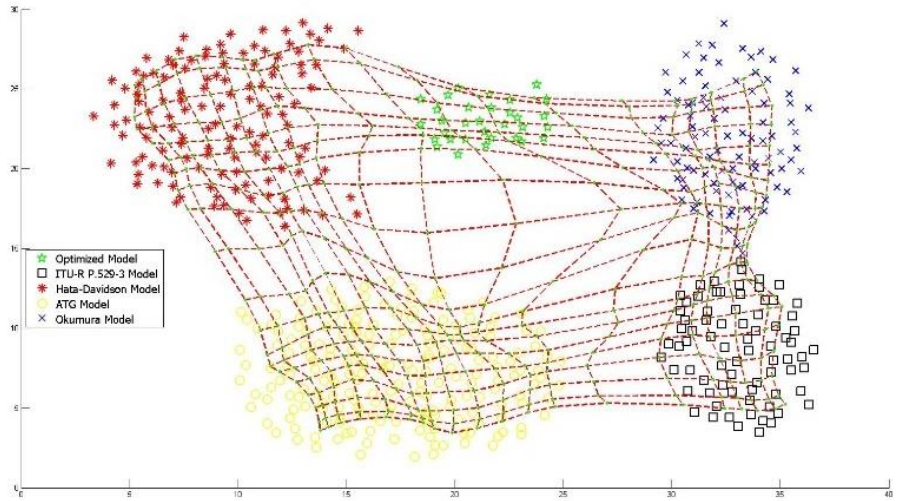

Figure 4.18: Parameter optimisation in a rural environment – HS

Table 4.6: Optimised predictions in a rural environment

Model	-PL (dB)	-RSS (dBm)	SINR (dB)	Throughput (Mb/S)	Radius (km)
Altitude of 0.2 km					
Optimised BS	100.68	26.31	4.65	3.87	8
Optimised HS	100.38	37.74	5.99	3.60	7
Altitude of 1 km					
Optimised BS	115.83	34.37	6.78	3.34	25
Optimised HS	117.70	46.79	7.69	3.18	17
Altitude of 2.5 km					
Optimised BS	133.42	59.87	8.24	1.95	59
Optimised HS	128.89	65.48	8.73	1.83	20
Altitude of 5 km					
Optimised BS	136.28	66.84	9.50	1.81	87
Optimised HS	132.64	70.63	10.91	1.69	24

Figures 4.13 through to 4.18 visualize the NN-SOM topology results into clusters according to their patterns in the input space after the network has been trained. The inputs are sourced from Tables 4.1 through to 4.3. The Figures reveal that there are patterns of five distinct clusters after 1000 iterations of evolving the parameters of the four propagation models. The simulation results offer predictions in relation to the propagation PL, RSS, SINR, throughput, and coverage footprint at various LAP altitudes. PL is kept as low as possible to achieve a certain level of reception with the smallest attenuated signal not exceeding the MAPL, i.e. between -146.5dB and -133.5dB for BS and HS respectively. SINR is maintained between 4dBi and 19dBi. RSS is kept as high as possible to achieve a wider wireless connectivity, and to avoid service degradation and/or interruption. A threshold for RSS and SINR for both BS and HS antennas depends on modulation methods and receiver sensitivity as in the WiMAX link budget specification. Thus, the maximum RSS value is kept between -85dBm and -91dBm. RSS, throughput and coverage radius are kept as high as possible for better signal strength and quality, higher data rates and wider connectivity.

4.1.3 Comparing Optimised Against Non-Optimised Predictions

Figures 4.19 through to 4.24 plot the predictions of the four adapted propagation models sourced from Tables 4.1 through to 4.3, against those of the optimised model sourced from Tables 4.4 through to 4.6 for both BS and HS and at different LAP altitudes and environments. M1, M2, M3, and M4 denote to ITU-R P.529-3, Okumura, Hata-Davidson, and ATG models respectively.

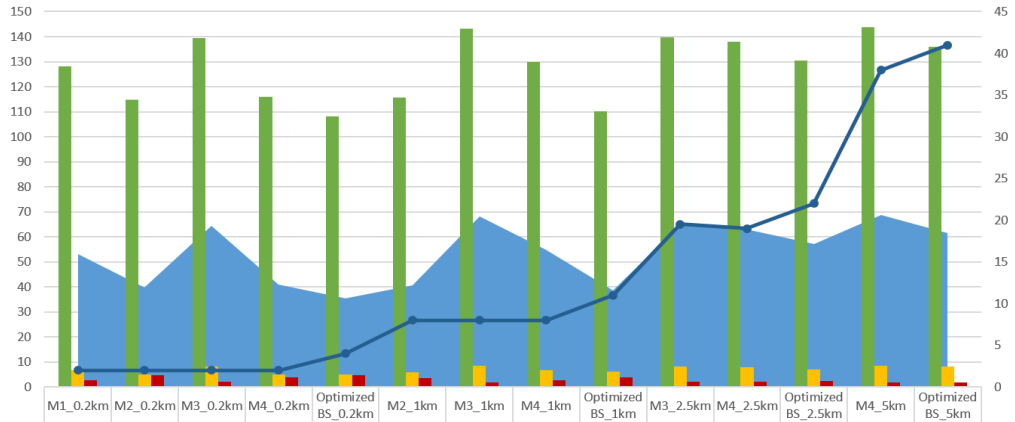

	M1_0.2km	M2_0.2km	M3_0.2km	M4_0.2km	Optimized BS_0.2km	M2_1km	M3_1km	M4_1km	Optimized BS_1km	M3_2.5km	M4_2.5km	Optimized BS_2.5km	M4_5km	Optimized BS_5km
RSS (dBm)	53.18	39.7	64.55	40.96	35.42	40.54	68.19	54.93	38.77	64.6	62.87	57.3	68.86	61.4
PL (dB)	128.18	114.7	139.55	115.96	108.11	115.54	143.19	129.93	110.23	139.6	137.87	130.53	143.86	135.83
SINR (dB)	6.65	4.97	8.07	5.12	5.17	5.94	8.52	6.87	6.11	8.07	7.86	7.18	8.61	8.21
Throughput (Mb/S)	2.83	4.65	2.09	3.87	4.78	3.7	1.96	2.7	3.86	2.09	2.19	2.34	1.86	1.95
Radius (km)	2	2	2	2	4	8	8	8	11	19.5	19	22	38	41

Figure 4.19: Optimised parameters in comparison to predictions with the four adapted models in an urban environment – BS

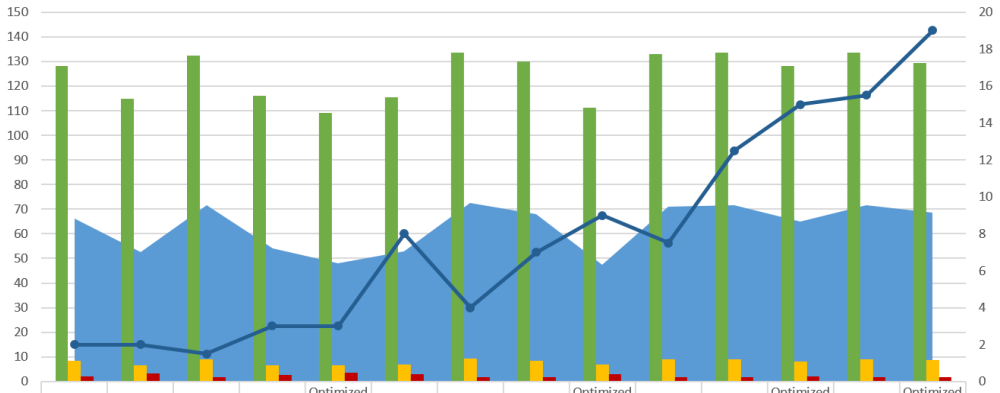

	M1_0.2km	M2_0.2km	M3_0.2km	M4_0.2km	Optimized HS_0.2km	M2_1km	M3_1km	M4_1km	Optimized HS_1km	M3_2.5km	M4_2.5km	Optimized HS_2.5km	M4_5km	Optimized HS_5km
RSS (dBm)	66.18	52.7	71.5	53.96	47.91	52.89	72.5	67.93	47.39	71.09	71.5	64.81	71.5	68.54
PL (dB)	128.18	114.7	132.5	115.96	109	115.54	133.5	129.93	111.2	133.09	133.5	128.2	133.5	129.4
SINR (dB)	8.27	6.58	9	6.74	6.54	6.89	9.2	8.49	6.97	8.89	8.95	8	8.95	8.84
Throughput (Mb/S)	2	3.13	1.71	2.77	3.46	2.87	1.63	1.91	2.93	1.75	1.72	1.92	1.7	1.77
Radius (km)	2	2	1.5	3	3	8	4	7	9	7.5	12.5	15	15.5	19

Figure 4.20: Optimised parameters in comparison to predictions with the four adapted models in an urban environment – HS

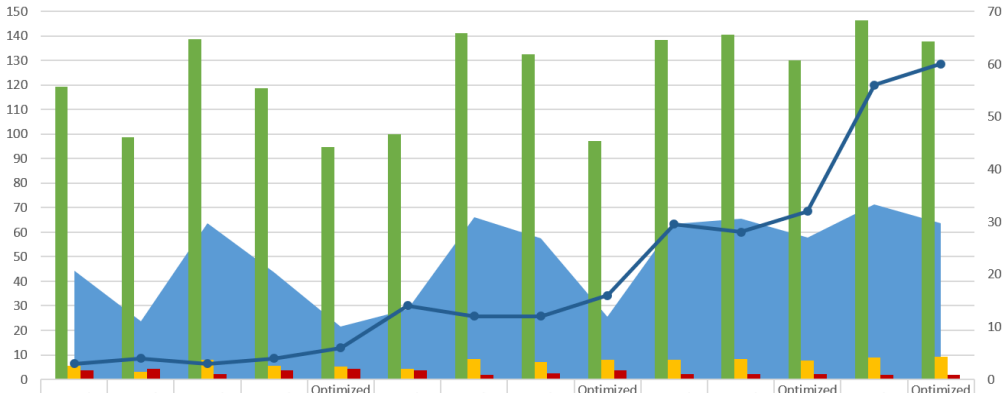

	M1_0.2km	M2_0.2km	M3_0.2km	M4_0.2km	Optimized BS_0.2km	M2_1km	M3_1km	M4_1km	Optimized BS_1km	M3_2.5km	M4_2.5km	Optimized BS_2.5km	M4_5km	Optimized BS_5km
RSS (dBm)	44.24	23.7	63.58	43.62	21.53	28.5	66.13	57.58	25.43	63.47	65.5	57.7	71.47	63.8
PL (dB)	119.24	98.7	138.58	118.62	94.68	100.03	141.13	132.58	97.1	138.47	140.5	130.16	146.47	137.89
SINR (dB)	5.53	3	7.94	5.45	5.11	4.22	8.27	7.2	8.11	7.93	8.18	7.61	8.93	9.29
Throughput (Mb/S)	3.56	4.3	2.15	3.62	4.41	3.6	2	2.52	3.81	2.15	2.04	2.29	1.74	1.87
Radius (km)	3	4	3	4	6	14	12	12	16	29.5	28	32	56	60

Figure 4.21: Optimised parameters in comparison to predictions with the four adapted models in a suburban environment – BS

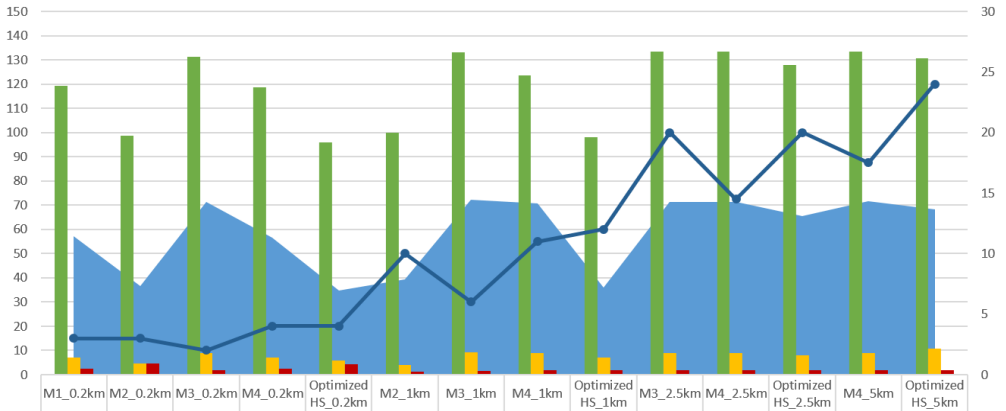

	M1_0.2km	M2_0.2km	M3_0.2km	M4_0.2km	Optimized HS_0.2km	M2_1km	M3_1km	M4_1km	Optimized HS_1km	M3_2.5km	M4_2.5km	Optimized HS_2.5km	M4_5km	Optimized HS_5km
RSS (dBm)	57.24	36.7	71.32	56.62	34.61	39.5	72.13	70.58	36.12	71.44	71.48	65.63	71.71	68.15
PL (dB)	119.24	98.7	131.32	118.62	95.91	100.03	133.13	123.58	98.06	133.44	133.48	128.01	133.5	130.66
SINR (dB)	7.15	4.59	8.91	7.07	5.86	4.05	9.15	8.82	6.96	8.93	8.93	7.91	8.96	10.74
Throughput (Mb/S)	2.54	4.65	1.74	2.58	4.38	1.08	1.64	1.78	1.94	1.74	1.73	1.86	1.69	1.69
Radius (km)	3	3	2	4	4	10	6	11	12	20	14.5	20	17.5	24

Figure 4.22: Optimised parameters in comparison to predictions with the four adapted models in a suburban environment – HS

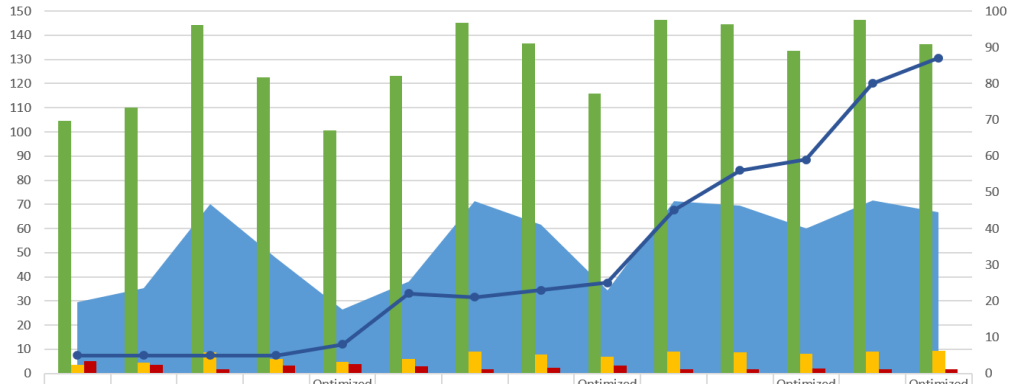

	M1_0.2km	M2_0.2km	M3_0.2km	M4_0.2km	Optimized BS_0.2km	M2_1km	M3_1km	M4_1km	Optimized BS_1km	M3_2.5km	M4_2.5km	Optimized BS_2.5km	M4_5km	Optimized BS_5km
RSS (dBm)	29.48	35.19	70.2	47.66	26.31	38.1	71.3	61.5	34.37	71.41	69.4	59.87	71.5	66.84
PL (dB)	104.48	110.19	144.2	122.66	100.68	123.1	145.3	136.5	115.83	146.41	144.4	133.42	146.5	136.28
SINR (dB)	3.68	4.39	8.74	5.96	4.65	5.85	8.99	7.69	6.78	8.93	8.67	8.24	8.92	9.5
Throughput (Mb/S)	5.14	3.47	1.8	3.2	3.87	3.01	1.62	2.26	3.34	1.74	1.83	1.95	1.7	1.81
Radius (km)	5	5	5	5	8	22	21	23	25	45	56	59	80	87

Figure 4.23: Optimised parameters in comparison to predictions with the four adapted models in a rural environment – BS

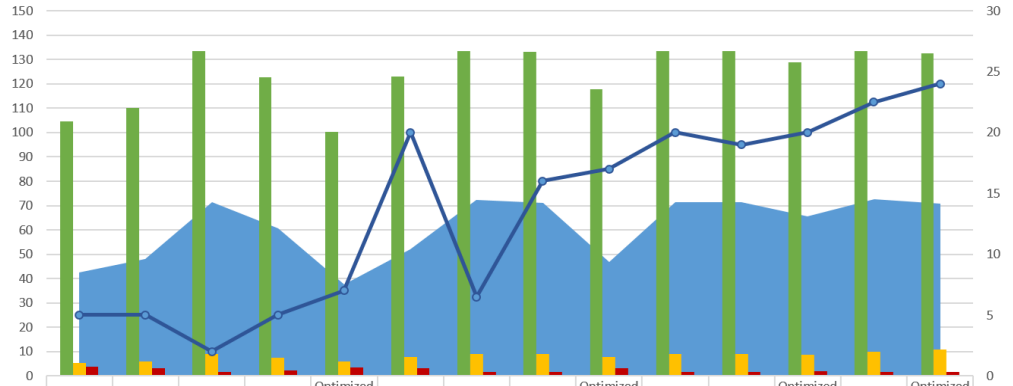

	M1_0.2km	M2_0.2km	M3_0.2km	M4_0.2km	Optimized HS_0.2km	M2_1km	M3_1km	M4_1km	Optimized HS_1km	M3_2.5km	M4_2.5km	Optimized HS_2.5km	M4_5km	Optimized HS_5km
RSS (dBm)	42.48	48.19	71.3	60.66	37.74	52.1	72.3	71.11	46.79	71.44	71.41	65.48	72.5	70.63
PL (dB)	104.48	110.19	133.3	122.66	100.38	123.1	133.3	133.11	117.7	133.44	133.41	128.89	133.5	132.64
SINR (dB)	5.31	6.02	8.91	7.58	5.99	7.87	9.02	8.88	7.69	8.93	8.96	8.73	10	10.91
Throughput (Mb/S)	3.73	3.22	1.74	2.32	3.6	3.16	1.7	1.75	3.18	1.74	1.73	1.83	1.65	1.69
Radius (km)	5	5	2	5	7	20	6.5	16	17	20	19	20	22.5	24

Figure 4.24: Optimised parameters in comparison to predictions with the four adapted models in a rural environment – HS

Optimised PL values float between -94.68dB and -136.28dB across all three environments with an improvement average between 4% to 15% in comparison to those of the four models. The optimised PL is also below the MAPL for BS and HS antennas across all environments. The optimised RSS achieves better predictions in comparison to ITU-R P.529-3, Hata-Davidson, and ATG models by an average of 3% through to 27%. However, the Okumura model tops for the highest RSS value. The RSS for the HS antenna is less than the value of BS because of the antenna gain values. Unsurprisingly, increasing the transmitter altitude or transmission power, increases both the coverage area and RSS. Keeping the transmission power constant at different transmitter altitudes yields varying levels of RSS.

Optimised SINR is kept within the acceptable average of 5.17dB and 10.91dB, with values below 4dB deemed unacceptable and considered inadequate, while any values above 19dBi are regarded as wasted transmitter power. SINR values in BS are higher than those in HS across all environments and altitudes due to achieved RSS results. Optimised throughput yields an improved predicted result between 2% and 10% in comparison to the four models. Throughput decreases with LAP altitudes in all terrains, and due to increases in path loss and distance, and shadowing.

The optimised radius predicts a wider wireless connectivity across the three environments with an average range between 2km and 6km. The modification that has been considered in the empirical models in calculating the coverage radius distance, i.e. the adoption of an elevation angle, instead of the traditional approach of coverage calculation seems more suitable to LAP quasi-stationary condition.

Overall, the optimised predictions show that PL is kept as low as possible to achieve a certain level of reception with the smallest attenuated signal. Radius, throughput and RSS are kept as high as possible to achieve a wider and stronger connectivity. The radius increases with transmitter altitude, as well as with changing from an urban to a rural environment, due to a decrease in the elevation angle. In addition to the limited effect of shadowing and reflection which in turn leads to an increase in distance.

Overall, the non-optimised predictions show that PL, RSS, and SINR values increase across all models and environments as the transmitter altitude increases, due to the increase in coverage. Throughput decreases as the transmitter altitude increases. It is observed that all the considered link budget parameters are different between HS and BS due to the differences in antenna gain. The receiver antenna height is set at 1m for HS and 5m for BS which yields an advantage for the Okumura model in achieving better coverage since a receiver antenna height of over 3m yields the same result. However, as the other adapted models accommodate receiver antenna heights of up to 30m, every increase in receiver antenna height impacts their coverage range.

The adoption of an elevation angle in calculating the coverage instead of the traditional coverage calculation, and the inclusion of MIMO diversity gain techniques to improve reliability in all four adapted models yield reasonable predictions. The improvement is evidenced in the low PL and extended coverage range. Thus, the combined antenna

and diversity gains are of importance to enhance RSS as low elevation angles leads to increase in the distance between platform and terrestrial users.

4.2 Validation of Predictions

This subsection validates the predictions of both the non-optimised and optimised propagation models at first using the NN Feed Forward Fitting Tool and then against those reported in the literature.

4.2.1 Validation using NN Feed Forward

This validation deploys the Levenberg-Marquardt backpropagation algorithm using MATLAB's NN Feed Forward Fitting Tool to evaluate the performance of the optimised against the non-optimised models. The NN-SOM output, and the predictions of the four non-optimised models are used as input in MATLAB's NN Feed Forward fitting tool. The percentage of Training, Validation, and Testing is set at 70, 15, and 15 respectively with the optimum number of hidden layers that yields best performance and regression set at 10. The aim is not to define an optimum number of neurons, but to see if this kind of network represents a solution. Assigning different number of neurons to the hidden layer obtains an approximation of how this impacts network performance. Small networks are trained easier, generalized better, and fewer training pairs are needed. The training is carried out and completed when all training sets are input through the learning algorithm in one epoch, i.e. the maximum number of iterations, before weights get updated. The process determines the optimal number of iterations during which validation produces a minimal value. A training simulation was carried out in MATLAB and the results are shown on Figures 4.25 through to 4.27.

Figure 4.25 depicts how the error function minimizes during training. Batch training is carried out and completed when all training data are input through the learning algorithm in one epoch, before weights get updated. The process determines the optimal number of iterations during which validation produces a minimal value. Validation uses regression plotting to determine that value. The performance is changed after each iteration of the training algorithm.

This training set and validation set decreases continuously to the point where overfitting happens. The network is trained for 18 epochs. After the 12th epoch the validation performance starts to increase to satisfy the condition of exhibiting an acceptable performance. After twelfth validation checks the network stops its training and returns to the state where the minimum validation performance is observed as indicated by the green circle. The result is fitting because, firstly, the final MSE is small, secondly, both the test and validation set errors have similar characteristics, thirdly, no significant overfitting occurs before iteration 12 after which the best validation performance occurs. The next step in validating is to create a regression plot of outputs in relation to the targets.

Figure 4.26 plots targets against training, validation, and test sets. Perfect fit means the data should fall along a 45-degree line, where the network outputs are equal to the targets. The dashed lines represent the targets which are equal to the difference between the perfect results and the outputs. The solid line indicates the best fit linear regression line between targets and outputs. The R value is a correlation coefficient, and indicates the relationship between the outputs and targets. If R = 1, then there is an exact linear relationship between the two vectors. If R is close to zero, then there is no such linear relationship. For this NN, the fit is practically good for most of the data sets, with R values in each case at 0.99 and above. Overall, the R values are satisfactory and represent the best levels of fitness.

Understanding the error histogram gives an additional verification of network performance, as Figure 4.27 shows. The blue, green and red bars indicate training data, validation data and testing data, respectively. The largest part of data fall on the zero-error line, which requires further examination of the outliers to decide if the data is correct, or if these data points are disparate than the rest of the data set. If it is the former, then the network is generalizing these points, which is exactly the case here.

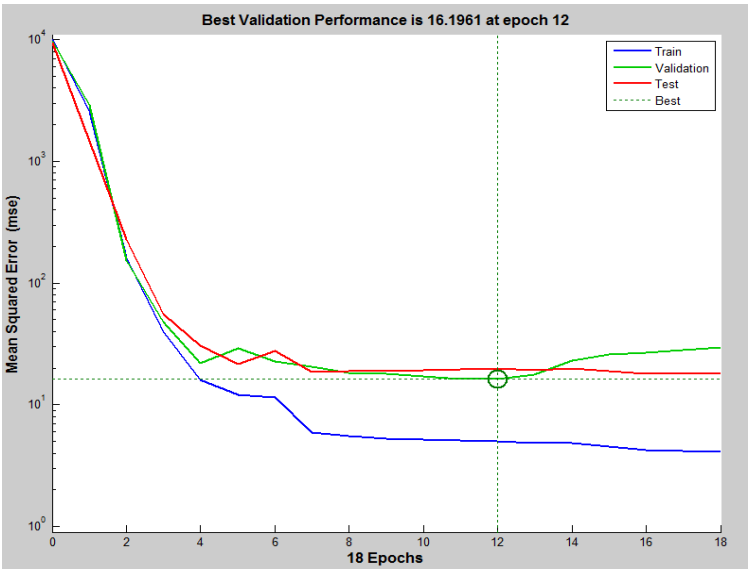

Figure 4.25: Training performance

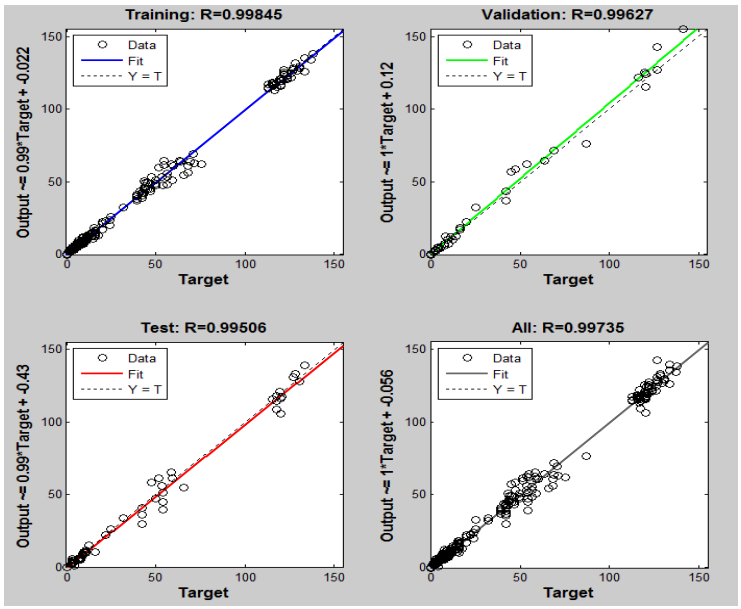

Figure 4.26: Regression plots

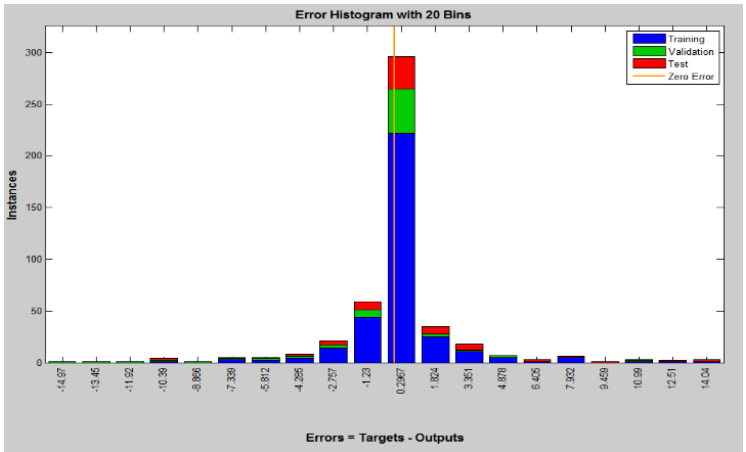

Figure 4.27: Error Histogram plot for Training data

Validation uses regression plotting to determine that value. After initial training of the NN model, the performance is changed after each iteration of the training algorithm. This training set and validation set decreases continuously to the point where overfitting happens, and thus the error rate increases. Understanding the NN training performance, Regression plots, and Error Histogram plot for Training data can give additional verification of network performance. Overall, R values are fitting and represent best fitness levels. Therefore, the NN optimised models deliver reasonable prediction results. Overfitting might happen during the training of the NN, which is undesirable, thus the MSE on the training set is already at a small value, so that is a reasonable indicator.

4.2.2 Validation Against the Results Reported in the Literature

Validation is carried out first against secondary data and then against primary data.

In [11] the Hata model LAP altitude is set at 0.2km, and frequency band is set at 1.5GHz in a rural environment with a reported PL of -135 dB and RSS of -72dBm in a 5km radius. On Table 4.3, at the same altitude and radius, and at a frequency of 3.5GHz, ITU-R P.529-3 model give better prediction results with PL of -104.48dB, RSS of -42.48dBm, whereas same with coverage. The optimised model produces better predictions at the same LAP altitude with PL of -107.38dB, RSS of -37.74dBm, and a radius of 5km.

In [2, 9] the ATG model LAP altitude is set at 1 km altitude, and frequency band at 2GHz, in an urban environment with a reported PL of -111dB and RSS of -47dBm in a 4km radius. On Table 4.1, at the same LAP altitude, but at a frequency of 3.5GHz, the Okumura model yields better predictions of RSS of -40dBm, and coverage of 8km, but at a marginally higher PL of -115.45dB. The optimised model produces better predictions at the same LAP altitude with RSS of 47.39dBm, radius of 9km, and PL of -111.20dB.

In [42] an ATG model at an altitude of 1km, and frequency band at 2.4GHz, in a suburban environment, with a reported path loss of -110dB in a 9km radius. On Table 4.2, at the same LAP altitude and radius, but at a frequency of 3.5GHz, the Okumura model yields better PL of -100.03dB, and a coverage of 14km. The optimised model produces better predictions at the same LAP altitude with PL of -98.06dB, and radius of 12km.

The optimised model was validated against a set of primary data collected in February 2017 on the PSATRI project in the capital city of KSA. Figure 4.28 shows some images in relation to the PSATRI project. One project outcome is a tethered platform that aims to measure the resistance and performance of a highly elevated tethered platform to achieve three main objectives: First, sustainability of the aerial system under different weather conditions, second, remote sensing measurements for security and emergency applications, and third, aerial imaging and live streaming. Figure 4.29 shows an overview of the PSATRI experiment parameters [122].

Figure 4.28:PSATRI in the Kingdom Saudi Arabia

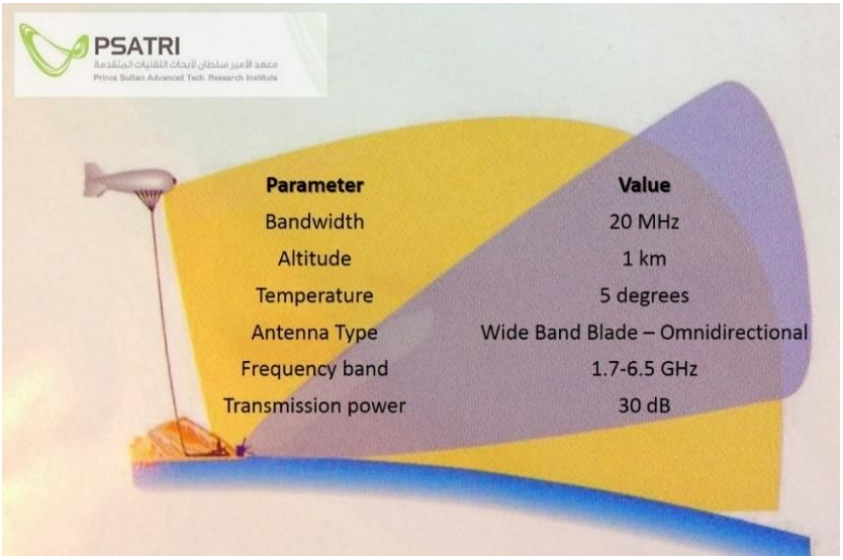

Figure 4.29: PSATRI experiment results with tethered balloon

The tethered balloon uses the ATG model in a rural environment at an altitude of 1km above ground. The results report a PL of -137.30dB in a 14km radius with an SNIR of 9dB, and a throughput of 0.15Mb/S. In comparison, the non-optimised model on Figure 4.24 shows that at the same LAP altitude and terrain, transmission power of 40dBm, the Okumura model produces a better prediction with a PL of -123dB, coverage of 20km, an SNIR of 7dB, and a throughput of 3Mb/s. The optimised model also produces better predictions at the same LAP altitude with a PL of -117.7dB, a coverage of 17km, an SNIR of 7.69dB, and a throughput of 3.18Mb/s.

Table 4.7 summarizes the predictions of the non-optimised and optimised propagation models against results reported in the literature. Based on Table 4.7 suggests that overall the link budget parameters of both the non-optimised and optimised propagation models deliver better predictions than those reported in the literature and field experiment at 0.2km and 1km LAP altitudes across different environments with an average float between 5% to 29% improvement.

Table 4.7: Validation against results reported in the literature

Model Type	Altitude (km)	Environment Type	PL (dB)	RSS (dBm)	Radius km
[11] - HATA	0.2	Rural	135	72	5
Non-Optimised - ITU-R P.529-3	0.2	Rural	104.48	42.48	5
NN- Optimised	0.2	Rural	107.38	37.74	7
[2, 9] - ATG	1	Urban	111	47	4
Non-Optimised - Okumura	1	Urban	115.45	40	8
NN Optimised	1	Urban	111.20	47.39	9
[42] - ATG	1	Suburban	110	-	9
Non-Optimised - Okumura	1	Suburban	100.03	-	14
NN Optimised	1	Suburban	98.06	-	12
PSATEI Experiment - ATG [122]	1	Rural	137.30	-	14
Non-Optimised - Okumura	1	Rural	123	-	20
NN Optimised	1	Rural	117.7	-	17

4.3 Validation through Deployment

This subsection attempts a validation through deployment in two proof-of-concept applications: Firstly, in a WSN in which Eb/No and BER of an AWGN channel are assessed, and secondly, in a cellular design in which the P_B performance is assessed.

4.3.1 Validation through Deployment in a WSN

The algorithm is sourced from equations 43 through to 47, and the predictions of the optimised and non-optimised models are used as inputs to predict BER for both large and small antenna gain using the "semilogy" function in MATLAB. Figures 4.30 to 4.32 predict the relationship between BER of a signal as a function of Eb/No across different environments at different LAP altitudes for both large and small antenna gain sensors. Tables 4.8 through to 4.10 show the numerical results of Eb/No and BER performance of the AWGN channel for both BS and HS across different environments.

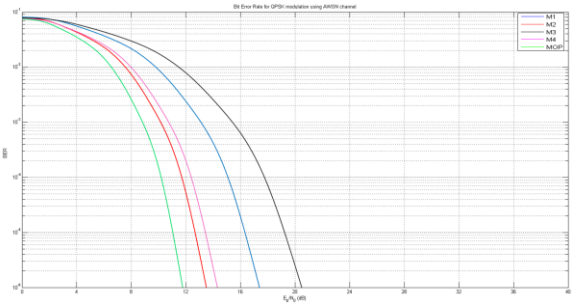

a) BS case at 0.2 km

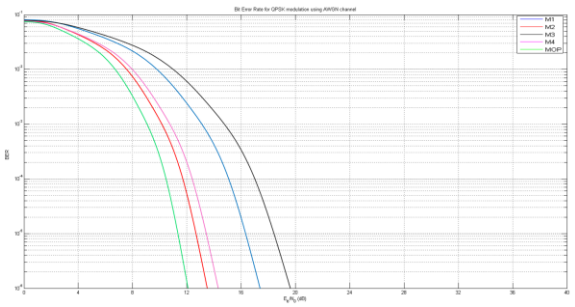

b) HS case at 0.2 km

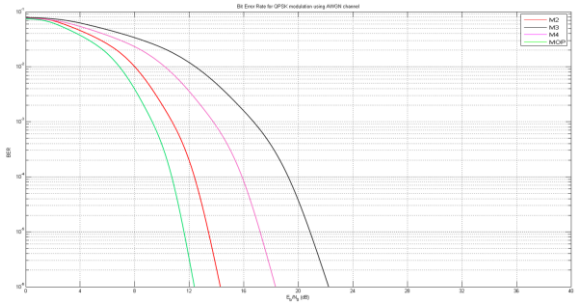

c) BS case at 1 km

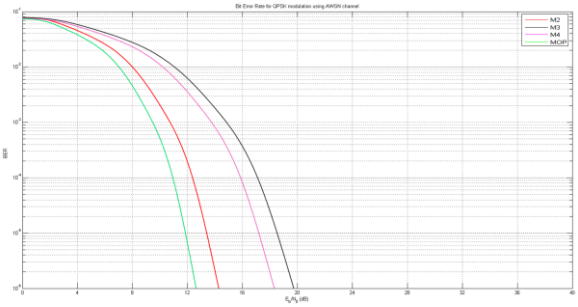

d) HS case at 1 km

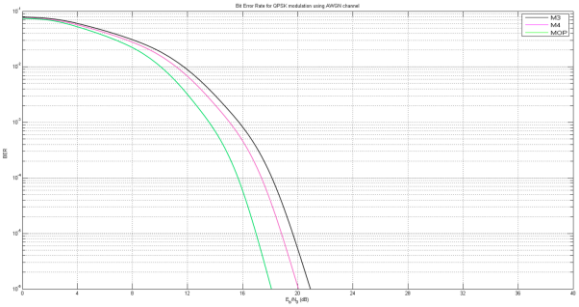

e) BS case at 2.5 km

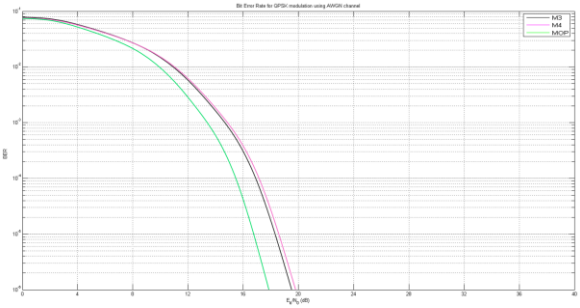

f) HS case at 2.5 km

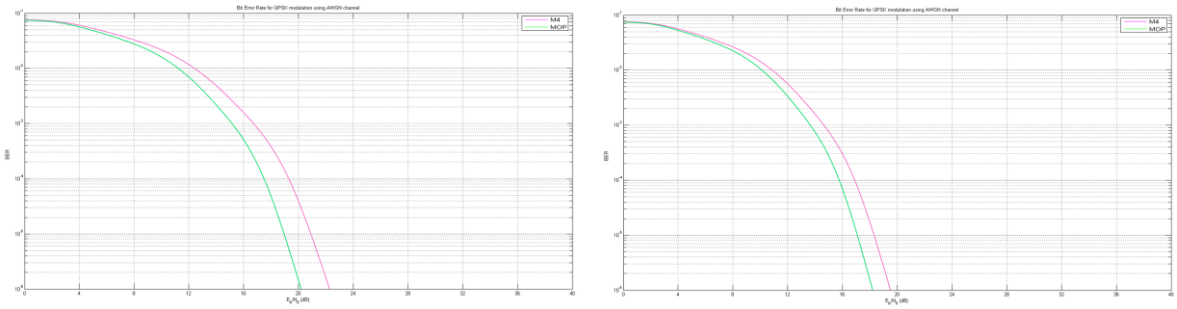

g) BS case at 5 km h) HS case at 5 km

M1: ITU-R P.529-3, M2: Okumura, M3: Hata-Davidson, M4: ATG, MOP: Optimised

Figure 4.30: BER of a signal as a function of Eb/No - Urban environment

Table 4.8: BER of a signal as a function of Eb/No - Urban environment

Model / *Parameter*	**M1**	**M2**	**M3**	**M4**	**MOP**
0.2km LAP Altitude - Large gain sensors					
Eb/No **(dB)**	17.90	13.87	21.31	14.24	12.16
0.2km LAP Altitude - Small gain sensors					
Eb/No (dB)	17.90	13.87	19.21	14.24	11.89
1km LAP Altitude - Large gain sensors					
Eb/No **(dB)**	0	14.12	22.42	18.43	12.82
1km LAP Altitude - Small gain sensors					
Eb/No **(dB)**	0	14.12	19.51	18.43	12.53
2.5km LAP Altitude - Large gain sensors					
Eb/No **(dB)**	0	0	21.34	20.80	18.61
2.5km LAP Altitude - Small gain sensors					
Eb/No **(dB)**	0	0	19.35	19.51	17.92
5km LAP Altitude - Large gain sensors					
Eb/No **(dB)**	0	0	0	22.61	20.20
5km LAP Altitude - Small gain sensors					
Eb/No **(dB)**	0	0	0	19.51	18.28
M1: ITU-R P.529-3, M2: Okumura, M3: Hata-Davidson, M4: ATG, MOP: Optimised					

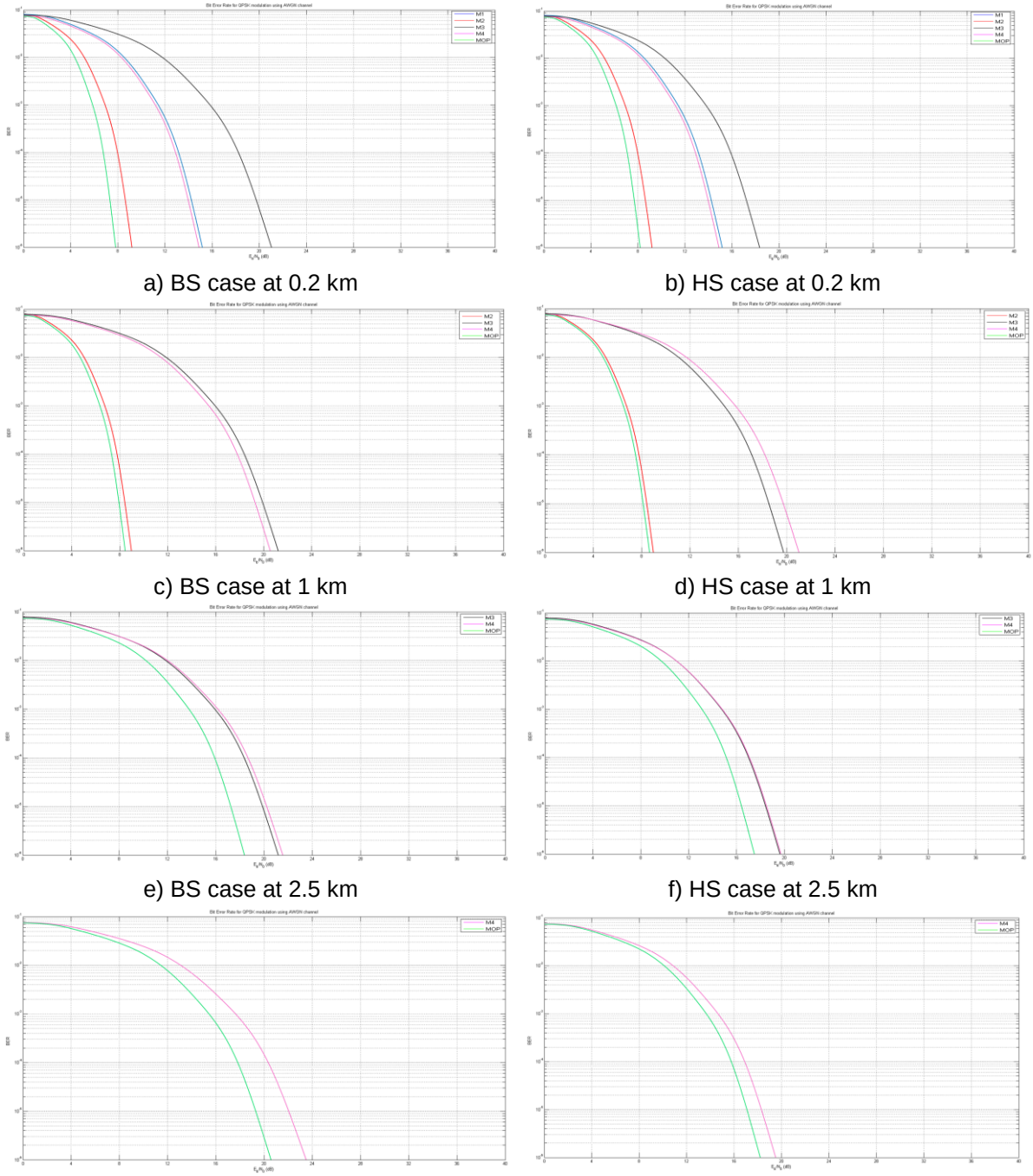

a) BS case at 0.2 km

b) HS case at 0.2 km

c) BS case at 1 km

d) HS case at 1 km

e) BS case at 2.5 km

f) HS case at 2.5 km

g) BS case at 5 km

h) HS case at 5 km

M1: ITU-R P.529-3, M2: Okumura, M3: Hata-Davidson, M4: ATG, MOP: Optimised

Figure 4.31: BER of a signal as a function of Eb/No - Suburban environment

Table 4.9: BER of a signal as a function of Eb/No - Suburban environment

Model / *Parameter*	**M1**	**M2**	**M3**	**M4**	**MOP**
0.2km LAP Altitude - Large gain sensors					
Eb/No **(dB)**	15.23	9.07	21.02	15.04	8.23
0.2k LAP Altitude - Small gain sensors					
Eb/No (dB)	15.23	9.07	18.85	15.04	7.86

1km LAP Altitude - Large gain sensors					
Eb/No **(dB)**	0	9.46	21.80	21.02	8.87
1km LAP Altitude - Small gain sensors					
Eb/No **(dB)**	0	9.46	19.39	21.02	8.59
2.5km LAP Altitude - Large gain sensors					
Eb/No **(dB)**	0	0	21	21.61	18.50
2.5km LAP Altitude - Small gain sensors					
Eb/No **(dB)**	0	0	19.49	19.50	17.86
5km LAP Altitude - Large gain sensors					
Eb/No **(dB)**	0	0	0	23.40	20.82
5km LAP Altitude - Small gain sensors					
Eb/No **(dB)**	0	0	0	19.51	18.65
M1: ITU-R P.529-3, M2: Okumura, M3: Hata-Davidson, M4: ATG, MOP: Optimised					

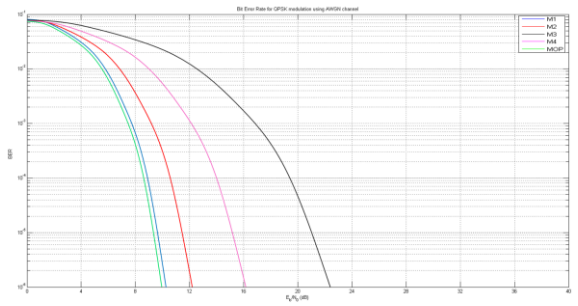

a) BS case at 0.2 km

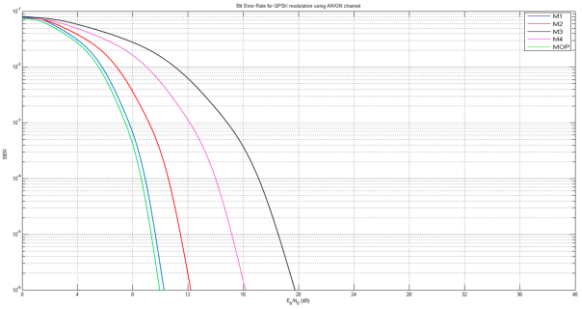

b) HS case at 0.2 km

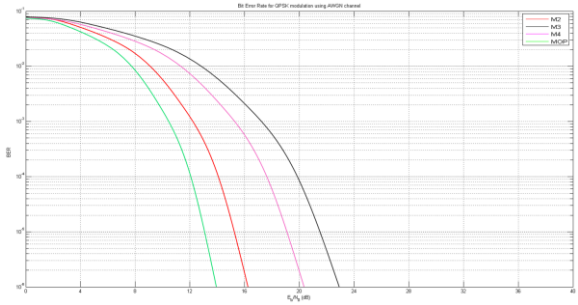

c) BS case a 1 km

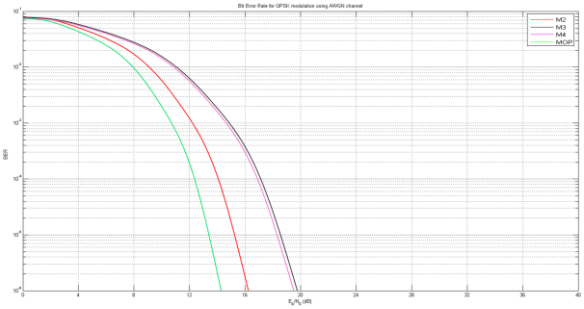

d) HS case at 1 km

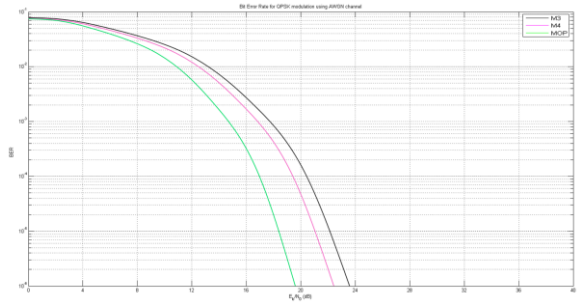

e) BS case at 2.5 km

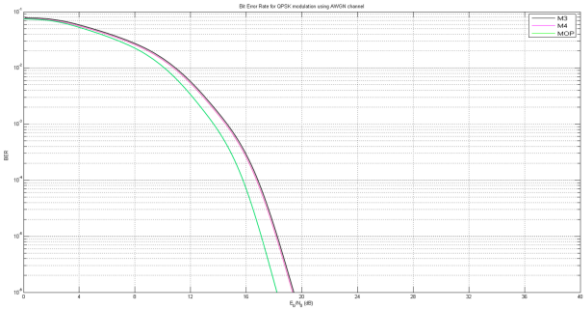

f) HS case at 2.5 km

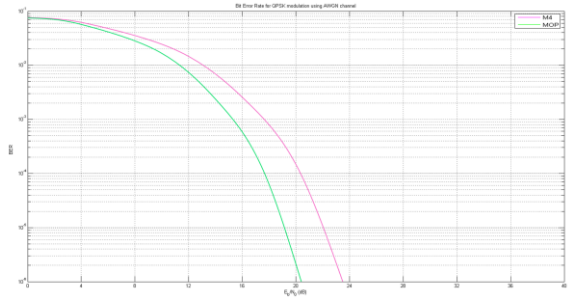

g) BS case at 5 km

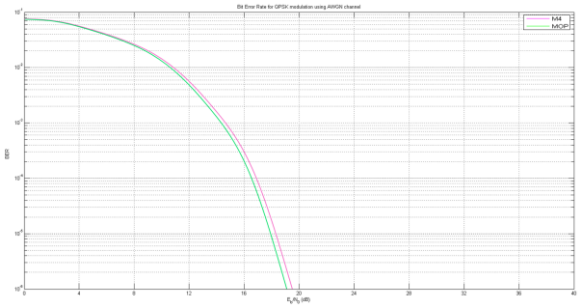

h) HS case at 5 km

M1: ITU-R P.529-3, M2: Okumura, M3: Hata-Davidson, M4: ATG, MOP: Optimised

Figure 4.32:BER of a signal as a function of Eb/No - Rural environment

Table 4.10: BER of a signal as a function of Eb/No - Rural environment

Model / *Parameter*	**M1**	**M2**	**M3**	**M4**	**MOP**
0.2km LAP Altitude - Large gain sensors					
Eb/No **(dB)**	10.80	12.51	22.72	16.25	10.67
0.2km LAP Altitude - Small gain sensors					
Eb/No (dB)	10.80	12.51	19.44	16.25	10.45
1km LAP Altitude - Large gain sensors					
Eb/No **(dB)**	0	16.39	23.05	20.40	14.77
1km LAP Altitude - Small gain sensors					
Eb/No **(dB)**	0	16.39	19.44	19.37	14.20
2.5km LAP Altitude - Large gain sensors					
Eb/No **(dB)**	0	0	23.37	22.77	19.48
2.5km LAP Altitude - Small gain sensors					
Eb/No **(dB)**	0	0	19.49	**19.47**	18.13
5km LAP Altitude - Large gain sensors					
Eb/No **(dB)**	0	0	0	23.41	20.34
5km LAP Altitude - Small gain sensors					
Eb/No **(dB)**	0	0	0	19.51	19.25
M1: ITU-R P.529-3, M2: Okumura, M3: Hata-Davidson, M4: ATG, MOP: Optimised					

The simulation results on Table 4.8 to 4.10 show the Eb/No performance of the the non-optimised models against optimised model at various LAP altitudes, receiver gains and across different environments at the lowest BER achived of $1x10^{-6}$. BER and Eb/No parameters are used interchangeably for monitoring the performance of a digital wireless system, and have been considred as two QoS indicators. The best link performance is the one that allows for the lowest possible BER with the lowest possible Eb/No. That describes a robust channel, where you can achieve low error rate without requiring a lot of transmission power.

Therefore, as can be seen from Figures 4.30 to 4.32 that at the lowest BER, the optimised model, drawn in green, exhibits the lowest Eb/No with range floats between 0.5dB to 15dB which helps optimise performance. It is observed that as PL decresses, both BER and Eb/No decreas and system performance improves. Both the Okumura and ATG models exhibit the second best Eb/No performance after the optimised model due to their low PL across all environments and altitudes. Varying LAP altitudes with an increase in distance across different geomorphologies also affects BER and Eb/No. Unsurprisingly, small gain sensors perform better than larger ones as a result of the antenna gains, but they transmit for shorter distance. The overall results of these two QoS indicators show reasonable improvement. This may lead to reduction in the required transmission power from sensors and an improved link performance between LAP and ground sensors, thus, increasing the lifetime and performance of the network.

4.3.2 Validation through Deployment in a Cellular Design

Figure 4.33 shows the percentage of wireless coverage area in each of the 13 regions in KSA in 2015. Figure 4.34 shows the ratio between population density per km² and the region size in 2015. Clearly, the region with the highest population is Jizan, and this region has also some of the harshest terrains and the lowest percentage in terms of a wireless communication infrastructure [52, 173]. Regions like Baha, Assir, and Hail are experiencing shortage in wireless coverage for the same reasons as Jizan.

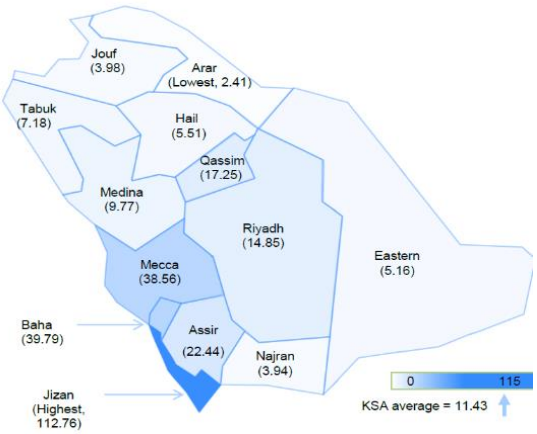

Figure 4.33: Ratio between population density per km² and region size

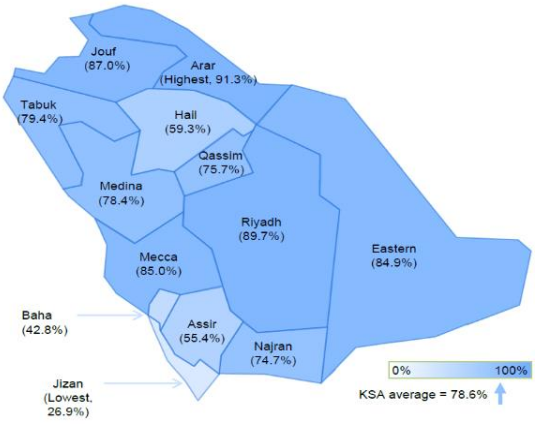

Figure 4.34: Percentage of wireless coverage

Literature reports two proposed cell planning configurations via aerial platforms that divide the coverage area into one or multiple cells [52, 71]. Each configuration has its own advantages and applications, but results show that the performance of multicell outweighs single cell configuration. In this validation, we consider a multiple cells configuration because it enhances the capacity due to frequency reuse through applying regular patterns of cells parameters to meet the demand or nature of target areas in KSA and it allows measuring of Erlang B. Our proposed cellular design uses parameters such as central cell radius, beam width and tiers, as well as the coverage size and population density. By tuning these parameters to meet the demand or nature of the target areas in KSA, predictions across three types of terrains evolve as representatives of their regions as Figures 4.35 to 4.40 illustrate.

The first type to consider is modern and developed cities, where neighbourhoods are paved, and population distribution is equal, moving from the city centre to the suburban. Riyadh is the best example of this type of region, as Figure 4.35 demonstrates. The proposed cell structure to cover such an area is shown on Figure 4.36. It consists of many adjacent small cells of equal size. The central cell radius is assumed to be 0.2km with 3.9° beam width and 15 tiers. The central cell radius and position is chosen by knowing the density of people in the covered area.

The second type of region to consider has a high population density in the city centre, and the density decreases as one moves toward the suburbs. Taif is an example of this type of region as Figure 4.37 shows. To cover such an area, the antenna will need to form small cells at the centre, and large cells at the edges by choosing the proper beam width. The central cell radius is assumed to be 1.5km, with 5.7° beam width and 13 tiers. Figure 4.38 shows the best cell structure pattern to cover such an area.

The third type is the empty region such as Al Rub' al Khali (or Empty Quarter desert) where it is scarce to find people living there, as Figure 4.39 shows. Such a place would need coverage for environmental and boundary monitoring or oil exploration. Such an area may be covered by large cells, because of the need for frequency reuse is low. The central cell radius is assumed to be 3km, with 10° beam width and 8 tiers. Figure 4.40 shows the best cell structure pattern to cover such an area.

Figure 4.35: Riyadh city – Urban

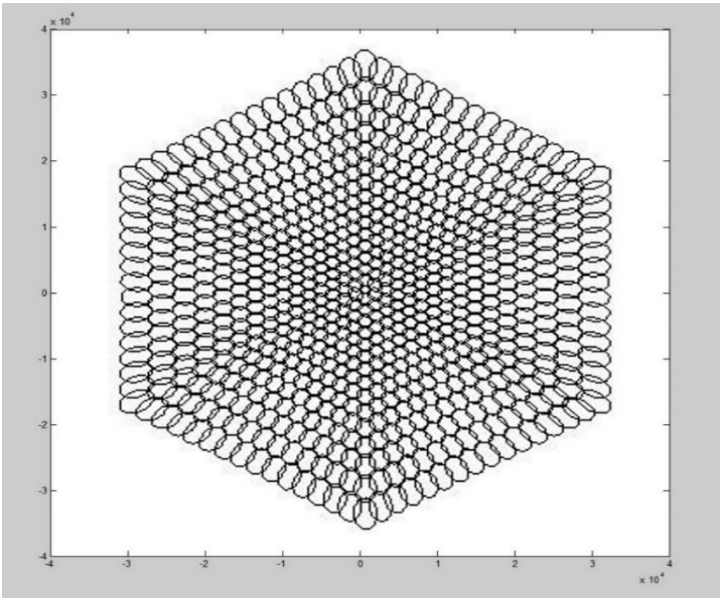

Figure 4.36: Cellular layout – Urban

Figure 4.37: Taif city – Suburban

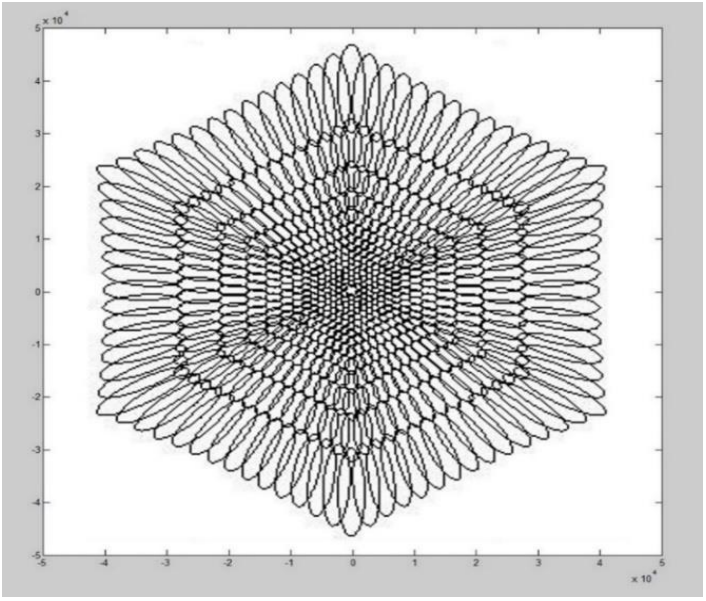

Figure 4.38: Cellular layout– Suburban

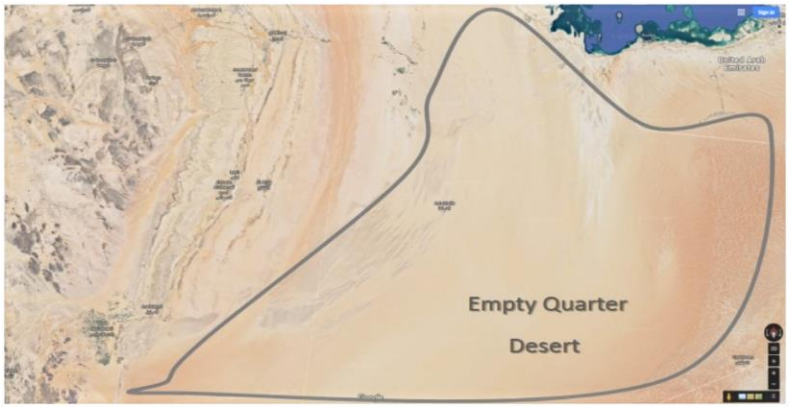

Figure 4.39: Empty Quarter desert – Rural

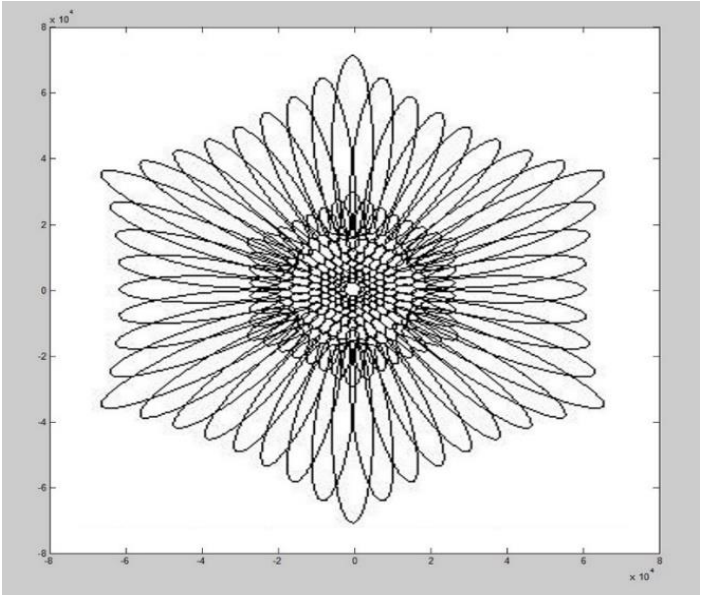

Figure 4.40: Cellular layout– Rural

A frequency reuse using smart adaptive spotbeam antenna which supports a beam shape formation that takes into consideration beam width, number of tiers and environment would cover the required area. The biggest benefit of this antenna is the ability to adjust a cell size, thus the division of the coverage area into many small cells would provide a larger system capacity. Therefore, a LAP-based cellular network design is significant in bridging the gap especially for sparsely populated and/or difficult terrains. Erlang B is used to evaluate the performance of the optimised against the adapted propagation models as Figures 4.41 to 4.43 visualize. The numerical results of the visual simulations presented on the figures are reported on Table 4.11 numerically of maximum P_B across three environments.

The P_B calculated as a function of traffic intensity in Erlang of different number of number of channels multiplied by obtained RSS of a model. Also, P_B is calculated at a 0.2km LAP altitude above ground across several environments. P_B suggests that a new call arriving is rejected because all servers (channels) are busy. This measures traffic congestion in the telephone network in cases of lost calls. P_B values in the case of optimised model, drawn in green, are lower than those of the non-optimised models with average range between 8% to 35%, because of better-optimised PL and RSS predictions. The correlation that exists between P_B and the environment yields a maximum traffic carried, A_c, across the different environments as the number of cells vary too, which again affects the P_B results. A desired probability of blocking can be set against the number of channels C to determine the maximum traffic that can be carried. Furthermore, the graph reveals the number of channels required to carry a specific amount of maximum traffic at a given GoS.

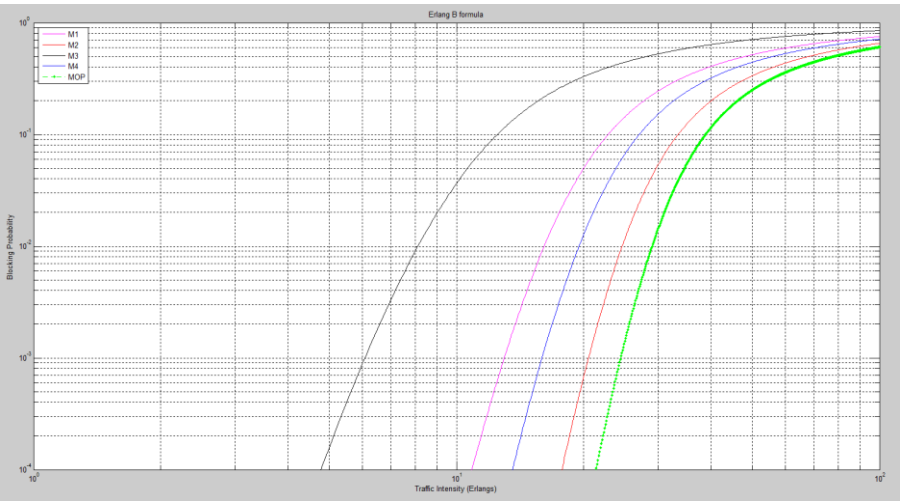

Figure 4.41: The probability of blocking – Urban

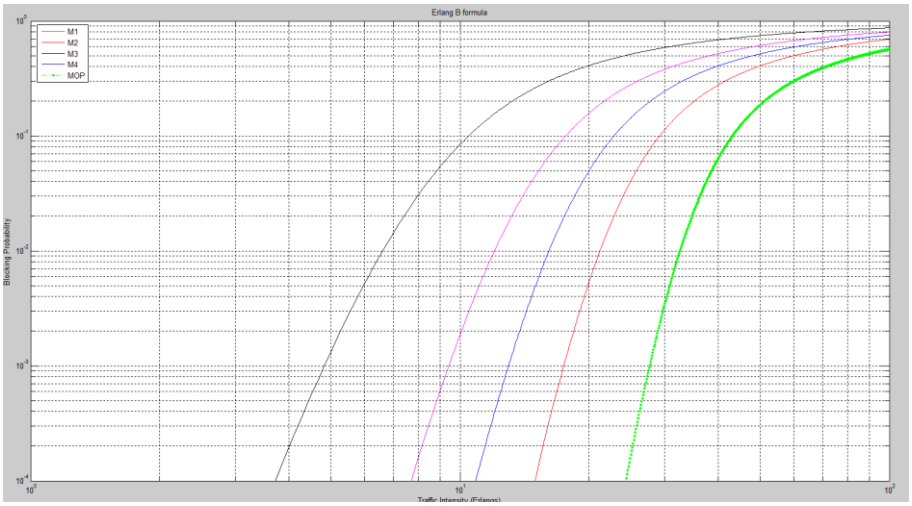

Figure 4.42: The probability of blocking – Suburban

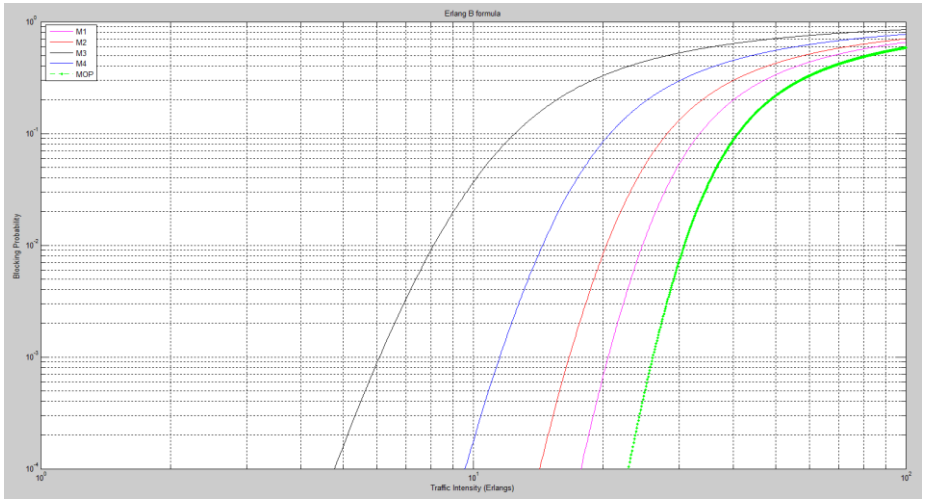

Figure 4.43: The probability of blocking – Rural

Table 4.11: The probability of blocking across the various environment

Environment	M1	M2	M3	M4	MOP
P_B- Urban	0.75	0.65	0.85	0.71	0.60
P_B- Suburban	0.80	0.69	0.87	0.75	0.56
P_B- Rural	0.65	0.70	0.85	0.77	0.58

4.4 Summary

In this chapter, the prediction results of the optimised model have been compared against those of the non-optimised propagation models. The simulation predictions that have been produced in MATLAB have been compared and analyzed based on the influence of variation of propagation conditions, distance, and receiver antenna height. In addition, when calculating the coverage radius, the elevation angle has been considered instead of the traditional approach. The predictions of both the non-optimised and optimised propagation models have been validated using the NN Feed Forward Fitting Tool and against those reported in the literature and a field experiment. The simulation results predict significant improvements with the optimised model in comparison to the non-optimised propagation models across the three environments at various altitudes.

The chapter has concluded with the validation of the optimised model through its deployment in two proof-of-concept applications; first a WSN in which the Eb/No and BER performance have been assessed, and second in a cellular network design in which the GoS has been assessed across different terrains in KSA through P_B. The predicted results in the WSN have shown that the optimised model produces the best performance in comparison to other models as it yields the lowest Eb/No at the lowest BER, which lead to reduction in the required transmission power from sensors. The assessment of P_B across the various terrains reveals that the predicted P_B values of the optimised model are also better in comparison to the non-optimised models. The following chapter summarizes the thesis and research contributions and makes suggestions for further research and development.

Chapter 5 : Concluding Discussion

This chapter gives a summary of the thesis and highlights the key research findings. It revisits the novelties underlining the three contributions made against the research objectives pursued. Finally, it makes recommendations for future research and development.

5.1 Thesis Summary

The first chapter investigates related research on last mile connectivity in relation to deploying LAPs as an aerial BSs. It identifies six key parameters that are used for measuring the link budget performance across various environments: path loss, elevation angle, LAP altitude and coverage area, power consumption, operational frequency, antenna specifications including gain, height, transmission power, and loss. It reports on a comparative review between terrestrial, aerial, both LAP and HAP, and satellite communication systems. The chapter draws an own research rationale that motivates the drafting of the research aim and objectives in relation to the research gaps identified.

The second chapter presents the design of an optimised propagation model that evolves from adapting four existing propagation models that are representatives of types that suite LAPs across different environments: ITU-R P.529-3, Okumura, Hata-Davidson, and ATG. The selected models are adapted to include the elevation angle in predicting the coverage footprint. This adaptation offers improved RSS and LoS service connectivity, and QoS service to ground receivers that generally experience low connectivity because of their distance, the earth's curvature, or terrain morphology. Optimisation is carried out in an NN-SOM that takes as inputs the non-optimised models at several LAP altitudes and clusters the results in SOM using a minimax technique. The Levenberg-Marquardt backpropagation algorithm is used to assess the performance of the evolved optimal set of parameters. The chapter concludes with a walkthrough example whose purpose is to compare the optimal model results against those of the four adapted models.

The third chapter presents the implementation of the design from the second chapter in four phases. During the first phase, the process of calibration of PL with each of the four adapted propagation models is mapped to its MATLAB code and the MAPL threshold is verified. During the second phase, the process of determining the link budget parameters, i.e. RSS, SINR, Throughput, and Radius with each propagation model is mapped to its MATLAB code. During the third phase, the evolution of the optimised propagation model using NN-SOM is mapped to its MATLAB code. During the last phase, the deployment of the optimised model is compared to the non-optimised models, at first, in a WSN in relation to the Eb/No and BER performance of an AWGN channel and then in a cellular design in relation to the GoS performance.

The fourth chapter validates the optimised model in four stages. During the first stage, the predictions of the four non-optimised models are obtained in relation to the propagation PL, RSS, SINR, throughput, and coverage footprint at various LAP altitudes and environments. During the second stage, these predictions are compared against the predictions of the optimised model under the same altitudes and environments. The optimised model aims at keeping PL as low as possible to achieve a certain level of reception with the smallest attenuated signal not exceeding the MAPL. SINR is maintained between 4dBi and 19dBi. RSS is kept as high as possible to achieve a wider wireless connectivity, and to avoid service degradation and/or interruption. Thus, the maximum RSS value is kept between -85dBm and -91dBm. RSS, throughput and coverage radius are kept as high as possible for improved signal strength and quality, higher data rates and wider connectivity. During the third stage, the Levenberg-Marquardt backpropagation algorithm is used to evaluate the performance of the optimised model against the non-optimised models in relation to predictions reported in literature. During the fourth stage, the optimised model is validated in the same two proof-of-concept applications, i.e. WSN and cellular design.

5.2 Thesis Contributions

Table 5.1 lists in order of priority the three research contributions made by this thesis against the relevant research objective.

Table 5.1: Research objectives versus contributions

Objectives	Contributions
Optimisation of a propagation model for LAPs	An optimal propagation model for last-mile connectivity evolved using Machine Learning
Implementation of the proposed optimised model as proof-of-concept	Two proof-of-concept applications, WSN and P_B, that use the optimal model
Improvement of selected existing propagation models	Adaptation of selected existing propagation models by inclusion of elevation angle in predicting coverage footprint

The first research contribution is the evolution of an optimal propagation model for last-mile connectivity using a machine learning approach, i.e. NN-SOM. This evolved model optimises path loss and RSS and minimizes transmission power and power consumption. The simulation results predict improvements to PL and RSS that average between 3% and 27% and to throughput that average between 2% and 10% across all three environments in comparison to those of the non-optimised models. In addition, the simulation results predict improvements to wireless connectivity across all three environments with the optimised radius that average between 2km and 6km.

The second contribution is the two proof-of-concept applications that utilise the optimised model, i.e. the WSN and the cellular design. The simulation results with the WSN at various LAP altitudes, receivers' gains and across different environments show that the NN-optimised model yields the lowest Eb/No that ranges between 0.5dB to 15dB at lowest BER achieved. Expectedly, large gain sensors perform better than the smaller ones because of the antenna gain values. This suggests a reduction in the required transmission power from sensors and improved link performance between the LAP and ground sensors, hence increasing the lifetime and performance of the network. The simulation results with the cellular design yield improved P_B predictions and an improved performance of Erlang B across the various environments with average range between 8% to 35%.

The third contribution is the adaptation of the propagation models for LAP to include the elevation angle to counteract the limitation of the antenna height. The simulation results with the adapted propagation models predict an improved coverage range because of LoS connectivity. Follows by addressing the suggestion that reported in the literature to consider MIMO antenna along with calculating fuller range of link budget parameters (i.e. RSS, SINR, throughput, coverage) in various scenarios at different LAP altitudes and environments. The inclusion of an elevation angle and the adoption of MIMO antenna functionality is a notable deviation from existing propagation models. With MIMO, the combined antenna and diversity gains are important to low elevation angles; as the distance between platform and ground users increases, this increases signal quality and minimizes interference and power consumption. The simulation results predict improvements with the four adapted models, in terms of extended coverage range, and RSS. Figure 5.1 puts together the three research contributions in order of priority.

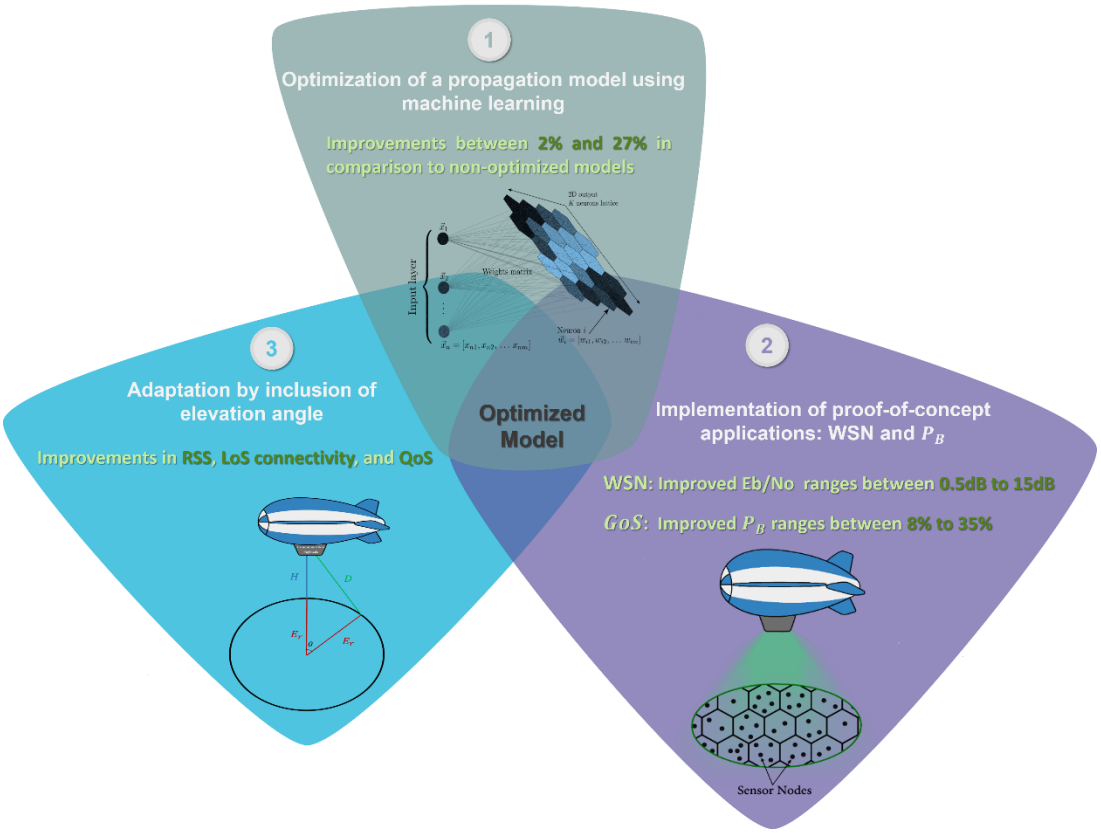

Figure 5.1: The three research contributions

5.3 Further Research and Development

Table 5.2 maps our considerations of further R&D against the three research contributions.

Table 5.2: Research objectives, contributions, and limitations or extension

Contributions	Limitations / Extension
An optimal propagation model for last-mile connectivity evolved using Machine Learning	• Variable frequency bands • Indoor and outdoor propagation models • Time overhead
Two proof-of-concept applications, WSN and P_B, that use the optimal model	• Tele-traffic data applications • Delay considerations
Adaptation of selected existing propagation models by inclusion of elevation angle in predicting coverage footprint	• Variable elevation angles • MIMO antenna considerations • Geolocations, i.e. google maps

In this work, only the 3.5 WiMAX frequency band has been considered in extending the footprint and achieving a low PL. Additional frequency bands may be considered for inclusion in the optimal model, which in turn may enhance RSS and maximize throughput especially for areas with limited coverage but significant number of users. One such frequency band is 28GHz/47GHz which may be shared with satellites [177]. Another such frequency band is 60GHz, which is dedicated for 5G WiGig. Future R&D may, for example, include 60GHz as an access point either in infrastructure or ad-hoc modes within a mesh network and then assessing the optimised model performance.

The optimised model in this work only includes parameters for outdoor propagation, i.e. FSPL and large-scale fading, at different altitudes. Therefore, future R&D may include parameters in relation to calculating indoor propagation, i.e. small-scale fading, building penetration loss. However, such a combination of indoor and outdoor parameters would only be suitable at “low” altitudes for serving mobile apps, otherwise the FSPL will dominate PL at high altitudes.

Although, the optimization process time takes an average between 2 to 3 hours to converge to optimum link budget values, still by far quicker and more accurate than the classic way of optimizing link budget parameters via what currently been used which is “trial and error approach”. As future extension of this work, time overhead can be reviewed in order to enhance time of optimization.

Measuring performance in relation to tele-traffic data is necessary for telecommunication networks planning to ensure that network costs are minimized without compromising QoS to the user. This work only considers one GoS benchmark in relation to QoS, i.e. P_B, in the second proof-of-concept. Therefore, including additional GoS benchmarks such as P_D to measure performance in relation to tele-traffic data may yield a more accurate result. This delay parameter comprises of several delays such as queueing, processing, transmission and propagation delays. We are currently exploiting this dimension and our preliminary findings have been reported in an IEEE conference paper which has been accepted for presentation [178].

Monitoring delay is not only significant to tele-traffic but also to handover performance. The optimised model the has evolved with this work aims at primarily enhancing connectivity for last mile by optimising coverage and RSS. However, including delay as one of the optimised parameters will directly interfere with RSS and coverage. Inclusion of this parameter might be of higher priority for emergency communications or during handover but of lower priority where, for example, coverage is the primary concern. Thus, optimising simultaneously RSS, coverage, throughput, and delay is not achievable if we are seeking to decrease the switching load whilst sustaining an acceptable level of QoS for connected devices.

Varying the elevation angle affects directly the LAP coverage area and LoS connectivity. Whilst a high elevation angle would yield a LAP coverage area of a relatively small radius a low elevation angle may reduce the LoS connectivity. Future R&D may involve varying of the elevation angle in relation to geomorphology and then assessing the optimised model performance.

In this work, only MIMO's spatial diversity is considered in improving reliability, coverage and power consumption. Future R&D may consider the inclusion of spatial multiplexing to improve data rates and reduce interference.

Integrating live geolocations sourced from google maps may provide a more realistic background to the environmental considerations whilst assessing propagation model performance. We are currently also exploiting this in [178] through a 3D RF tool, i.e. Remcom Wireless InSite, that enables us to respond to the ad hoc structure of disaster relief, and measure the performance of rescue teams, e.g. in Florida state in the USA during Hurricane Irma in August 2017.

References

[1] D. Grace, T. Jiang, S. Allsopp, and L. Reynaud, 'Integrated Project ABSOLUTE - Aerial Base Stations with Opportunistic Links for Unexpected & Temporary Events', Oct. 2013.

[2] A. l-Hourani, S. Kandeepan, and S. Lardner, 'Optimal LAP Altitude for Maximum Coverage', *IEEE Wireless Communications Letters*, vol. 3, no. 6, pp. 569–572, Dec. 2014.

[3] J.Kosmerl and A. Vilhar, 'Base stations placement Optimisation in wireless networks for emergency communications', *2014 IEEE International Conference on Communications Workshops (ICC)*, Sydney, Australia, Jun. 2014, pp.200-204.

[4] L. Reynaud and T. Rasheed, 'Deployable aerial communication networks: challenges for futuristic applications', *Proceedings of the 9th ACM symposium on Performance evaluation of wireless ad hoc, sensor, and ubiquitous networks - PE-WASUN '12*, Paphos, Cyprus, 2012, pp.9-16.

[5] M. Shahajahan and A. Hes-Shafi, "Analysis of Propagation Models for WiMAX at 3.5 GHz", PhD thesis, Blekinge Institute of Technology, Sweden, 2009.

[6] P. Prajesh, R. Singh 'A Survey on Various Propagation Model for Wireless Communication', in *5th IEEE International Conference on Advanced Computing & Communication Technologies [ICACCT-2011]*, Qafqaz University Baku, Azerbaijan, Oct. 2011, pp. 61–64,

[7] D. Nalineswari and N. Rakesh, 'Link budget analysis on various terrains using IEEE 802.16 WIMAX standard for 3.5 GHz frequency', *IEEE International Conference on Electrical, Computer and Communication Technologies (ICECCT)*, Coimbatore, India, Mar. 2015, pp.1-5.

[8] C. Phillips, D. Sicker, and D. Grunwald, "A survey of wireless path loss prediction and coverage mapping methods," *IEEE Communications Surveys & Tutorials*, vol. 15, no. 1, pp. 255–270, 2013.

[9] A. Al-Hourani and S. Kandeepan, 'Cognitive Relay Nodes for airborne LTE emergency networks', *7th International Conference on Signal Processing and Communication Systems (ICSPCS)*, Carrara, Australia, Dec. 2013, pp.1-9.

[10] "Recommendation ITU-R P.1411-6 Propagation data and prediction methods for the planning of short-range outdoor radio communication systems and radio local area networks in the frequency range 300 MHz to 100 GHz", International Telecommunication Union (ITU), 2015.

[11] S. A. Khaleefa, S. H. Alsamhi, and N. S. Rajput, 'Tethered balloon technology for telecommunication, coverage and path loss', *2014 IEEE Students' Conference on Electrical, Electronics and Computer Science*, Bhopal, India, Mar. 2014, pp.1-4.

[12] S. Alsamhi, S. Gapta, N. Rajput and R. Saket, "Network Architectures Exploiting Multiple Tethered Balloon Constellations for Coverage Extension", *6th International Conference on Advances in Engineering Sciences and Applied Mathematics*, Kuala Lumpur, Malaysia, Dec. 2016, pp.1-6.

[13] A. Rubina, O. Andryeyev, M. Harounabadi, A. Al-Khani, and O. Artemenko, "Investigation and Adaptation of Signal Propagation Models for a Mixed Outdoor-Indoor Scenario Using a Flying GSM Base Station", *Springer Ad Hoc Networks*, Ottawa, vol. 184, pp. 128–139, 2016.

[14] S. Chandrasekharan, A. Al-Hourani, K. Gomez, S. Kandeepan, R. Evans, L. Reynaud, and S. Scalise, "Performance Evaluation of LTE and WiFi Technologies in Aerial Networks", *IEEE Globecom Workshops (GC Wkshps), Washington,* USA, Dec. 2016, pp.1-7.

[15] A. Guillen-Perez, R. Sanchez-Iborra, M. Cano, J. Sanchez-Aarnoutse, and J.Garcia-Haro, "WiFi NETWORKS ON DRONES", *ITU Kaleidoscope: ICTs for a Sustainable World (ITU WT)*, Bangkok Thailand, Jan. 2017, pp.1-8.

[16] N. Goddemeier, K. Daniel and C. Wietfeld, "Coverage Evaluation of Wireless Networks for Unmanned Aerial Systems", *IEEE GLOBECOM Workshops (GC Wkshps)*, Miami, USA, Jan. 2011, pp.1760 – 1765.

[17] A. Al-Hourani, S. Kandeepan, and A. Jamalipour, 'Modeling air-to-ground path loss for low altitude platforms in urban environments', *2014 IEEE Global Communications Conference*, Austin, USA, Dec. 2014, pp. 2898 – 2904.

[18] K. Gomez, A. Hourani, L. Goratti, R. Riggio, S. Kandeepan, I. Bucaille, 'Capacity evaluation of Aerial LTE base-stations for public safety communications', *European Conference on Networks and Communications (EuCNC)*, Paris, France, Jun. 2015, pp. 133 – 138.

[19] L. Zhao, J. Yi, F. Adachi, C. Zhang, and H. Zhang, 'Power-Efficient Radio Resource Allocation for Low-Medium-Altitude Aerial Platform Based TD-LTE Networks', *IEEE Vehicular Technology Conference (VTC Fall)*, Quebec, Canada, Sep. 2012, pp.1-4.

[20] L. Bing, "Study on Modelling of Communication Channel of UAV", *Procedia Computer Science*, vol. 107, pp. 550–557, 2017.

[21] A. AL-Hourani, S. Chandrasekharan, G. Kaandorp, W. Glenn, A. Jamalipour, and S. Kandeepan, "Coverage and rate analysis of aerial base stations", *IEEE Transactions on Aerospace and Electronic Systems*, vol. 52, pp. 3077-3081, 2016.

[22] J. S¨ae, S. Yunas, and J. Lempiainen, "Coverage aspects of temporary LAP network," *12th annual conference on wireless on-demand network systems and services (WONS)*, Cortina d'Ampezzo, Italy, August 2016, pp.1-4.

[23] E. Kalantari, H. Yanikomeroglu and A. Yongacoglu, "On the Number and 3D Placement of Drone Base Stations in Wireless Cellular Networks", *84th IEEE Vehicular Technology Conference (VTC-Fall),* Montreal, Canada, Sep. 2017, pp.1-6.

[24] S. Chandrasekharan, K. Gomez, A. Al-Hourani, S. Kandeepan, T. Rasheed, L. Goratti, L. Reynaud, D. Grace, I. Bucaille, T. Wirth, and S. Allsopp, "Designing and implementing future aerial communication networks," *IEEE Communications Magazine*, vol. 54, pp. 26-34, 2016.

[25] M. Helmy, T. Baykas, and H. Arslan, "Optimisation of aerial base station location in LAP for disaster situations," *IEEE Conference on Standards for Communications and Networking (CSCN)*, Tokyo, Japan, Oct. 2015, pp. 240 – 244.

[26] F. Teixeira, "Tethered Balloons and TV White Spaces: A Solution for Real-time Marine Data Transfer at Remote Ocean Areas", *IEEE Third Underwater Communications and Networking Conference (UComms)*, Lerici, Italy, August 2016, pp.1-5.

[27] 'A Practical Introductory Guide on Using Satellite Technology for Communications', *International Telecommunications Satellite Organization (INTELSAT)*, 11-Aug-2014. [Online]. Available: http://www.intelsat.com/wp-content/uploads/2013/01/5941-SatellitePrimer-2010.pdf. [Accessed: 01-Apr-2015].

[28] B. G. Evans, 'The role of satellites in 5G', IEEE *7th Advanced Satellite Multimedia Systems Conference and the 13th Signal Processing for Space Communications Workshop (ASMS/SPSC)*, Livorno, Italy, Jan. 2014, pp. 197 – 202.

[29] J. S. Seybold, *Introduction to RF propagation*. UK: Wiley-Blackwell Ney jersy, USA, 2005.

[30] D. Grace and M. Mohorcic, *Broadband communications via high-altitude platforms*. United Kingdom: Wiley-Blackwell (an imprint of John Wiley & Sons Ltd), 2010.

[31] A. Aragón-Zavala, J. Cuevas-Ruíz, and J. Delgado-Penín, *High-altitude platform systems for wireless communications*. United Kingdom: Wiley-Blackwell (John Wiley & Sons Ltd), 2008.

[32] J. Holis and P. Pechac, "Elevation dependent shadowing model for mobile communications via high altitude platforms in built-up areas," *IEEE Transactions on Antennas and Propagation*, vol. 56, pp. 1078–1084, 2008.

[33] K. Siwiak, "Radio wave Propagation: Urban and Suburban Paths," in *Radiowave propagation and antennas for personal communications*, Y. Bahreini, Ed. Boston, MA: Artech House Publishers, 1995.

[34] M. Ryu and O. Masayuki, "*Wireless Communications System Using Stratospheric Platforms: R and D Program on Telecom and Broadcasting System Using High Altitude Platform Stations*", Journal of the Communication Research Laboratory, vol. 48, pp. 33–48, 2001.

[35] F. Dong, H. Han, X. Gong, J. Wang and H. Li, "*A Constellation Design Methodology Based on QoS and User Demand in High-Altitude Platform Broadband Networks*", IEEE Transactions on Multimedia, vol. 18, pp. 2384-2397, 2016.

[36] Wen-Qin Wang and Dingde Jiang, "*Integrated Wireless Sensor Systems via Near-Space and Satellite Platforms: A Review*", IEEE Sensors Journal, vol. 14, pp. 3903-3914, 2014.

[37] Z. Yang, 'Coexistence, Deployment and Business Models of Heterogeneous Wireless Systems Incorporating High Altitude Platforms', PhD thesis, Blekinge Institute of Technology, SWEDEN, 2013.

[38] A. Habib, "MIMO Channel Modeling for Integrated High Altitude Platforms , Geostationary Satellite / Land Mobile Satellite and Wireless Terrestrial Networks", *Journal of Space Technology*, vol. 3, pp.19-26, 2013.

[39] A. Mohammed, A. Mehmood, F.-N. Pavlidou, and M. Mohorcic, 'The Role of High-Altitude Platforms (HAPs) in the Global Wireless Connectivity', *Proceedings of the IEEE*, vol. 99, pp. 1939–1953, 2011.

[40] M. Letizia, 'Circularly Polarized multi-beam Antenna System for High-Altitude-Platforms', PhD thesis, ÉCOLE POLYTECHNIQUE FÉDÉRALE DE LAUSANNE, Switzerland, 2013.

[41] G. Laštovička-Medin, "Nano/pico/femto-satellites: Review of challenges in space education and science integration towards disruptive technology", *5th Mediterranean Conference on Embedded Computing (MECO)*, Bar, Montenegro, June 2016, pp. 357 – 362.

[42] M. Helmy, Z. Esat Ankaralı, M. Siala, T. Baykaş, and H. Arslan, "Dynamic Utilization of Low-Altitude Platforms in Aerial Heterogeneous Cellular Networks", *IEEE 18th Wireless and Microwave Technology Conference (WAMICON),* Cocoa Beach, USA, April 2017, pp.1-6.

[43] N. Hossein Motlagh, T. Taleb and O. Arouk, "*Low-Altitude Unmanned Aerial Vehicles-Based Internet of Things Services: Comprehensive Survey and Future Perspectives*", IEEE Internet of Things Journal, vol. 3, pp. 899-922, 2016.

[44] I. Dalmasso, I. Galletti, R. Giuliano, F. Mazzenga, 'WiMAX networks for emergency management based on UAVs', *2012 IEEE First AESS European Conference on Satellite Telecommunications (ESTEL)*, Rome, Italy, Oct 2012, pp.1-6.

[45] K. Du and M. Swamy, *Wireless communication systems*. Cambridge, UK: Cambridge University Press, 2010.

[46] D. P. Agrawal and Q.-A. Zeng, *Introduction to wireless and mobile systems*. United States: CENGAGE Learning Custom Publishing, 2011.

[47] M. Richharia, *Mobile satellite communications: principles and trends*. United States: John Wiley & Sons Inc, 2014.

[48] V. Gawande, P. Bilaye, A. Gawale, R. Pant, and U. Desai, 'Design and Fabrication of an Aerostat for Wireless Communication in Remote Areas',*7th AIAA ATIO Conf, 2nd CEIAT Int'l Conf on Innov and Integr in Aero Sciences,17th LTA Systems Tech Conf; followed by 2nd TEOS Forum*, Belfast, Northern Ireland, Sep. 2007, pp.1-14.

[49] A. Vilhar, A. Hrovat, T. Javornik, and M. Mohorcic, 'Experimental analysis of wireless temporary networks deployed by low altitude platforms', IEEE 18th International Workshop on Computer Aided Modeling and Design of Communication Links and Networks (CAMAD), Berlin, Germany, Sep. 2013, pp.238 – 242.

[50] P. Bilaye, V. Gawande, U. Desai, A. Raina, and R. Pant, 'Low Cost Wireless Internet Access for Rural Areas using Tethered Aerostats', *IEEE Third International Conference on Industrial and Information Systems*, Kharagpur, India, Dec. 2008, pp.1-5.

[51] S. H. Alnajjar, F. Malek, M. Razalli, and M. Ahmad, 'Low-Altitude Platform to Enhance Communications Reliability in Disaster Environments', *Journal of Advances in Information Technology*, vol. 5, pp. 21-30, 2014.

[52] F. Almalki, M. Angelides, "Considering near space platforms to close the coverage gap in wireless communications; the case of the Kingdom of Saudi Arabia", *FTC 2016 - Future Technologies Conference*, San Francisco, USA, Dec. 2016, pp. 224 – 230.

[54] Iskandar and A. Abubaker, 'Co-channel interference mitigation technique for mobile WiMAX downlink system deployed via Stratospheric Platform', *2014 8th International Conference on Telecommunication Systems Services and Applications (TSSA)*, Kuta, Indonesia, Oct. 2014, pp.1-5.

[55] K. Namuduri, Y. Wan, and M. Gomathisankaran, 'Mobile ad hoc networks in the sky: State of the Art, Opportunities, and Challenges',*Proceedings of the second ACM MobiHoc workshop on Airborne networks and communications - ANC '13*, Bangalore, India , July 2013, pp.25-28.

[56] S. Dawoud, A. Uzun, S. Gondor, and A. Kupper, "Optimizing the Power Consumption of Mobile Networks Based on Traffic Prediction," *IEEE 38th Annu. Comput. Softw. Appl. Conf.*, Vasteras, Sweden, July 2014, pp. 279–288.

[57] U. B. Antonio Capone Ilario Filippini Bernd Gloss, "Rethinking Cellular System Architecture for Breaking Current Energy Efficiency Limits," *Sustain. Internet ICT Sustain. (SustainIT),* Pisa, Italy, Oct. 2012, pp.1-5.

[58] G. Baldini, S. Karanasios, D. Allen, and F. Vergari, 'Survey of Wireless Communication Technologies for Public Safety', *IEEE Communications Surveys & Tutorials*, vol. 16, pp. 619–641, Jan. 2014.

[59] International Telecommunication Union (ITU), 'Utilization of telecommunications/ICTs for disaster preparedness, mitigation and response', 2014. [Online]. Available: http://www.itu.int/dms_pub/itu-d/opb/stg/D-STG-SG02.22.1-2014-PDF-E.pdf. [Accessed: 28- Feb- 2015].

[60] Y. Zeng, R. Zhang and T. Lim, "*Wireless communications with unmanned aerial vehicles: opportunities and challenges*", IEEE Communications Magazine, vol. 54, pp. 36-42, 2016.

[61] K. Gomez, K. Sithamparanathan, V. Mut, B. Vincent, R Raquel, H. Romain, R. Tinku, G. Leonardi, R. Laurent, G. David, Z. Qiyang, H. Yunbo, R. Salahedin, M. Nils, J. Tao, B. Isabelle, W. Thomas, C. Roberta, and J.Tomaz, "*Aerial base stations with opportunistic links for next generation emergency communications*", IEEE Communications Magazine, vol. 54, pp. 31-39, 2016.

[62] A. Valcarce, T. Rasheed, K. Gomez, S. Kandeepan, L. Reynaud, R. Hermenier, A. Munari, M. Mohorcic, M. Smolnikar, and I. Bucaille, 'Airborne Base Stations for Emergency and Temporary Events', in *Lecture Notes of the Institute for Computer Sciences, Social Informatics and Telecommunications Engineering*, Springer Science amd Business Media, pp 13-25, 2013.

[63] A. Kaadan, D. Zhou, H. Refai, P. LoPresti, 'Modelling of aerial-to-aerial short-distance free-space optical links', *Integrated Communications, Navigation and Surveillance Conference (ICNS)*, Herndon, USA, Apr. 2013, pp.1-12.

[64] K. M. Gajra and R. S. Pant, 'SoPTAS: Solar powered tethered aerostat system', *1st International Conference on Non Conventional Energy (ICONCE 2014)*, Kalyani, India, Jan. 2014, pp.65-68.

[65] I. Bucaille, S. Hethuin, T. Rasheed, A. Munari, R. Hermenier, and S. Allsopp, 'Rapidly Deployable Network for Tactical Applications: Aerial Base Station with Opportunistic Links for Unattended and Temporary Events ABSOLUTE Example', *MILCOM 2013 - IEEE Military Communications Conference*, San Diego, USA, Nov. 2013, pp.1116-1120.

[66] O. Andryeyev, O. Artemenko and A. Mitschele-Thiel, "Improving the System Capacity Using Directional Antennas With a Fixed Beam on Small Unmanned Aerial Vehicles", *European Conference on Networks and Communications (EuCNC)*, Paris, France, 2015, pp. 139-143.

[67] S. Zhang, Z. Wang, M. Qiu and M. Liu, "*BER-based Power Scheduling in Wireless Sensor Networks*", Journal of Signal Processing Systems, vol. 72, pp. 197-208, 2013.

[68] D. Duan, "Optimizing the Battery Energy Efficiency in Wireless Sensor Networks", *IEEE International Conference on Signal Processing, Communications and Computing (ICSPCC)*, Xi'an, China, Sep. 2011, pp.1-6.

[69] T. Wang, W. Heinzelman and A. Seyedi, "Minimization of Transceiver Energy Consumption in Wireless Sensor Networks with AWGN Channels", *46th Annual Allerton Conference on Communication, Control, and Computing*, Urbana-Champaign, USA, Sep. 2008, pp.62-66.

[70] M. Poulakis, S. Vassaki and A. Panagopoulos, "Satellite-Based Wireless Sensor Networks: Radio Communication Link Design", *7th European Conference on Antennas and Propagation (EuCAP)*, Gothenburg, Sweden, April 2013, pp. 2620 – 2624.

[71] Z. Yang and A. Mohammed, “High Altitude Platforms for Wireless Sensor Network applications,” IEEE International Symposium on Wireless Communication Systems, Reykjavik, Iceland, Oct. 2008, pp. 613 – 617.

[72] C., Robert M, *The technical collection of intelligence*. Washington, DC: CQ Press, 2010.

[73] G. S. Rao, *Mobile Cellular Communication*. India: Pearson Education India, 2013.

[74] ‘state of the satellite industry report 2014’, *The Satellite Industry Association (SIA)*, Sep-2014. [Online]. Available: http://www.sia.org/wp-content/uploads/2014/09/SSIR-September-2014-Update.pdf. [Accessed: 30-Mar-2015].

[75] J. N. Pelton, S. Madry, S. Camacho-Lara, and editors., *Handbook of Satellite Applications: 2013*. United States: Springer-Verlag New York Inc., 2013.

[76] S. More and D. K. Mishra, "4G revolution: WiMAX technology," *Third Asian Himalayas International Conference on Internet*, Kathmandu, Nepal, Nov. 2012, pp.1-4.

[77] A. Al-Kandari, M. Al-Nasheet, and A. R. Abdulgafer, "WiMAX vs. LTE: An analytic comparison," *2014 Fourth International Conference on Digital Information and Communication Technology and its Applications (DICTAP)*, Bangkok, Thailand, May 2014, pp. 389-393.

[78] U. R. Mori, P. Chandarana, G. Gajjar, and S.Dasi , "Performance comparison of different modulation schemes in advanced technologies WiMAX and LTE," *IEEE International Advance Computing Conference (IACC)*, Banglore, India, Jun. 2015, pp. 286 – 289.

[79] I. Aldmour, "LTE and WiMAX: Comparison and future perspective," *Communications and Network*, vol. 05, pp. 360–368, 2013.

[80] D. Eberle, "LTE vs. WiMAX 4th generation telecommunication networks,". [Online]. Available: https://www.snet.tu-berlin.de/fileadmin/fg220/courses/WS1011/snet-project/lte-vs-wimax_eberle.pdf. Accessed [Jan. 6, 2016].

[81] D. Astely, "LTE release 12 and beyond," *IEEE Communications Magazine*, vol. 51, pp. 154–160, Jul. 2013.

[82] T. A. Benmusa, A. J. Belgassem, and M. A. S. Ibrahim, "Planning and dimensioning a high speed 4G WiMAX network in Tripoli area," *14th International Conference on Sciences and Techniques of Automatic Control & Computer Engineering - STA’2013*, Sousse, Tunisia, Dec. 2013, pp. 318 – 324.

[83] D. Bankov, E. Khorov, A. Lyakhov, and E. Stepanova, "Fast centralized authentication in Wi-Fi HaLow networks", *IEEE International Conference on Communications*, Paris, France, May 2017, pp.1-6.

[84] E. Mohamed, K. Sakaguchi and S. Sampei, "Wi-Fi Coordinated WiGig Concurrent Transmissions in Random Access Scenarios", *IEEE Transactions on Vehicular Technology*, vol. 66, pp. 10357-10371, 2017.

[85] A. A. Ekram Hossain, Mehdi Rasti, Hina Tabassum, “Evolution Toward 5G MULTI -TIER Cellular Wireless Networks : An Interference Management Perspective,” *IEEE Wirel. Commun.*, vol. 21, pp. 118–127, 2014.

[86] J. Cao, Maode, H. Li, Y. Zhang, and Z. Luo, ‘A Survey on Security Aspects for LTE and LTE-A Networks’, *IEEE Communications Surveys & Tutorials*, vol. 16, pp. 283–302, Jan. 2014.

[87] K. Gomez, T. Rasheed, L. Reynaud, and S. Kandeepan, ‘On the performance of aerial LTE base-stations for public safety and emergency recovery’, *IEEE Globecom Workshops (GC Wkshps)*, Atlanta, USA, Dec. 2013, pp. 1391 – 1396.

[88] M. A. Rahman, ‘Enabling drone communications with WiMAX Technology’, *The 5th International Conference on Information, Intelligence, Systems and Applications*, Chania, Greece, Jul. 2014, pp. 323-328.

[89] E. C. Cook, ‘Broad area wireless networking via High Altitude Platforms.’, PhD thesis, Naval postgraduate school, USA, 2013.

[90] Z. Yang and A. Mohammed, "Deployment and capacity of mobile WiMAX from high altitude platform," *2011 IEEE Vehicular Technology Conference*, San Francisco, USA Sep. 2011, pp.1-5.

[91] B. Dusza and C. Wietfeld, "Performance Evaluation of IEEE 802.16e mobile WiMAX for Long Distance Control of UAV Swarms", *IEEE International Conference on Wireless Information Technology and Systems (ICWITS),* Honolulu, HI, USA, August 2011, pp.1-4.

[92] O. Andryeyev and A. Mitschele-Thiel, "Increasing the Cellular Network Capacity Using Self-Organized Aerial Base Stations", *3rd Workshop on Micro Aerial Vehicle Networks, Systems, and Applications (DroNet '17),* New York, USA, June 2017, pp. 37-42.

[93] M. Silva, A. Correia, R. Dinis, N. Souto, J. Silva, *Transmission techniques for emergent multicast and broadcast systems.* Boca Raton, FL: CRC Press / Taylor & Francis, 2010.

[94] L. L. Hanzo, *MIMO-OFDM for LTE, Wi-Fi, and WiMAX: Coherent versus non-coherent and cooperative turbo-transceivers*. United States: John Wiley & Sons, 2011.

[95] *J. R. Hampton, Introduction to MIMO communications. Cambridge: Cambridge University Press, 2013.*

[96] *H. Arslan, Ed., Cognitive radio, software defined radio, and Adaptive wireless systems (signals and communication technology). Dordrecht: Springer-Verlag New York, 2007.*

[97] S. Ghafoor, P. Sutton, C. Sreenan, and K. Brown, 'Cognitive radio for disaster response networks: survey, potential, and challenges', *IEEE Wireless Communications*, vol. 21, pp. 70–80, Jan. 2014.

[98] H. Sharma and B. P, 'A communication approach for aerial surveillance of long linear infrastructures in non-urban terrain', *Twenty First National Conference on Communications (NCC)*, Mumbai, India, Feb. 2015, pp.1-6.

[99] S. Aljahdali, 'Enhancing the Capacity of Stratospheric Cellular Networks Using Adaptive Array Techniques', *International Journal of Computer Network and Information Security*, vol. 5, pp. 1–10, 2013.

[100] H. Li, X. Xu, M. Yang, and Q. Guo, 'Compensative mechanism based on steerable antennas for High Altitude Platform movement', *6th International ICST Conference on Communications and Networking in China (CHINACOM)*, Harbin, China, Aug. 2011, pp. 870 – 874.

[101] "MIMO or AAS: Key technology choice in deploying WiMAX," Nortel Networks Corporation. [Online]. Available: https://app.refme.com/home#/project/1637337/reference/manual?type=report. Accessed [06/01/2016].

[102] "Advanced Antenna Systems for WiMAX," in *Nokia Siemens networks*. [Online]. Available: file:///C:/Users/farisbj/Downloads/Advanced_Antenna_WiMAX_071129.pdf. Accessed: [Jan. 6, 2016].

[103] "A Complete Range of WiMAX Solutions," Airspan Networks. [Online]. Available: file:///C:/Users/farisbj/Downloads/ASMAX_lowres.pdf. Accessed: [Jan. 6, 2016].

[104] M. Deruyck E. Tanghe; W. Joseph; W. Vereecken; M. Pickavet; L. Martens; and B. Dhoedt, "Model for power consumption of wireless access networks," *IET Science, Measurement & Technology*, vol. 5, pp.155-161, 2011.

[105] Y. Xu, X. Xia, K. Xu and Y. Wang, "*Three-Dimension Massive MIMO for Air-to-Ground Transmission: Location-Assisted Precoding and Impact of AoD Uncertainty*", IEEE Access,vol. 5, pp. 15582-15596, 2017.

[106] A. Alajmi, A. Vulpe and O. Fratu, "*UAVs for Wi-Fi Receiver Mapping and Packet Sniffing with Antenna Radiation Pattern Diversity*", Springer Wireless Personal Communications, vol. 92, pp. 297-313, 2016.

[107] S. Kapri and P. Singh, "Internet Penetration And Google Loon As A Last Mile Solution", *Springer International Journal of Aerospace and Mechanical Engineering*, vol. 3, pp. 41-45, 2017.

[108] K. Faheem, D. Rafique and D. Saeed, "Last Mile Access Solution For the Provisioning Of Affordable Internet In The Rural & Semi Urban Areas.", *International Journal of Advanced Research*, vol. 4, pp. 307-311, 2016.

[109] 'STRATOSPHERIC BROADBAND', *CAPANINA*. [Online]. Available: http://www.capanina.org. [Accessed: 06-Feb-2017].

[110] F. D'Oliveira, F. Melo and T. Devezas, "High-Altitude Platforms - Present Situation and Technology Trends", *Journal of Aerospace Technology and Management*, vol. 8, pp. 249-262, 2016.

[111] ‘Lindstrand Technologies Ltd - A world leading manufacturer of Aerostats, Hangars, Helium Airships and Bespoke Inflatable Buildings’. [Online]. Available: http://www.lindstrandtech.com/. [Accessed: 17-Mar-2017].

[112] ‘StratXX near space technology’. [Online]. Available: http://www.stratxx.com/. [Accessed: 06-Feb-2017].

[113] "Hybrid Air Vehicles", [Online]. Available: https://www.hybridairvehicles.com/. [Accessed: 26- Nov- 2017].

[114] ‘Hybrid Air Vehicles Ltd - For Persistent Surveillance and Heavy Lift Logistics’, *Hybrid Air Vehicles*. [Online]. Available: http://www.hybridairvehicles.com/Default.aspx. [Accessed: 17-Mar-2017].

[115] M. Letizia, ‘Circularly Polarized multi-beam Antenna System for High-Altitude-Platforms’, PhD thesis, ÉCOLE POLYTECHNIQUE FÉDÉRALE DE LAUSANNE, Switzerland, 2013.

[116] ‘JAXA Japan Aerospace Exploration Agency’. [Online]. Available: http://global.jaxa.jp/. [Accessed: 06-Feb-2017].

[117] ‘ABSOLUTE : Aerial Base Stations with Opportunistic Links for Unexpected & Temporary Events’, 31-Oct-2012. [Online]. Available: http://www.absolute-project.eu/images/WPcontent/2012_10_31_Project_Presentation_Absolute.pdf. [Accessed: 20-Apr-2017].

[118] ‘TECH – UPDATER“s: An Internet Balloon - Google Project ”LOON" ???’,*TECH – UPDATER’s*. [Online]. Available: http://tech-updaters.blogspot.co.uk/2013/07/an-internet-balloon-google-project-loon.html. [Accessed: 17-Mar-2017].

[119] ‘Facts and Figures - Project Loon’, *Google Loon Project*. [Online]. Available: https://sites.google.com/a/pressatgoogle.com/project-loon/facts-and-figures. [Accessed: 19-Mar-2017].

[120] ‘New Zealand pilot test – Project Loon – Google’, *Google Loon project*. [Online]. Available: http://www.google.com/loon/where/. [Accessed: 19-Mar-2017].

[121] ‘Lockheed Martin · Lockheed Martin’. [Online]. Available: http://www.lockheedmartin.com/. [Accessed: 17-Mar-2017].

[122] “Prince Sultan Advanced Tech. Research Institute (PSATRI)", [Online]. Available: https://psatri.ksu.edu.sa/en. [Accessed: 26- Nov- 2017].

[123] "King Abdulaziz City for Science and Technology (KACST)", [Online]. Available: https://www.kacst.edu.sa/eng/Pages/default.aspx. [Accessed: 26- Nov- 2017].

[125] R. Wieringa, *Design Science Methodology for Information Systems and Software Engineering*. Berlin, Heidelberg: Springer Berlin Heidelberg, 2014.

[126] M. Lipsey, *Design Sensitivity: Statistical Power for Experimental Research (Applied Social Research Methods)*. Newbury Park, Sage, 2000.

[127] M. Miles, A. Huberman and J. Saldana, *Qualitative data analysis: a methods sourcebook*. London: Sage, 2014.

[128] H. Hassani, “Research Methods in Computer Science: The Challenges and Issues”, *arXiv preprint*, 2017.

[129] Cash, T. Stanković and M. Štorga, *Experimental Design Research: Approaches, Perspectives, Applications*. Springer, 2016.

[130] O. Eris, *Effective inquiry for innovative engineering design: From Basic Principles to Applications*. Springer, 2012.

[131] L. Blessing, A. Chakrabarti and L. Blessing, *DRM, a Design research methodology. Springer*, 2009.

[132] M. Alshami, T. Arslan, J. Thompson, and A. Erdogan, "Evaluation of path loss models at WiMAX cell-edge, "*4th IFIP International Conference on New Technologies, Mobility and Security*, Paris, France, Feb. 2011, pp.1-5.

[133] E. Kristiansand, "3.4-3.8 GHz band propagation models," Electronic Communication Committee-33 Orange Network, Sep. 2012.

[134] N. Rakesh, B. Maheswari, and S. Srivatsa, "Performance analysis of propagation models in different terrain conditions for IEEE standard 802.16e WiMAX," *2014 International Conference on Communication and Signal Processing*, Melmaruvathur, India, Apr. 2014, pp.142 – 146.

[135] N. Rakesh and D. Nalineswari, "Comprehensive performance analysis of path loss models on GSM 940MHz and IEEE802.16 WIMAX frequency 3.5GHz on different terrains," *International Conference on Computer Communication and Informatics*, Coimbatore, India Jan. 2015, pp.1-7.

[136] M. Lustgarten and J. Madison, "An empirical propagation model (EPM-73)," *IEEE Transactions on Electromagnetic Compatibility*, vol.19, pp. 301–309, Aug. 1977.

[137] S. Kasampalis, P. Lazaridis, Z. Zaharis, A. Bizopoulos, S. Zettas, J.Cosmas, "Comparison of Longley-Rice, ITU-R P.1546 and Hata-Davidson propagation models for DVB-T coverage prediction," *IEEE International Symposium on Broadband Multimedia Systems and Broadcasting*, Beijing, China, Jun. 2014m pp.1-4.

[138] L. Jordanova, "PROVIDING A QUALITY RECEPTION OF DVB-T SIGNALS," *JOURNAL OF APPLIED ELECTROMAGNETISM (JAE)*, vol. 17, pp. 16–18, 2015.

[139] W. Jiang, H. Cao, L. Goratti, M. Wiemeler, and T. Kaiser, "Opportunistic relaying over aerial-to-terrestrial and device-to-device radio channels," *IEEE International Conference on Communications Workshops (ICC)*, Sydney, Australia, Jun. 2014, pp.206-211.

[140] "LENS ANTENNAS FOR COMMUNICATIONS FROM HIGH-ALTITUDE PLATFORMS," in *Modern lens antennas for communications engineering*. United States: John Wiley & Sons, 2013.

[141] Q. Feng, J. Mcgeehan, E. Tameh, and A. Nix, "Path loss models for air-to-ground radio channels in urban environments, "*IEEE 63rd Vehicular Technology Conference*, Melbourne, Australia, May 2006, pp.2901–2905.

[142] ITU Radiocommunication Bureau (BR), "F.1500 - preferred characteristics of systems in the fixed service (FS) using high altitude platforms operating in the bands 47.2-47.5 GHz and 47.9-48.2 GHz," 2010. [Online]. Available: https://www.itu.int/dms_pubrec/itu-r/rec/f/R-REC-F.1500-0-200005-I!!PDF-E.pdf. Accessed: May 11, 2016.

[143] W. L. Tan, P. Hu, and M. Portmann, "Experimental evaluation of measurement-based SINR interference models," *IEEE International Symposium on a World of Wireless, Mobile and Multimedia Networks (WoWMoM)*, San Francisco, USA, Jun. 2012, pp.1-9.

[144] A. Vlavianos, L. Law, I. Broustis, S. Krishnamurthy, and M. Faloutsos, "Assessing link quality in IEEE 802.11 wireless networks: Which is the right metric?", *IEEE 19th International Symposium on Personal, Indoor and Mobile Radio Communications*, Cannes, France, Sep. 2008, pp1-6.

[145] Z.H. Talukder, S. Islam, D. Mahjabeen, A. Ahmed, S. Rafique and M. Rashid, "Cell coverage evaluation for LTE and WiMAX in wireless communication system," *World Applied Sciences Journal*, vol. 22, pp. 1486–1491, 2013.

[146] M. Malkowski, "Link-level comparison of IP-OFDMA (mobile WiMAX) and UMTS HSDPA," *IEEE 18th International Symposium on Personal, Indoor and Mobile Radio Communications*, Athens, Greece, Sep. 2007, pp.1-5.

[147] F. Almalki, M. Angelides, “Optimisation of a Propagation Model for Last-Mile Connectivity using a Low Altitude Platform,” unpublished.

[148] K. Raivio, O. Simula, J. Laiho, and P. Lehtimaki, "Analysis of mobile radio access network using the self-organizing map," *IFIP/IEEE Eighth International Symposium on Integrated Network Management,* Colorado Springs, USA, March 2003, pp.439 – 451.

[149] H. Agius and M. Angelides, "Modelling and filtering of MPEG-7-compliant meta-data for digital video", *ACM Symposium on Applied Computing,* Nicosia, Cyprus, March 2004, pp. 1248-1252.

[150] Y. Lin and H. Ye, "Input Data Representation for Self-Organizing Map in Software Classification", in *Second International Symposium on Knowledge Acquisition and Modelling*, Wuhan, China, Nov. 2009, pp.350 - 353.

[151] M. Angelides and A. Tong, "Implementing multiple tutoring strategies in an intelligent tutoring system for music learning", *Journal of Information Technology*, vol. 10, pp. 52-62, 1995.

[152] "Computation visualization programming neural network Toolbox for use with MATLAB ® user's guide,". [Online]. Available: http://www.image.ece.ntua.gr/courses_static/nn/matlab/nnet.pdf. Accessed: Oct. 4, 2016.

[153] M. C. Angelides and H. Agius, "An MPEG-7 scheme for semantic content modelling and filtering of digital video," *Multimedia Systems*, vol. 11, pp. 320–339, Oct. 2006.

[154] V. Jain, A. Singh, V. Chauhan, and A. Pandey, "Analytical study of wind power prediction system by using feed forward neural network," *International Conference on Computation of Power, Energy Information and Communication (ICCPEIC)*, Chennai, India, Apr. 2016, pp.303-306.

[155] R. Singh and S. Kansal, "Artificial neural network based spectrum recognition in cognitive radio," *IEEE Students' Conference on Electrical, Electronics and Computer Science (SCEECS)*, Bhopal, India, Mar. 2016, pp.1-6.

[156] D. Abinoja, R. Bedruz, and K. Jovellanos, A. Bandala, "Wireless user estimation using artificial neural networks," *International Conference on Humanoid, Nanotechnology, Information Technology, Communication and Control, Environment and Management*, Cebu, Philippines, Dec. 2015, pp.1-5.

[157] M. Angelides and R. Paul, "Towards a Framework for Integrating Intelligent Tutoring Systems and Gaming Simulation", *Proceedings of Winter Simulation Conference - (WSC '93)*, Los Angeles, USA, Dec. 1993, pp.1281-1289.

[158] F. A. Almalki, M. C. Angelides, "Empirical Evolution of a Propagation Model for Low Altitude Platforms", *Computing Conference 2017*, London, UK, July 2017, pp.1-6.

[159] J. C. Delos Angeles and E. P. Dadios, "Neural network-based path loss prediction for digital TV macrocells," *International Conference on Humanoid, Nanotechnology, Information Technology, Communication and Control, Environment and Management*, Cebu, Philippines, Dec. 2015, pp.1-9.

[160] "Airspan networks, leaders in 4G technology,". [Online]. Available: http://www.airspan.com/about-airspan/. Accessed [Jan. 10, 2016]

[161] ITU Radiocommunication Bureau (BR), "F.1500 - preferred characteristics of systems in the fixed service (FS) using high altitude platforms operating in the bands 47.2-47.5 GHz and 47.9-48.2 GHz," 2010. [Online]. Available: https://www.itu.int/dms_pubrec/itu-r/rec/f/R-REC-F.1500-0-200005-I!!PDF-E.pdf. Accessed: May 11, 2016.

[162] J. Hoy, *Forensic radio survey techniques for cell site analysis*. United States: John Wiley & Sons, pp.170, 2014.

[163] A. Valcarce, ", Airborne Base Stations for Emergency and Temporary Events," Lecture Notes of the Institute for Computer Sciences, Social Informatics and Telecommunications Engineering Personal Satellite Services, 2017.

[164] Y. Albagory and O. Said, "Performance enhancement of high-altitude platforms wireless sensor networks using concentric circular arrays," *AEU - International Journal of Electronics and Communications*, vol. 69, pp. 382–388, 2015.

[165] O. Said and Y. Albagory, "Internet of Things-Based Free Learning System: Performance Evaluation and Communication Perspective," *IETE Journal of Research*, vol. 63, pp. 31–44, 2016.

[166] S. H. Alsamhi, and N. S. Rajput, S.K. Gupta "Performance Evaluation of Broadband Service Delivery via Tethered Balloon Technology," *6th International Conference on Advances in Engineering Sciences and Applied Mathematics*, Kuala Lumpur Malaysia, January, 2017, pp.1-6.

[167] J. Agbinya, M. Aguayo-Torres and R. Klempous, *4G wireless communication networks: Design Planning and Applications*. Aalborg, Denmark: River Publishers, 2013.

[168] J. Deaton, "High Altitude Platforms for Disaster Recovery: Capabilities, Strategies, and Techniques for Emergency Telecommunications", *EURASIP Journal on Wireless Communications and Networking*, vol. 2008, pp. 31–44, 2008.

[169] "Central department of statistics & information," [Online]. Available: http://www.cdsi.gov.sa/english/. Accessed [Jan. 18, 2016].

[170] Business Monitor International Ltd., ‘Saudi Arabia Telecommunications Report & Forecasts Series.’, UK, 2015.

[171] I. Iskandar, "Performance Evaluation of Broadband WiMAX Services over High Altitude Platforms (HAPs) Communication Channel*", the fourth IEEE international conference on wireless and mobile communications ICWMC 2008*, Athens, Greece, July 2008, pp. 55-59.

[172] B. El-Jabu and R. Steele, "Cellular communications using aerial platforms," *IEEE Transactions on Vehicular Technology*, vol. 50, pp. 686–700, May 2001.

[173] M. I. Dessouky, H. A. Sharshar, and Y. A. Albagory, " Design of High Altitude Platforms Cellular Communication," *Progress In Electromagnetics Research*, vol. 67, pp. 251–261, 2007.

[174] "General Authority for Statistics in Kingdom of Saudi Arabia", [Online]. Available: https://www.stats.gov.sa/en. [Accessed: 26- Nov- 2017].

[175] M. Mozaffari, W. Saad, M. Bennis, and M. Debbah, "Drone small cells in the clouds: Design, deployment and performance analysis," *IEEE Global Communications Conference*, San Diego, USA, Dec. 2015, pp.1-6.

[176] H. Li, S. Habibi, and G. Ascheid, "Handover prediction for long-term window scheduling based on SINR maps," *IEEE 24th Annual International Symposium on Personal, Indoor, and Mobile Radio Communications*, London, UK, Sep. 2013, pp. 917 - 921

[177] "Methodologies for interference evaluation from the downlink of the fixed service using high altitude platform stations to the uplink of the fixed-satellite service using the geostationary satellites within the band 28.5-47.35 GHz", ITU, 2015.

[178] F. Almalki, M. Angelides, “Propagation modelling and performance assessment of aerial platforms deployed during emergencies”, *12th IEEE International Conference for Internet Technology and Secured Transactions (ICITST-2017)*, Cambeidge university, UK, Dec. 2017, pp.1-6.